

AL-TR-1992-0001

AD-A252 116



**COMPARATIVE STUDY OF THE MTFA, ICS,  
AND SQRI IMAGE QUALITY METRICS FOR  
VISUAL DISPLAY SYSTEMS (U)**

Robert J. Beaton  
Willard W. Farley

KEYSTONE ENGINEERING LIMITED  
P.O. BOX 11046  
BLACKSBURG, VIRGINIA 24062-1046

SEPTEMBER 1991



FINAL REPORT FOR PERIOD JUNE 1990 TO SEPTEMBER 1991

Approved for public release; distribution is unlimited.

92 6 16 03:5

92-15666



AIR FORCE SYSTEMS COMMAND  
WRIGHT-PATTERSON AIR FORCE BASE, OHIO 45433-6573

ARMSTRONG

LABORATORY

## NOTICES

When US Government drawings, specifications, or other data are used for any purpose other than a definitely related Government procurement operation, the Government thereby incurs no responsibility nor any obligation whatsoever, and the fact that the Government may have formulated, furnished, or in any way supplied the said drawings, specifications, or other data, is not to be regarded by implication or otherwise, as in any manner licensing the holder or any other person or corporation, or conveying any rights or permission to manufacture, use, or sell any patented invention that may in any way be related thereto.

Please do not request copies of this report from the Armstrong Aerospace Medical Research Laboratory. Additional copies may be purchased from:

National Technical Information Service  
5285 Port Royal Road  
Springfield, Virginia 22161

Federal Government agencies and their contractors registered with the Defense Technical Information Center should direct requests for copies of this report to:

Defense Technical Information Center  
Cameron Station  
Alexandria, Virginia 22314

## TECHNICAL REVIEW AND APPROVAL

AL-TR-1992-0001

This report has been reviewed by the Office of Public Affairs (PA) and is releasable to the National Technical Information Service (NTIS). At NTIS, it will be available to the general public, including foreign nations.

This technical report has been reviewed and is approved for publication.

FOR THE COMMANDER



KENNETH R. BOFF, Chief  
Human Engineering Division  
Armstrong Laboratory

REPORT DOCUMENTATION PAGE			Form Approved OMB No. 0704-0188	
<small>Public reporting burden for this collection of information is estimated to average 1 hour per response, including the time for reviewing instructions, searching existing data sources, gathering and maintaining the data needed, and completing and reviewing the collection of information. Send comments regarding this burden estimate or any other aspect of this collection of information, including suggestions for reducing this burden, to Washington Headquarters Services, Directorate for Information Operations and Reports, 1215 Jefferson Davis Highway, Suite 1204, Arlington, VA 22202-4302, and to the Office of Management and Budget, Paperwork Reduction Project (0704-0188), Washington, DC 20503.</small>				
1. AGENCY USE ONLY (Leave blank)		2. REPORT DATE SEPT 1991		3. REPORT TYPE AND DATES COVERED FINAL June 1990 - Sept 1991
4. TITLE AND SUBTITLE  Comparative Study of The MTFA, ICS, and SQRI Image Quality Metrics for Visual Display Systems.			5. FUNDING NUMBERS C: F33615-89-C-0532 PE: 62202F PR: 7184 TA: 10 WU: 44	
6. AUTHOR(S) R.J. Beaton & W.W. Farley Keystone Engineering Limited Blacksburg, VA 24061-0118				
7. PERFORMING ORGANIZATION NAME(S) AND ADDRESS(ES) Logicon Technical Services, Inc. P.O. Box 317258 Dayton, OH 4543107258			8. PERFORMING ORGANIZATION REPORT NUMBER	
9. SPONSORING / MONITORING AGENCY NAME(S) AND ADDRESS(ES) Armstrong Laboratory, Crew Systems Directorate Human Engineering Division HSD, AFSC Wright-Patterson AFB, OH 45433-6573			10. SPONSORING / MONITORING AGENCY REPORT NUMBER  AL-TR-1992-0001	
11. SUPPLEMENTARY NOTES				
12a. DISTRIBUTION / AVAILABILITY STATEMENT  Approved for public release; distribution is unlimited.			12b. DISTRIBUTION CODE  A	
13. ABSTRACT (Maximum 200 words)  This effort was a review of and analytic comparison between several of the most widely reported display image quality metrics: Modulation Transfer Function Area (MTFA), Integrated Contrast Sensitivity (ICS) metric, and the Square-Root Integral (SQRI) metric. Differences were found with regard to weightings applied to the psychovisual data which underline each metric. The SQRI metric was found to be sensitive to many variations in display viewing but was also found to exhibit large computational errors which were difficult to bring into control. The MTFA and ICS metrics were found to be somewhat less sensitive to display viewing parameters but also to exhibit greater computational robustness.				
14. SUBJECT TERMS  Image Quality, Display, Modulation Transfer Function			15. NUMBER OF PAGES 105	
			16. PRICE CODE	
17. SECURITY CLASSIFICATION OF REPORT  UNCLASSIFIED	18. SECURITY CLASSIFICATION OF THIS PAGE  UNCLASSIFIED	19. SECURITY CLASSIFICATION OF ABSTRACT  UNCLASSIFIED	20. LIMITATION OF ABSTRACT  UNLIMITED	

## PREFACE

This report was prepared by Keystone Engineering Limited for the U.S. Air Force Armstrong Laboratory under Contract No. F33615-89-C-0532 (Subcontract No. 07-014-09S). This report documents the project activities for the contract period June 1990 to September 1991. Robert J. Beaton was the Principal Investigator on the contract.

This project was performed in support of the Crew System Integration Branch, Human Engineering Division, Work Unit 7184 10 44, "Advanced Strategic Cockpit Engineering and Research." Gilbert G. Kuperman was the technical focal point for the research.

The authors gratefully acknowledge the contributions of Michael Miller who assisted in initial literature search and data collection activities.



Accession For	
NTIS GRA&I	<input checked="checked" type="checkbox"/>
DTIC TAB	<input type="checkbox"/>
Unannounced	<input type="checkbox"/>
Justification	
By	
Distribution/	
Availability Codes	
Dist	Avail and/or Special
A-1	

## TABLE OF CONTENTS

LIST OF FIGURES.....	vi
LIST OF TABLES .....	x
LIST OF SYMBOLS.....	xii
1.0 INTRODUCTION .....	1
1.1 Purpose of Project.....	5
2.0 METHODS.....	6
2.1 Computer Resources .....	6
2.2 Computational Parameters .....	7
2.3 Modulation Transfer Function Parameters.....	8
2.3.1 Pixel Shape. ....	8
2.3.2 Pixel Resolution. ....	9
2.3.3 Pixel Addressability. ....	10
2.3.4 Display Size. ....	10
2.3.5 Ambient Glare. ....	13
2.3.6 Viewing Distance.....	14
2.4 Contrast Threshold Function Parameters .....	15
2.4.1 Low-Pass Model. ....	15
2.4.2 Band-pass Model. ....	17
2.4.3 Extended Band-pass Model.....	19
2.4.4 CTF Model Verification and Selection. ....	22
3.0 METRIC COMPUTATIONS .....	27
3.1 Standard Conditions for Display and Observer .....	27
3.2 Baseline Values for Image Quality Metrics.....	28
3.2.1 MTFA Metric. ....	28
3.2.2 ICS Metric. ....	30

3.2.3 SQRI Metric. ....	33
3.3 Comparison of Normalized Integrands .....	35
3.4 Maximum Values for Image Quality Metrics .....	37
3.5 Sensitivity to Parameter Changes .....	38
3.5.1 Display Size. ....	38
3.5.2 Resolution/Addressability. ....	42
3.5.3 Peak, Glare, and Adaptation Luminance. ....	46
3.5.4 Viewing Distance. ....	53
3.6 Empirical Metric Computations .....	56
3.6.1 Empirical Metric Expressions. ....	57
3.6.2 Computational Issues. ....	58
3.6.2.1 Number of Samples. ....	58
3.6.2.2 LSF Sampling Interval. ....	58
3.6.2.3 LSF Scan Period. ....	59
3.6.2.4 Lower Spatial Frequency Limit. ....	60
3.6.2.5 Upper Spatial Frequency Limit. ....	61
3.6.2.6 Removing Glare Offset. ....	62
3.6.3 Empirical Metric Computations. ....	63
3.6.3.1 Empirical MTFA Metric. ....	64
3.6.3.2 Empirical ICS Metric. ....	66
3.6.3.2 Empirical SQRI Metric. ....	67
<b>4.0 PERFORMANCE CORRELATIONS .....</b>	<b>69</b>
4.1 Westerink and Roufs (1988) .....	69
4.1.1 Description of Experiment. ....	69
4.1.2 Metric v. Performance Correlations. ....	69
4.1.2.1 MTFA Metric. ....	72
4.1.2.2 ICS Metric. ....	73
4.1.2.3 SQRI Metric. ....	74
4.2 van der Zee and Boesten (1980) .....	75
4.2.1 Description of Experiment. ....	75
4.2.2 Metric v. Performance Correlations. ....	75

4.2.2.1	MTFA Metric.....	77
4.2.2.2	ICS Metric.....	78
4.2.2.2	SQRI Metric.....	79
4.3	Knox (1987).....	80
4.3.1	Description of Experiment.....	80
4.3.2	Metric v. Performance Correlations.....	81
4.3.2.1	MTFA Metric.....	82
4.3.2.2	ICS Metric.....	83
4.3.2.3	SQRI Metric.....	84
4.4	Beaton (1984) .....	85
4.4.1	Description of Experiment.....	85
4.4.2	Metric v. Performance Correlations.....	85
4.4.2.1	MTFA Metric.....	86
4.4.2.2	ICS Metric.....	87
4.4.2.3	SQRI Metric.....	89
4.5	Hunter (1988) .....	90
4.5.1	Description of Experiment.....	90
4.5.2.	Metric v. Performance Correlations.....	90
4.5.2.1	MTFA Metric.....	92
4.5.2.2	ICS Metric.....	94
4.5.2.3	SQRI Metric.....	96
5.0	CONCLUSIONS .....	99
6.0	REFERENCES .....	102

## LIST OF FIGURES

Figure 1. Infante (1984) model of the human visual contrast threshold function. ....	16
Figure 2. Barten (1987) model of the human visual contrast threshold function. ....	18
Figure 3. Barten (1989) model of the human visual contrast threshold function. ....	20
Figure 4. MTF and Barten 1989 CTF used in MTFA evaluation of standard conditions. ....	29
Figure 5. MTFA integrand function used in evaluation of standard conditions. ....	30
Figure 6. Barten 1989 CSF used in ICS and SQRI evaluation of standard conditions. ....	32
Figure 7. ICS integrand used in evaluation of standard conditions. ....	33
Figure 8. SQRI integrand used in evaluation of standard conditions. ....	35
Figure 9. Normalized integrands for MTFA, ICS, and SQRI metrics used in evaluation of standard conditions. ....	36
Figure 10-A. Effect of display size on the MTFA image quality metric. ....	41
Figure 10-B. Effect of display size on the ICS image quality metric. ....	41
Figure 10-C. Effect of display size on the SQRI image quality metric. ....	42
Figure 11-A. Effect of resolution/addressability on the MTFA image quality metric. ....	44
Figure 11-B. Effect of resolution/addressability on the ICS image quality metric. ....	45

Figure 11-C. Effect of resolution/addressability on the SQRI image quality metric. ....	45
Figure 12-A. Effect of peak-to-glare luminance ratio on the MTFA image quality metric. ....	49
Figure 12-B. Effect of peak-to-glare luminance ratio on the ICS image quality metric. ....	49
Figure 12-C. Effect of peak-to-glare luminance ratio on the SQRI image quality metric. ....	50
Figure 13-A. Effect of adaptation luminance ratio on the MTFA image quality metric. ....	52
Figure 13-B. Effect of adaptation luminance ratio on the ICS image quality metric. ....	52
Figure 13-C. Effect of adaptation luminance ratio on the SQRI image quality metric. ....	53
Figure 14-A. Effect of viewing distance on the MTFA image quality metric. ....	55
Figure 14-B. Effect of viewing distance on the ICS image quality metric. ....	56
Figure 14-C. Effect of viewing distance on the SQRI image quality metric. ....	56
Figure 15. Empirical MTFA metric values as a function of number of samples and lens magnification.....	65
Figure 16. Empirical ICS metric values as a function of number of samples and lens magnification.....	67
Figure 17. Empirical SQRI metric values as a function of number of samples and lens magnification.....	68

Figure 18. Scattergram of subjective image quality judgments reported in Westerink and Roufs (1988) and empirically computed MTFA metric values. ....	72
Figure 19. Scattergram of subjective image quality judgments reported in Westerink and Roufs (1988) and empirically computed ICS metric values. ....	73
Figure 20. Scattergram of subjective image quality judgments reported in Westerink and Roufs (1988) and empirically computed SQRI metric values. ....	74
Figure 21. Scattergram of subjective quality judgments reported in van der Zee and Boesten (1980) and empirically computed MTFA metric values. ....	78
Figure 22. Scattergram of subjective image quality judgments reported in van der Zee and Boesten (1980) and empirically computed ICS metric values. ....	79
Figure 23. Scattergram of subjective image quality judgments reported in van der Zee and Boesten (1980) and empirically computed SQRI metric values. ....	80
Figure 24. Scattergram of subjective image quality judgments reported in Knox (1987) and empirically computed MTFA metric values. ....	83
Figure 25. Scattergram of subjective image quality judgments reported in Knox (1987) and empirically computed ICS metric values. ....	84
Figure 26. Scattergram of subjective image quality judgment reported Knox (1987) and empirically computed SQRI metric values. ....	85
Figure 27. Scattergram of subjective image quality judgments reported in Beaton (1984) and empirically computed MTFA metric values. ....	88

Figure 28. Scattergram of subjective image quality judgments reported in Beaton (1984) and empirically computed ICS metric values. ....	88
Figure 29. Scattergram of subjective image quality judgment reported Beaton (1984) and empirically computed SQRI metric values. ....	89
Figure 30. Scattergram of subjective image quality judgments reported in Hunter (1988) and empirically computed MTFA metric values for the low-resolution display condition. ....	93
Figure 31. Scattergram of subjective image quality judgments reported in Hunter (1988) and empirically computed MTFA metric values for the high-resolution display condition. ....	94
Figure 32. Scattergram of subjective image quality judgments reported in Hunter (1988) and empirically computed ICS metric values for the low-resolution display condition. ....	95
Figure 33. Scattergram of subjective image quality judgments reported in Hunter (1988) and empirically computed ICS metric values for the high-resolution display condition. ....	96
Figure 34. Scattergram of subjective image quality judgment reported Hunter (1988) and empirically computed SQRI metric values for the low-resolution display conditions. ....	97
Figure 35. Scattergram of subjective image quality judgment reported Hunter (1988) and empirically computed SQRI metric values for the high-resolution display conditions. ....	98

## LIST OF TABLES

Table 1. Parameters of Image Quality Metric Algorithms .....	7
Table 2. Average Display Area Calculations .....	21
Table 3-A. Comparison of Actual and Computed CTF Values (0.0001 cd/m <sup>2</sup> adaptation luminance) .....	23
Table 3-B. Comparison of Actual and Computed CTF Values (0.001 cd/m <sup>2</sup> adaptation luminance) .....	23
Table 3-C. Comparison of Actual and Computed CTF Values (0.01 cd/m <sup>2</sup> adaptation luminance) .....	24
Table 3-D. Comparison of Actual and Computed CTF Values (0.1 cd/m <sup>2</sup> adaptation luminance) .....	24
Table 3-E. Comparison of Actual and Computed CTF Values (1.0 cd/m <sup>2</sup> adaptation luminance) .....	25
Table 3-F. Comparison of Actual and Computed CTF Values (10.0 cd/m <sup>2</sup> adaptation luminance) .....	25
Table 4. Parameter Settings for Standard Conditions .....	27
Table 5. Baseline MTFA Values for Standard Conditions <sup>1</sup> . ....	28
Table 6. Baseline ICS Values for Standard Conditions <sup>1</sup> . ....	31
Table 7. Baseline SQRI Values for Standard Conditions <sup>1</sup> . ....	34
Table 8. Maximum Values for MTFA, ICS, and SQRI Metrics .....	37
Table 9. Parameters for Display Size Computations. ....	40
Table 10. Parameters for Resolution/Addressability Computations .....	43

Table 11. Parameters for Peak-To-Glare Luminance Ratio Computations.....	48
Table 12. Parameters for Adaptation Luminance Computations. ....	51
Table 13. Parameters for Viewing Distance Computations.....	54
Table 14. Computational Parameters for Empirical Metric Evaluations.....	64
Table 15. Empirical MTFA Values Computed Across $N_{LSF}$ and MAG .....	65
Table 16. Empirical ICS Values Computed Across $N_{LSF}$ and MAG .....	66
Table 17. Empirical SQRI Values Computed Across $N_{LSF}$ and MAG .....	68
Table 18. 50% Width Calculations for Westerink and Roufs (1988). ....	71
Table 19. Computational Parameters for Westerink and Roufs (1988).....	71
Table 20. Screen Size Calculations for van der Zee and Boesten (1988) .....	76
Table 21. Computational Parameters for van der Zee and Boesten (1980) .....	77
Table 22. Resolution/Addressability Ratio Calculations for Knox (1987).....	81
Table 23. Display Size Calculations for Knox (1987).....	81
Table 24. Computational Parameters for Knox (1987) .....	82
Table 25. 50% Width Calculations for Beaton (1984) .....	86
Table 26. Computational Parameters for Beaton (1984).....	87
Table 27. Computational Parameters for Hunter (1988).....	92

## LIST OF SYMBOLS

$a \ll b$	a is much less than b
$a \gg b$	a is much greater than b
% Error	Percent error statistic
A	Pixel addressability in millimeters
$\arctan (.)$	Arc tangent operation in radians
$b_0, b_1, b_2$	Empirical coefficients or constants
CTF(.)	Contrast Threshold Function
D	Distance of observer from display screen in millimeters
$\Delta d$	Spatial sampling interval in millimeters
DS	Display size
DW	Display width
DH	Display height
DD	Display diagonal
DA	Display area
$\overline{DA}$	Average display area
$\Delta v$	Summation interval in cycles per degree
G	Reflected glare luminance in $\text{cd/m}^2$
I	Incident illumination level in lux
ICS	Integrated Contrast Sensitivity metric
$\text{int} (.)$	Integer round-up operation

$\text{int} (.)$	Integer round-down operation
IQ	Perceived image quality level
$L_{\max}$	Maximum pixel luminance in $\text{cd/m}^2$
$L_{\min}$	Minimum pixel luminance in $\text{cd/m}^2$
$L_{\text{adapt}}$	Adaptation luminance level in $\text{cd/m}^2$
$L_{\text{ave}}$	Average scene luminance in $\text{cd/m}^2$
$L_{\text{peak}}$	Peak screen luminance in $\text{cd/m}^2$
M	Modulation (normalized luminance contrast)
MAG	Lens magnification factor
MTF(.)	Modulation Transfer Function
MTFA	Modulation Transfer Function Area metric
N	Number of measurement points
PGR	Peak-to-Glare Ratio metric
$P_{\text{LSF}}$	LSF measurement period
R	Reflectivity value
RAR	Resolution-to-Addressability Ratio metric
S	Size of object in millimeters
FWHM	Full-Width Half-Maximum metric
s	Pixel (spot) width
$\sigma$	Standard deviation with respect to the spatial location
SQRI	Square Root Integral metric

$T$	Transmissivity value
$\nu$	Angular spatial frequency in cycles per degree
$\nu_l$	Lower limit of integration in cycles per degree
$\nu_u$	Upper limit of integration in cycles per degree
$\omega$	Linear spatial frequency in cycles per distance
$\omega_l$	Lower limit of integration in cycles per distance
$\omega_u$	Upper limit of integration in cycles per distance
$\omega_{-6 \text{ dB}}$	Linear spatial frequency in cycles per distance corresponding to -6 dB MTF point
$\tilde{\omega}_{Ny}$	Nyquist limit of discrete MTF analysis in cycles per distance
$x$	Spatial position on display screen in distance units

## 1.0 INTRODUCTION

Image quality is the key concept underlying many engineering decisions made during the design of visual display systems. Fundamentally, the concept of image quality refers to the amount of task-appropriate information presented to an observer from viewable regions of a display screen. From an engineering standpoint, there are several physical characteristics that limit the levels of image quality achievable from a display system, such as bandwidth, resolution, addressability, color gamut, and luminance contrast.

The relationships among physical display characteristics and perceived image quality are complex. For example, perceived image quality can increase faster with increasing display bandwidth at low luminance contrast levels as compared to high luminance contrast levels. Many perceptual relationships involving physical display characteristics and perceived image quality levels have been studied over the past 50 years. The display design principles derived from these studies have been captured in quantitative measures or so-called "metrics" of image quality (see, for reviews, Beaton, 1984; Snyder, 1985).

Most image quality metrics are based on spatial frequency-domain representations of the display device and the human observer. Specifically, the capacity of a display system to transmit a signal is indexed by the Modulation Transfer Function (MTF). The MTF expresses the relative amount of modulation (i.e., normalized luminance contrast) produced by a display system as a function of the spatial frequency components comprising an image signal. Each value of the MTF is the ratio of output-to-input modulation at a particular spatial frequency value. For all realizable display systems, the MTF decreases with increasing spatial frequency, and, thus, all displays possess a finite capacity (bandwidth) to transmit information signals (see, for details, Snyder, 1980).

While the MTF expresses the capacity of a display system to transmit visual signals, a similar spatial frequency-domain function can be used to index the capacity of human observer to perceive those signals. The Contrast

Threshold Function (CTF) expresses the amount of modulation required by the human visual system to detect the spatial frequency components of an image signal. Each CTF value represents the minimum amount of modulation required by the human visual system to detect a particular spatial frequency component. In general, the CTF increases with increasing spatial frequency; however, the CTF magnitudes are affected by viewing conditions. Nevertheless, the general shape of the CTF indicates that the human visual system has finite capacity to detect spatial frequency components of image signals (see, for details, Snyder, 1980).

The MTF and CTF describe fundamental aspects of the concept of image quality; that is, the MTF quantifies the amount of signal modulation available from a display system, whereas the CTF quantifies the amount of signal modulation required by a human observer. Using these two quantitative functions, numerous unitary metrics of image quality have been formulated to help engineers account for the perceptual tradeoffs associated with alternate display design decisions.

Among available image quality metrics, the best-known one is the Modulation Transfer Function Area (MTFA; Borough, Fallis, Warnock, and Britt, 1967; Snyder, 1973). The MTFA image quality metric is defined as:

$$MTFA = \int_{v_l}^{v_u} MTF(v) - CTF(v) \, dv \quad (\text{Eq. 1})$$

in which,

- MTF(v)      denotes the Modulation Transfer Function,
- CTF(v)      denotes the Contrast Threshold Function,
- v            denotes angular spatial frequency in cycles per degree of visual angle,

- $\nu_l$  denotes the lower spatial frequency limit of integration in cycles per degree of visual angle,
- $\nu_u$  denotes the upper spatial frequency limit of integration in cycles per degree of visual angle,

The MTFA metric is a scalar index of the total amount of visually-detectable signal modulation presented by a system as a function of spatial frequency. The MTFA metric has enjoyed a history of use in the photographic and optical imaging industries. And, it has been adopted as the *de facto* standard metric in the electronic display industry (see, ANSI/HFS 100-1988).

Despite its acceptance within the visual displays engineering community, the MTFA metric is not a flawless predictor of image quality across all display viewing conditions. Indeed, workers in this arena have recognized several limitations of the MTFA metric and have sought to develop improved image quality metrics (see, for review, Beaton, 1984).

One limitation of the MTFA metric is its low numerical sensitivity to subtle changes in the CTF, such as those caused by changes in observer's luminance adaptation level or image noise levels. The low sensitivity of the MTFA metric to CTF shifts stems from the fact that typical MTF magnitudes are large in comparison to CTF magnitudes, particularly at lower spatial frequency values (i.e., less than 10 cycles per degree of visual angle). In other words, the subtraction of disparate but small CTF values from larger MTF values may not produce substantial changes in MTFA values.

The Integrated Contrast Sensitivity (ICS) metric (van Meeteren, 1973) purportedly affords greater sensitivity to subtle changes in the CTF as compared to the MTFA metric. The ICS is defined as

$$ICS = \int_{\nu_l}^{\nu_u} \frac{MTF(\nu)}{CTF(\nu)} d\nu \quad (Eq. 2)$$

in which all symbol definitions are identical to Eq. 1.

The analytical form of the ICS embodies the operation of "cascading" component transfer functions from linear systems theory. That is, the MTF is point-by-point multiplied with the inverse CTF. The inverse CTF has been interpreted by visual science researchers as a transfer function of the human visual system. The inverse CTF is referred to as the Contrast Sensitivity Function (CSF). Since the ICS metric integrand is the product of the MTF and inverse CTF, ICS values may change rapidly with changes in CTF or MTF values.

A theoretical limitation of the ICS metric (and MTF-A metric as well) is that modulation levels are weighted uniformly across the spatial frequency passband. In the metric formulation, a unit of modulation at a low spatial frequency influences the metric value by the same amount as a unit of modulation at a high spatial frequency. Several workers in this field, however, have noted that the contribution of modulation to perceived image quality levels varies nonuniformly across the spatial frequency passband (cf. Carlson, 1988; Carlson and Cohen, 1980).

The recently-proposed Square-Root Integral (SQRI) metric (Barten, 1987, 1988, 1989a, 1989b, 1989c, 1989d, 1990a, 1990b, 1991) is based on a non-linear scaling of modulation across spatial frequencies. The SQRI metric is defined as:

$$SQRI = \frac{1}{\ln 2} \int_{v_l}^{v_u} \sqrt{\frac{MTF(v)}{CTF(v)}} \frac{\partial v}{v} \quad (Eq. 3)$$

in which all symbol definitions are identical to Eq. 1.

The SQRI metric scales visually-weighted modulation levels by two compressive operations: (1) a square root operator and (2) a logarithmic integration (i.e.,  $\frac{\partial v}{v}$ ). These analytic operations emphasize the contributions

of lower modulation levels at lower spatial frequencies in the SQRI metric value. Purportedly, the compressive scaling performed by the SQRI metric matches observed patterns in human suprathreshold contrast discriminations. The SQRI metric is claimed to provide an improved index of image quality effects associated with physical display parameters in comparison to the MTFA and ICS metrics.

The SQRI metric has received much attention recently in the visual displays engineering community, and some workers have suggested adopting the SQRI metric as an alternative to the MTFA and ICS metrics. Unfortunately, there has not been a comprehensive evaluation of the SQRI metric assessing its image quality modelling capability or computational requirements in relation to existing metrics.

## **1.1 PURPOSE OF PROJECT**

As new image quality metrics emerge from the display engineering and visual science disciplines, it is understood that their inherent advantages and limitations must be examined carefully in relation to extant image quality standards. This engineering doctrine is founded on the premise that image quality factors substantially determine the efficiency of the visual interface between operators and their input/output activities while interacting with a system. Thus, the knowledge of image quality levels derived from metrics plays a critical role in the design optimization of display systems.

The project reported herein examines the MTFA, ICS, and SQRI image quality metrics. Specifically, the three image quality metrics are examined in terms of analytical properties and behaviors, computational requirements and pitfalls, as well as statistical correlations with subjective image quality judgments across numerous visual display conditions. This work highlights advantages and disadvantages among the MTFA, ICS, and SQRI image quality metrics.

## 2.0 METHODS

Two phases of work were completed in this project. In the first phase, analytical properties of the MTFA, ICS, and SQRI image quality metrics were studied. This portion of work examined the numerical behavior of the metrics across various display device and viewing condition parameters (e.g., display size, resolution and addressability, peak luminance, ambient glare, observer viewing distance, and adaptation luminance). Additionally, computational requirements associated with the metrics were examined.

In the second phase, the capacity of the metrics to predict human performance across image quality levels was examined. A review of select engineering literature on subjective image quality judgments was used to establish a correlational database for comparisons among the metrics.

### 2.1 COMPUTER RESOURCES

Computational algorithms for the image quality metrics were implemented in the *Mathematica*<sup>TM</sup> (Wolfram Research, Version 1.2.1.e for Apple Macintosh) and C (Symantec, Think C<sup>TM</sup>, Version 5.0.5 for Apple Macintosh; Microsoft C, Version 6.0a for IBM/DOS) programming languages. The computations were performed on an Apple Macintosh IIx (Operating System Version 7.0) and an IBM PS-2 Model 30 (DOS Operating System Version 4.0) microcomputers, each configured with floating-point numeric coprocessors.

The *Mathematica*<sup>TM</sup> program computed all metrics using an adaptive numerical integration algorithm with 15 digits of precision, 10 digits of accuracy, a minimum of two interval subdivisions, and a maximum of 100 interval subdivisions.

The C-language programs performed the numerical integrations using Simpson's 1/3- and 4/3-Rules without end-correction in 64-bit floating-point numerics. The Fourier transforms implemented in the C-language for this project were based on the algorithm of Bergland and Doland (1979).

## 2.2 COMPUTATIONAL PARAMETERS

The software programs developed for the project allow the user to define numerous computational parameters for the metric evaluations. A brief listing of these parameters is shown in Table 1.

Table 1. Parameters of Image Quality Metric Algorithms

<b>Display Parameters</b>		<b>Description</b>
Display Size		Height and width of screen
Resolution		Size and shape of picture elements
Addressability		Distance between picture elements
Peak Luminance		Maximum screen light intensity
Reflected Glare		Reflected light intensity from screen
<b>Observer Parameters</b>		
Viewing Distance		Distance of observer from screen
Contrast Sensitivity		Empirical CTF model
Adaptation Luminance		Average light exposure level
<b>Computational Parameters</b>		
Integration Limits		Spatial frequency passband
Integration Type		Numerical integration algorithm

## 2.3 MODULATION TRANSFER FUNCTION PARAMETERS

**2.3.1 Pixel Shape.** Pixel shape refers to the spatial distribution of luminance that defines an individual picture element (pixel) on a display screen. The luminance distribution or profile of a pixel is referred to as the Line Spread Function (LSF). For monochrome Cathode Ray Tube (CRT) display devices, the LSF often is approximated by a Gaussian function, such as defined below (Infante, 1984):

$$\text{LSF}(x) = L_{\max} \exp\left[\frac{-4 \ln 2 x^2}{s^2}\right] \quad (\text{Eq. 4})$$

in which

- |            |   |
|------------|---|
| $x$        | denotes spatial position on the display screen,   |
| $L_{\max}$ | denotes the maximum pixel luminance, and          |
| $s$        | denotes the 50%-width of the pixel (see, §2.3.2). |

It should be noted that Eq. 4 does not account for electron beam artifacts, such as astigmatism, which can cause defocused or "blurry" images on monochrome CRT screens.

The MTF is computed from the LSF by a forward Fourier transform. For certain LSF shapes, the MTF is known analytically. For example, the MTF of the Gaussian LSF in Eq. 4 is given by (Infante, 1984):

$$\text{MTF}(\omega) = \exp\left[\frac{-\pi^2 s^2 \omega^2}{4 \ln 2}\right] \quad (\text{Eq. 5})$$

in which

- |          |   |
|----------|---|
| $\omega$ | denotes linear spatial frequency in cycles per unit distance (i.e., cycles per millimeter). |
|----------|---|

By inspection of Eqs. 4 and 5, we note that a Gaussian LSF and its corresponding MTF are related inversely through the 50%-width parameter. That is, MTF width decreases with increasing LSF width.

To combine the MTF and visual functions (i.e., CTF or CSF), the linear spatial frequency units must be referred to angular spatial frequency units. The conversion of spatial frequency units used in this work is given by

$$v = \frac{\pi}{180 \arctan \left[ \frac{1}{\omega D} \right]} \quad (\text{Eq. 6})$$

in which

- $v$  denotes angular spatial frequency in cycles per degree of visual angle,
- $\arctan [.]$  denotes the arc tangent function in radians, and
- $D$  denotes the distance between the observer and display screen.

It is important to note that  $D$  must be expressed in the same units of length used for  $\omega$  and  $s$  in Eq. 5 (i.e., millimeters, inches, etc.). Also, Eq. 6 assumes that the observer's line-of-sight forms a single right-angle with the object (screen) plane.

**2.3.2 Pixel Resolution.** Pixel resolution refers to the size or width of individual picture elements on the display screen. In this report, pixel resolution is defined as the Full-Width at Half-Maximum (FWHM) luminance or the 50% width point. In general, since the MTF is computed by transforming the LSF, the bandwidth of the MTF is related inversely to pixel resolution. Also, FWHM is related to other measures of the width of a pixel intensity distribution (Bracewell, 1986). For example, with the Gaussian pixel shape given in Eq. 4,

$$\text{FWHM} = 2.355 \sigma \quad (\text{Eq. 7})$$

in which

$\sigma$  denotes the standard deviation with respect to the spatial dimension axis (e.g., mm, cm, mils, etc.).

**2.3.3 Pixel Addressability.** Pixel addressability refers to the distance or separation between adjacent pixels or raster lines on the display screen. Specifically, pixel addressability is defined as the linear distance between centroids of two adjacent pixels or raster lines. For analog display systems, it should be appreciated that pixel addressability is undefined since pixels can be located at any position on the screen. However, for discretely addressed display systems, pixel locations are constrained to fixed positions on the raster structure.

Pixel addressability has an impact on the highest spatial frequency that can be produced by a discretely addressed display system. That is, according to the Nyquist sampling theory, at least two samples per cycle are necessary to represent a spatial frequency component without aliasing. Thus, the upper limit of the spatial frequency passband for a discretely addressed display system is given as

$$\omega_u = \frac{1}{2 A} \quad (\text{Eq. 8a})$$

$$v_u = \frac{\pi}{180 \arctan \left[ \frac{2 A}{D} \right]} \quad (\text{Eq. 8b})$$

in which

$A$  denotes the pixel addressability in distance units (e.g., mm, cm, mils, etc.).

**2.3.4 Display Size.** Display size refers to the spatial extent of the active picture area on a display device. Display size usually specifies the

linear distance along the horizontal, vertical, or diagonal dimensions of the active screen area, although some authors intend it to specify display area. Since image quality metrics utilize various forms of the display size parameter, it is convenient to define the following terms:

Display Width:  $DW_{mm}$  denotes the horizontal display dimension in mm (Eq. 9a)

$$DW_{deg} = \frac{180}{\pi} \arctan\left[\frac{DW_{mm}}{D}\right] \quad (\text{Eq. 9b})$$

Display Height:  $DH_{mm}$  denotes the vertical display dimension in mm (Eq. 10a)

$$DH_{deg} = \frac{180}{\pi} \arctan\left[\frac{DH_{mm}}{D}\right] \quad (\text{Eq. 10b})$$

Display Diagonal:

$$DD_{mm} = \sqrt{DW_{mm}^2 + DH_{mm}^2} \quad (\text{Eq. 11a})$$

$$DD_{deg} = \frac{180}{\pi} \arctan\left[\frac{DD_{mm}}{D}\right] \quad (\text{Eq. 11b})$$

Display Area:

$$DA_{mm} = DW_{mm} DH_{mm} \quad (\text{Eq. 12a})$$

$$DA_{deg} = \frac{32400}{\pi^2} \arctan\left[\frac{DW_{mm}}{D}\right] \arctan\left[\frac{DH_{mm}}{D}\right] \quad (\text{Eq. 12b})$$

Average (Geometric Mean) Display Area:

$$\overline{DA}_{mm} = \sqrt{DW_{mm} DH_{mm}} \quad (\text{Eq. 13a})$$

$$\overline{DA}_{deg} = \frac{180}{\pi} \sqrt{\arctan\left[\frac{DW_{mm}}{D}\right] \arctan\left[\frac{DH_{mm}}{D}\right]} \quad (\text{Eq. 13b})$$

Note that Eqs. 12b and 13b define area values in terms of subtended linear dimensions, rather than in terms of the subtended area dimensions.

Display size determines the lowest spatial frequency that can be produced by a display system. Since at least one cycle per display size is required to render a spatial frequency component without aliasing, the lower spatial frequency passband limit for a display system is given as

$$\omega_l = \frac{1}{DS_{mm}} \quad (\text{Eq. 14a})$$

$$\nu_l = \frac{\pi}{180 \arctan\left[\frac{DS_{mm}}{D}\right]} \quad (\text{Eq. 14b})$$

in which

$DS_{mm}$  denotes display size along a particular screen dimension (i.e.,  $DW_{mm}$  for the horizontal dimension or  $DH_{mm}$  for the vertical dimension).

Since many visual display screens are rectangular in shape (i.e., non-equal horizontal and vertical dimensions), the setting of the display size parameter is problematic in computations of one-dimensional image quality metrics. Barring *a priori* reasons to emphasize one spatial display dimension over another, it is reasonable to use the average display area to set the lower passband limit using Eq. 13:

$$\omega_l = \frac{1}{\overline{DA}_{mm}} \quad (\text{Eq. 15a})$$

$$v_l = \frac{1}{DA_{deg}} \quad (\text{Eq. 15b})$$

**2.3.5 Ambient Glare.** Ambient glare refers to the amount of light reflected from a display screen from sources within the work place environment. Specifically, ambient glare is defined as the diffuse luminance reflected from the dark or inactive regions of a display screen. For most display screens, ambient glare may be measured using a large-area integrating photometer or calculated from the measured illumination and screen reflectivity values. Moreover, since it is impossible from a practical viewpoint to catalog the ambient environments of all display workstations, we make the simplifying assumption that ambient glare is reflected uniformly from the display screen.

Ambient glare exerts a direct effect on the luminance modulation obtainable from a display device. Specifically, since reflected glare luminance adds to luminance emitted from a display, modulation decreases with increasing ambient glare levels, as given by

$$M = \frac{L_{max} - L_{min}}{L_{max} + L_{min} + 2 G} \quad (\text{Eq. 16})$$

in which

$L_{max}, L_{min}$      denote the maximum, minimum luminance of the  
    spatial frequency component without glare, and  
 $G$                      denotes the ambient reflected glare luminance.

In terms of MTF values, the effect of ambient glare is given by a simple scaling constant (Farley, 1989):

$$\text{MTF}(\nu)_{\text{glare}} = \left[ \frac{L_{\text{peak}}}{L_{\text{peak}} + 2G} \right] \text{MTF}(\nu)_{\text{no glare}} \quad (\text{Eq. 17})$$

in which

$L_{\text{peak}}$  denotes the peak luminance emitted from a display screen for a zero spatial frequency (i.e., DC level or all pixels set to maximum value) input signal.

Note that  $L_{\text{peak}}$  is not guaranteed to equal  $L_{\text{max}}$  due to luminance response nonlinearities inherent to certain display technologies (i.e., CRTs).

**2.3.6 Viewing Distance.** Viewing distance refers to the linear distance between the display screen and the observer's eye point. Although viewing distances vary across display applications (e.g., 430–635 mm for desktop displays and 710–815 mm for aircraft cockpits), the minimum distance value is constrained to about 150–254 mm by the human visual system's ability to accommodate (focus) on the display screen.

Viewing distance affects the angular size of objects at the observer's eye point. This fact has important consequences for the image quality of visual displays, since observer's visual ability to resolve spatial details in a scene is related directly to the angular size of the details on the retina. The conversion from linear distance units to angular size units is given as

$$\text{Visual Angle (degrees)} = \frac{180}{\pi} \arctan \left[ \frac{S}{D} \right] \quad (\text{Eq. 18})$$

in which

$S$  denotes the linear size of the object.

It should be mentioned that the small angle approximation to the arctangent function (i.e.,  $\frac{180}{\pi} \left[ \frac{H}{D} \right]$ ) may be used instead of Eq. 18 for angles

less than about 5 degrees. However, use of this approximation is discouraged strongly for image quality metric evaluations since substantial errors accumulate in computations involving low spatial frequency values (e.g., SQRI metric).

## 2.4 CONTRAST THRESHOLD FUNCTION PARAMETERS

In this section, several computational models for the human visual CTF are discussed.

The CTF indexes the amount of modulation necessary for a human observer to detect visual sinusoidal patterns of varying spatial frequency values. Since the units of the CTF (or CSF) are compatible quantitatively with the MTF of a display system, the CTF has been used to represent the role of the human visual system in image quality metrics. However, the CTF is not a static entity. Rather, the CTF is influenced by numerous variables in a viewing environment. For example, the CTF decreases with increasing light adaptation levels and increasing number of cycles per spatial frequency component. Some of the models discussed below account for these viewing environment effects on the CTF.

**2.4.1 Low-Pass Model.** Infante (1984) reports a statistically derived model of the CTF for human vision. The Infante 1984 model is given as

$$\text{CTF}(v) = b_0 \exp[b_1 v] \quad (\text{Eq. 19})$$

in which

$$b_0 = 7.6546310\text{E-}4 \text{ and}$$

$$b_1 = 0.166404.$$

Figure 1 presents a plot of the Infante 1984 model across the visual spatial frequency passband. The Infante model reportedly is a least-squares regression fit to an estimated average CTF for adults with normal visual capabilities. The original CTF data applies to viewing conditions in which

the display screen size is greater than 5 degrees of visual angle and the space-average luminance (i.e., adaptation level) is greater than 20 cd/m<sup>2</sup> (cf. Snyder, 1980, p. 213).

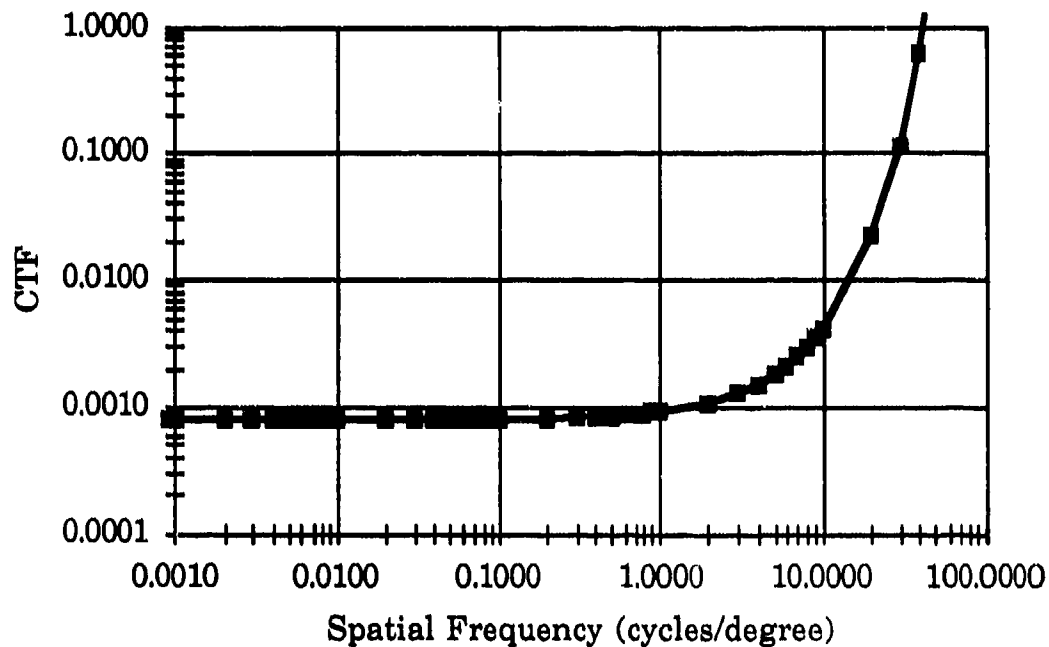


Figure 1. Infante (1984) model of the human visual contrast threshold function.

Interpretation of CTF data is straightforward. At each spatial frequency, the minimum modulation (contrast threshold) required by the human visual system to detect the pattern is plotted. A spatial frequency component possessing less than the required threshold modulation (i.e., a subliminal object) is not detected by an observer's visual system. On the other hand, a spatial frequency pattern possessing at least the threshold amount of modulation (i.e., a suprathreshold object) will be detected with a 0.5 or greater probability.

Although the Infante 1984 model is simple to compute, this model treats the CTF as a static quantity — that is, the model does not account for shifts in the CTF with changes in the viewing environment. Moreover, the

Infante 1984 model represents the visual system with a low-pass characteristic sensitivity to spatial frequency signals. In the visual science community, however, it generally is accepted that the human visual system possesses a band-pass characteristic sensitivity to spatial frequency patterns viewed under at least mesopic adaptation levels (Van Nes and Bouman, 1967). A low-pass characteristic sensitivity is obtained only by "correcting" CTFs for number of visible cycles in the lower (i.e., less than 8 cycles per degree) spatial frequency range (Hoekstra, van der Goot, van den Brink, and Bilsen, 1974).

**2.4.2 Band-pass Model.** Barten (1987) reports an empirical CTF equation that accounts for the effect of adaptation luminance on contrast thresholds. The Barten 1987 model is given as

$$CTF(v) = \frac{1}{b_0 v \exp[-b_1 v] \sqrt{1 + b_2 \exp[b_1 v]}} \quad (\text{Eq. 20})$$

in which

$$b_0 = 440 \left[ 1 + \frac{0.7}{L_{\text{adapt}}} \right]^{0.2},$$

$$b_1 = 0.30 \left[ 1 + \frac{100}{L_{\text{adapt}}} \right]^{0.15}, \text{ and}$$

$$b_2 = 0.06, \text{ and}$$

$L_{\text{adapt}}$  denotes the adaptation level of the observer in  $\text{cd/m}^2$  luminance units.

Figure 2 presents a plot of the Barten 1987 model across the entire visual spatial frequency passband for several adaptation luminance levels. The Barten 1987 model reportedly was developed from the CTF data of van Meeteren (1973).

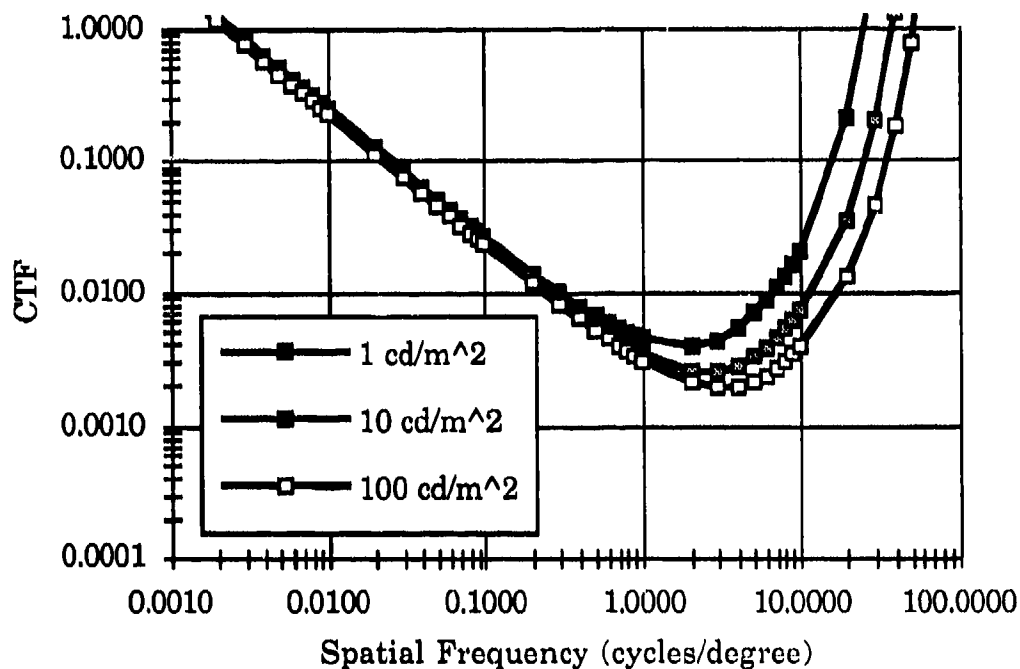


Figure 2. Barten (1987) model of the human visual contrast threshold function.

As seen in Figure 2, the Barten 1987 model computes a bandpass characteristic shape for the CTF. In other words, the CTF shape indicates a lower threshold for spatial frequency components in the 1–8 cycle per degree range as compared to spatial frequency components either below or above this passband range.

Additionally, the Barten 1987 model indexes the decrease in CTF with increasing adaptation level. In van Meeteren (1973), the term “adaptation

level" refers to the space-averaged luminance level (i.e., average luminance integrated over the entire two-dimensional extent of display area).

Since the Barten 1987 model is parameterized by a viewing environment variable, it does not treat the CTF as a static quantity. Thus, the Barten 1987 model is an improvement over the Infante 1984 model.

**2.4.3 Extended Band-pass Model.** Barten (1989a,b,c,d) extended his earlier CTF model to account for the effect of display size in addition to adaptation luminance on contrast thresholds. The Barten 1989 model is given as

$$CTF(v) = \frac{1}{b_0 v \exp[-b_1 v] \sqrt{1 + b_2 \exp[b_1 v]}} \quad (\text{Eq. 21})$$

in which

$$b_0 = \frac{540 \left[ 1 + \frac{0.7}{L_{\text{adapt}}} \right]^{0.2}}{1 + \frac{12}{\overline{DA}_{\text{deg}} \left[ 1 + \frac{v}{3} \right]^2}},$$

$$b_1 = 0.30 \left[ 1 + \frac{100}{L_{\text{adapt}}} \right]^{0.15}, \text{ and}$$

$$b_2 = 0.06.$$

Figure 3 presents a plot of the Barten 1989 model across the entire visual spatial frequency passband for several display sizes (i.e., average display area in degrees) and an adaptation luminance level of 10 cd/m<sup>2</sup>. The effect of display size on the CTF in Barten's 1990 model reportedly was developed from the data of Carlson (1982).

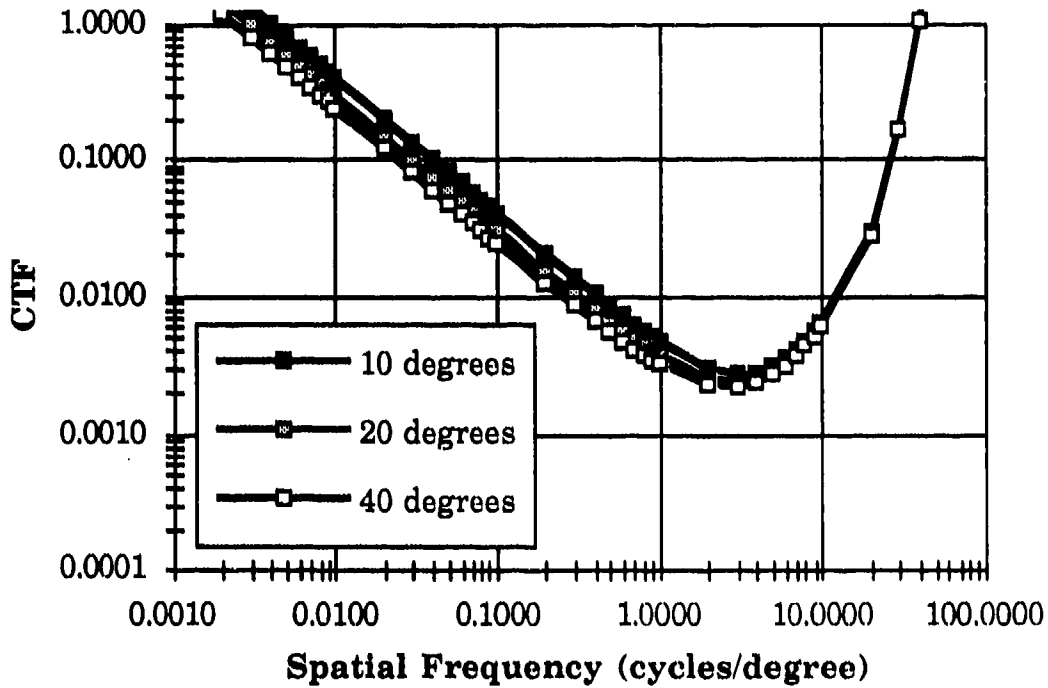


Figure 3. Barten (1989) model of the human visual contrast threshold function.

To illustrate the display size calculations involved in Barten's 1989 model, consider the following:

Assume that  $DD_{mm}$ ,  $D$ , and the width-to-height Aspect Ratio (AR) of the active screen area have been specified, where

$$AR = \frac{DW_{mm}}{DH_{mm}}. \quad (\text{Eq. 22})$$

Then, the linear extents of the screen area are computed as

$$DW_{mm} = AR \sqrt{\frac{DD_{mm}^2}{(AR^2 + 1)}} \quad (\text{Eq. 23})$$

and

$$DH_{mm} = \sqrt{\frac{DD_{mm}^2}{(AR^2 + 1)}} \quad (\text{Eq. 24})$$

Next, the linear size dimensions are converted into degree of visual angle units as

$$DW_{deg} = \frac{180}{\pi} \arctan\left[\frac{DW_{mm}}{D}\right] \quad (\text{Eq. 25})$$

and

$$DH_{deg} = \frac{180}{\pi} \arctan\left[\frac{DH_{mm}}{D}\right] \quad (\text{Eq. 26})$$

And, finally, the average display area is computed as

$$\overline{DA}_{deg} = \sqrt{DW_{deg} DH_{deg}} \quad (\text{Eq. 27})$$

Table 2 shows the results of the display size calculations for a 4:3 width-to-height aspect ratio display screen viewed from 762 mm (30 in). Note that display sizes shown in Table 2 approximate those used in Figure 3.

Table 2. Average Display Area Calculations

$DD_{mm}$	$\overline{DA}_{deg}$
178	9.2
406	20.3
889	38.8

The Barten 1989 model indexes the band-pass characteristic of the human visual system to spatial frequency signals. This model also indexes the decrease in contrast thresholds with increasing display size and increasing adaptation luminance. Thus, the Barten 1989 model is the most elaborate "engineering" model of human CTFs known to the authors.

It is important to note that the CTF models presented above produce nonsensical values greater than unity outside of the visual passband. Therefore, it is the responsibility of the user to handle these computational artifacts.

**2.4.4 CTF Model Verification and Selection.** Given the three CTF models reviewed above, it is instructive to examine the validity of the model values with respect to CTF data measured from human observers. For this purpose, the Barten 1987 and 1989 CTF model predictions were compared to the empirical CTF data obtained by van Meeteren (1973). The van Meeteren data show the effects of adaptation luminance (i.e., 0.0001, 0.001, 0.01, 0.1, 1.0, and 10.0  $\text{cd/m}^2$ ) on human CTFs for a 17 by 11 degree field of view. The Infante 1984 model was excluded from this validation test since it indexes "average" CTFs across viewing conditions.

For the model validation, CTF graphs reported by van Meeteren (1973) were enlarged through photocopying and, then, digitized into computer-readable format with a high-precision graphics touch tablet. Next, the Barten CTF 1987 and 1989 models were computed for the specified adaptation luminance levels. Numerical differences (i.e., percentage error) between van Meeteren's measured data and Barten's computed CTF values were assessed. Tables 3-A through 3-F present the numerical comparisons corresponding to adaptation levels of 0.0001, 0.001, 0.01, 0.1, 1.0, and 10.0  $\text{cd/m}^2$ , respectively.

Table 3-A. Comparison of Actual and Computed CTF Values (0.0001 cd/m<sup>2</sup> adaptation luminance)

Van Meeteren 1973		Barten 1987		Barten 1989	
Cyc/Deg	CTF	CTF	% Error <sup>1.</sup>	CTF	% Error <sup>1.</sup>
0.471	0.0999	0.0800	19.87	0.1080	-8.09
0.803	0.1236	0.0950	23.10	0.1197	3.13
1.945	0.2569	0.2640	-2.74	0.2846	-10.75
3.241	0.9131	0.7969	12.73	0.7809	14.47

Note 1. % Error =  $\frac{100[\text{CTF}_{\text{Measured}} - \text{CTF}_{\text{Computed}}]}{\text{CTF}_{\text{Measured}}}$

Table 3-B. Comparison of Actual and Computed CTF Values (0.001 cd/m<sup>2</sup> adaptation luminance)

Van Meeteren 1973		Barten 1987		Barten 1989	
Cyc/Deg	CTF	CTF	% Error	CTF	% Error
0.476	0.0333	0.0371	-11.59	0.0500	-50.35
0.821	0.0353	0.0368	-4.21	0.0462	-30.86
1.871	0.0710	0.0681	4.08	0.0740	-4.17
4.016	0.4467	0.2512	43.77	0.2375	46.83

Table 3-C. Comparison of Actual and Computed CTF Values ( $0.01 \text{ cd/m}^2$  adaptation luminance)

Van Meeteren 1973		Barten 1987		Barten 1989	
Cyc/Deg	CTF	CTF	% Error	CTF	% Error
0.470	0.0138	0.0189	-36.65	0.0255	-84.37
0.800	0.0155	0.0161	-4.27	0.0203	-31.43
1.898	0.0218	0.0216	0.91	0.0234	-7.32
4.048	0.0717	0.0567	21.03	0.0535	25.42
6.286	0.1442	0.1471	-2.02	0.1309	9.26
12.473	0.9307	2.9968	-222.01	2.5224	-171.03

Table 3-D. Comparison of Actual and Computed CTF Values ( $0.1 \text{ cd/m}^2$  adaptation luminance)

Van Meeteren 1973		Barten 1987		Barten 1989	
Cyc/Deg	CTF	CTF	% Error	CTF	% Error
0.458	0.0090	0.0106	-17.76	0.0144	-59.31
0.792	0.0073	0.0080	-9.51	0.0101	-38.23
1.851	0.0082	0.0078	4.30	0.0085	-4.15
3.958	0.0142	0.0150	-6.05	0.0143	-0.51
6.154	0.0297	0.0295	0.49	0.0263	11.28
13.826	0.1268	0.3518	-177.37	0.2946	-132.31
19.851	0.3678	3.1297	-750.89	2.5887	-603.80

Table 3-E. Comparison of Actual and Computed CTF Values ( $1.0 \text{ cd/m}^2$  adaptation luminance)

Van Meeteren 1973		Barten 1987		Barten 1989	
Cyc/Deg	CTF	CTF	% Error	CTF	% Error
0.466	0.0052	0.0069	-31.80	0.0093	-78.02
0.832	0.0042	0.0048	-13.63	0.0060	-42.36
1.900	0.0041	0.0038	7.77	0.0041	0.13
4.060	0.0056	0.0055	1.99	0.0052	7.50
6.158	0.0096	0.0089	7.53	0.0080	17.56
14.109	0.0329	0.0501	-52.49	0.0419	-27.61
19.211	0.0713	0.1701	-138.54	0.1408	-97.48
27.578	0.2558	1.4551	-468.80	1.1956	-367.38

Table 3-F. Comparison of Actual and Computed CTF Values ( $10.0 \text{ cd/m}^2$  adaptation luminance)

Van Meeteren 1973		Barten 1987		Barten 1989	
Cyc/Deg	CTF	CTF	% Error	CTF	% Error
0.471	0.0057	0.0058	-0.92	0.0078	-36.11
0.743	0.0042	0.0041	2.17	0.0052	-24.63
1.892	0.0029	0.0026	9.75	0.0028	2.18
4.097	0.0031	0.0028	9.71	0.0027	14.90
6.212	0.0051	0.0039	22.41	0.0035	30.89
13.963	0.0128	0.0133	-3.99	0.0111	12.94
19.361	0.0306	0.0311	-1.79	0.0257	15.75
27.264	0.0955	0.1210	-26.62	0.0994	-4.07
40.221	0.2498	1.3282	-431.65	1.0868	-335.03

Several points are noteworthy regarding the numerical comparisons tabulated above. First, it is appreciated that adaptation luminance levels within the range of  $0.0001 \text{ cd/m}^2$  to  $0.1 \text{ cd/m}^2$  rarely occur in real-world

display application environments. Rather, these extremely low adaptation levels are representative of controlled laboratory environments.

Second, the CTF values computed from Barten's 1987 and 1989 models exhibit consistent deviations from one another across the spatial frequency and adaptation luminance levels examined. Specifically, at low spatial frequencies, Barten's 1987 model computes smaller CTF values as compared to Barten's 1989 model. However, at high spatial frequencies, the converse trend is observed between Barten's 1987 and 1989 models.

Third, and most importantly, it can be seen from Tables 3-A through 3-F, that Barten's 1987 and 1989 CTF models fail to track the measured CTF well. In other words, the percent error statistic often ranges between 50% and 200% across the spatial frequencies within any adaptation level. It should be mentioned that log-log plots of these actual and computed values de-emphasize the magnitude of the error deviations (cf. Barten, 1989a,b,c,d, 1990a,b).

From these observations, the following recommendations are made regarding the use of CTF models in image quality evaluations. First, the Infante 1984 model should be excluded from general-purpose usage since it does not account for important viewing environment parameters (i.e., adaptation luminance and display size). Second, because Barten's 1987 model is not more accurate than his 1989 model, there is little reason to consider it for general-purpose usage. Finally, despite the errors observed in Table 3, Barten's 1989 model is recommended for general-purpose image quality computations pending the development of a more accurate CTF model. Additional comments to support these recommendations are presented in subsequent sections of the report.

### 3.0 METRIC COMPUTATIONS

This section of the report presents the image quality metric computations completed during the project. Computational conditions, metric value comparisons, and model parameters effects are discussed.

#### 3.1 STANDARD CONDITIONS FOR DISPLAY AND OBSERVER

To facilitate comparisons among the image quality metrics, it is convenient to define a set of standard display device and observer viewing conditions. Since an underlying objective of this work was to assess the utility of the metrics for real-world display evaluation projects, the standard conditions established herein reflect contemporary visual display systems and their application environments. Table 4 lists the parameter values for the standard display device and observers conditions, hereafter referred to simply as the *standard conditions*.

Table 4. Parameter Settings for Standard Conditions

Display Device Parameters	Value
Device Type	Monochrome CRT
Screen Height	280 mm (11.02 in)
Screen Width	380 mm (14.96 in)
Pixels Per Height	1024
Pixels Per Width	1280
Pixel Shape	Gaussian
Pixel Width (FWHM)	0.300 mm (0.012 in)
Peak Luminance	100 cd/m <sup>2</sup> ( 29.19 fL)
Reflected Glare	20 cd/m <sup>2</sup> (5.84 fL)

Observer Parameters	Value
Viewing Distance	500 mm (19.69 in)
Adaptation Luminance	20 cd/m <sup>2</sup> (5.84 fL)

## 3.2 BASELINE VALUES FOR IMAGE QUALITY METRICS

The MTFA, ICS, and SQRI metrics were computed for the standard conditions using the *Mathematica*<sup>TM</sup> algorithms. Since these algorithms use an adaptive integration technique as well as high numerical precision (15 digits) and accuracy (10 digits), the *Mathematica*<sup>TM</sup> results were interpreted as near-exact solutions for the image quality metric equations.

**3.2.1 MTFA Metric.** The MTFA values computed for the standard conditions are listed in Table 5. The three MTFA values shown in Table 5 represent alternate metric solutions corresponding to each of the CTF models discussed in §2.4. Across the CTF models, the range of MTFA values is small (i.e., 0.028951 or 0.3% of the minimum MTFA value). This finding indicates that the MTFA metric is robust (insensitive) to changes in CTF shape, at least for the standard conditions used in the computations. This finding, however, is not surprising since the MTFA metric value is determined primarily by the subtraction of small magnitude CTF values from relatively much larger MTF values at low spatial frequencies.

Table 5. Baseline MTFA Values for Standard Conditions<sup>1</sup>.

CTF Model	MTFA
Infante 1984	7.958642
Barten 1987	7.929691
Barten 1989	7.940036

Note 1. Metric values listed were determined with lower ( $v_l$  from Eq. 15b) and upper ( $v_u$  from Eq. 8b) limits of integration equal to 0.026856 and 14.697516 cycles per degree of visual angle, respectively.

Figure 4 shows the MTF and Barten 1989 CTF curves used in the MTFA metric computation for the standard conditions. Note that these curves cross one another at 25.130257 cycles per degree of visual angle.

However, the upper limit of integration ( $\nu_u$ ) was set to the lower value of 14.697516 as determined from Eq. 8b. The data shown in Figure 4 indicate that the image quality level defined by the standard conditions corresponds to a display-limited system, since the MTF-CTF crossover frequency (i.e., 25.130257 cycles per degree of visual angle) is greater than the Nyquist limit of the display system (i.e., 14.697516 cycles per degree of visual angle).

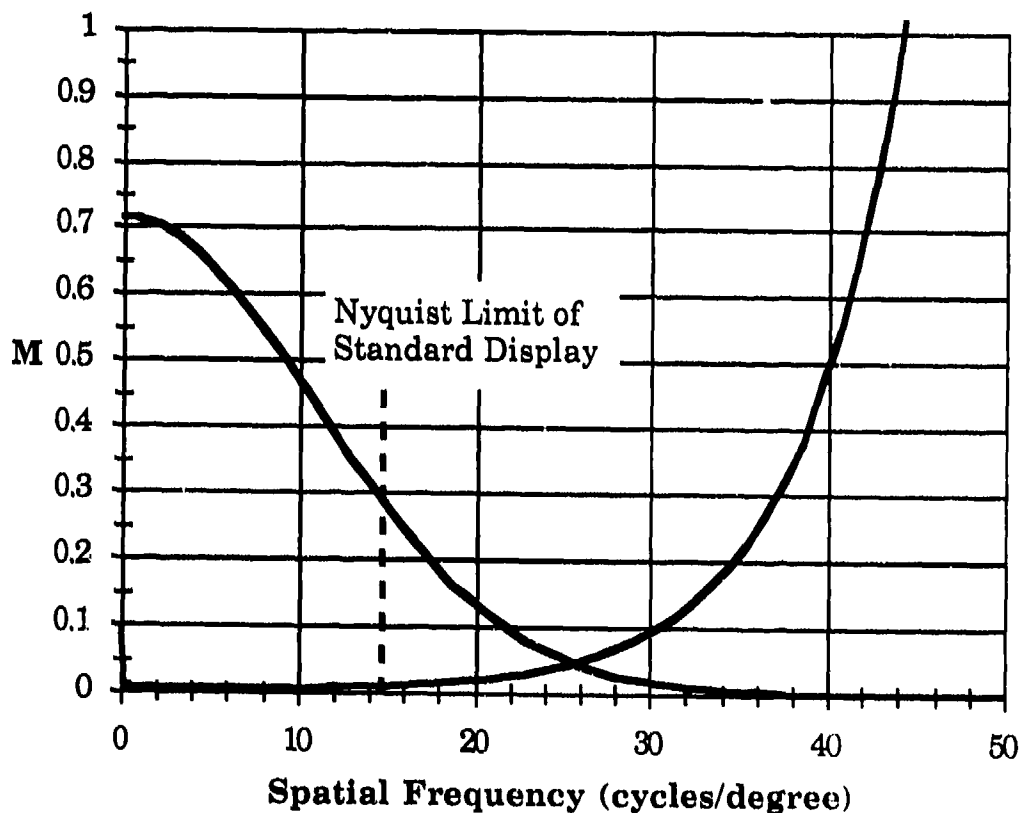


Figure 4. MTF and Barten 1989 CTF used in MTFA evaluation of standard conditions.

Figure 5 shows the MTFA metric integrand (i.e.,  $[MTF(\nu) - CTF(\nu)]$ , in which the CTF is determined by Barten's 1989 model) used in the evaluation of the standard conditions. These data indicate the amount of perceivable modulation at each spatial frequency that contributes to the total

MTFA metric value. Under the standard conditions, there is more perceivable modulation at lower spatial frequencies as compared to higher spatial frequencies.

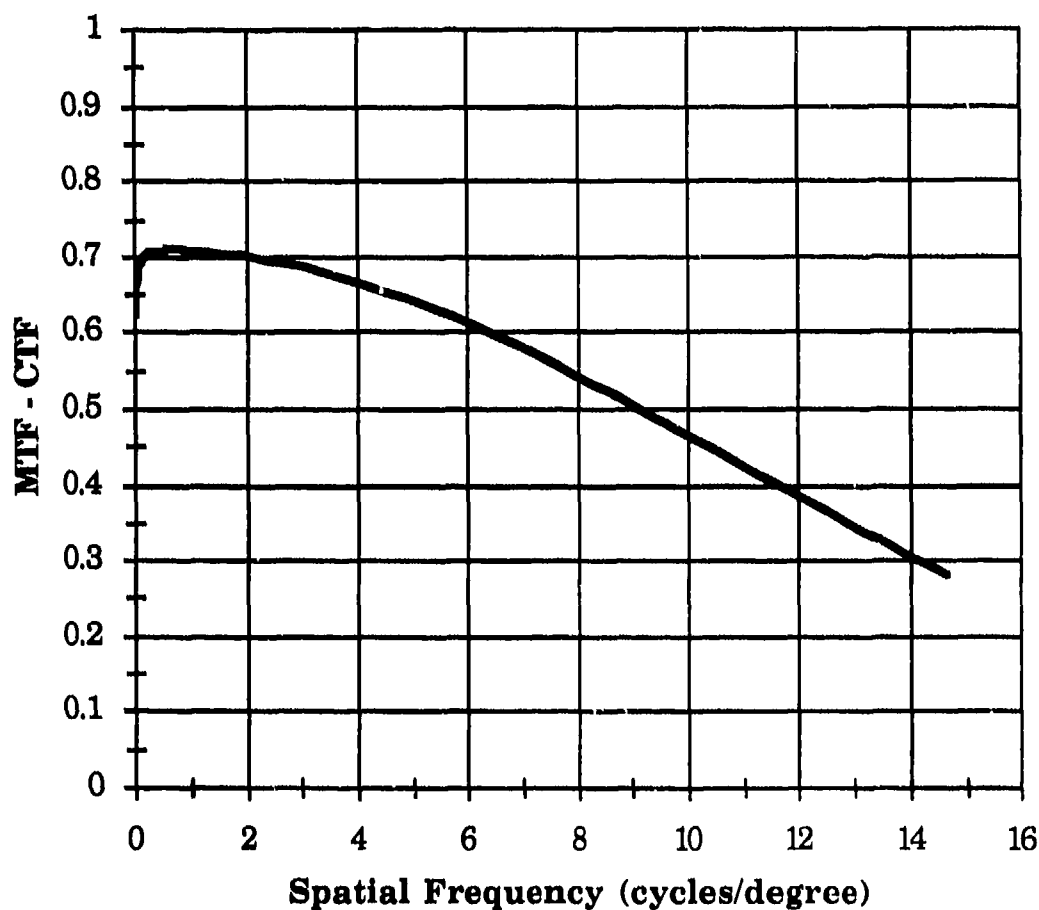


Figure 5. MTFA integrand function used in evaluation of standard conditions.

**3.2.2 ICS Metric.** Computed ICS values for the standard conditions are listed in Table 6. Again, the three ICS values correspond to separate calculations using each of the CTF models discussed in §2.4. From these computations, clearly the ICS values vary substantially across the CTF

models (i.e., range is 2261.02774 ICS units or 102% of the minimum ICS value).

Table 6. Baseline ICS Values for Standard Conditions<sup>1</sup>.

CTF Model	ICS
Infante 1984	4475.452504
Barten 1987	2214.424764
Barten 1989	2527.491690

Note 1. Metric values listed were determined with lower ( $v_l$  from Eq. 15b) and upper ( $v_u$  from Eq. 8b) limits of integration equal to 0.026856 and 14.697516 cycles per degree of visual angle, respectively.

The variance in ICS values shown in Table 6 stems from two sources. The first source involves the differently-shaped CTF (or, more appropriately for the ICS metric, differently-shaped CSF) curves computed by the three perceptual models. Specifically, recall that the Infante 1984 model computes a low-pass CTF, whereas Barten's 1987 and 1989 models compute band-pass CTFs. In other words, the CTF values computed by the Infante 1984 model at low spatial frequencies are much smaller than the corresponding values computed by Barten models. Therefore, the Infante-based ICS value is expected to be larger than either of the Barten-based ICS values.

The second source of ICS variance involves the mathematical operation used to combine the MTF and CTF data. That is, the ICS metric multiplies the MTF and inverse CTF on a point-by-point (pair-wise) basis. Since the operation of multiplication (division) is non-linear with respect to addition (subtraction), ICS values are influenced more by numerically large MTF-CSF pair values than by small MTF-CSF pair values. This analytical property contributes to the larger ICS value obtained with the Infante 1984 model in comparison to the two Barten models.

Figure 6 shows the Barten 1989 CSF curve used in the ICS metric computation for the standard conditions. As mentioned earlier, the CSF is the reciprocal of the CTF. It should be mentioned that the CSF shown in Figure 6 also was used in the SQRI metric computations presented below.

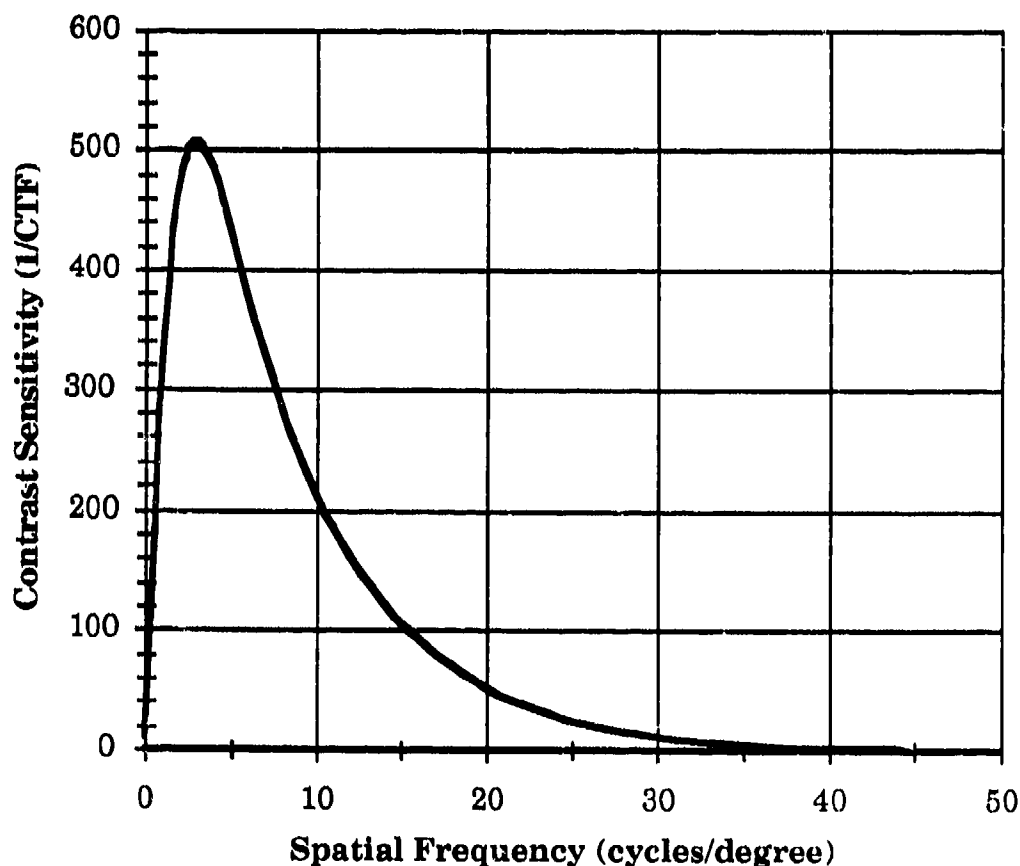


Figure 6. Barten 1989 CSF used in ICS and SQRI evaluation of standard conditions.

Figure 7 shows the ICS metric integrand (i.e.,  $[MTF(v) CSF(v)]$ , in which CSF is determined by Barten's 1989 model) computed for the standard conditions. These data indicate the amount of "visually-weighted" modulation at each spatial frequency that contributes to the total ICS metric value. For the standard conditions, the ICS metric value is determined

primarily by visually-weighted modulation within the spatial frequency passband of 1-5 cycles per degree of visual angle.

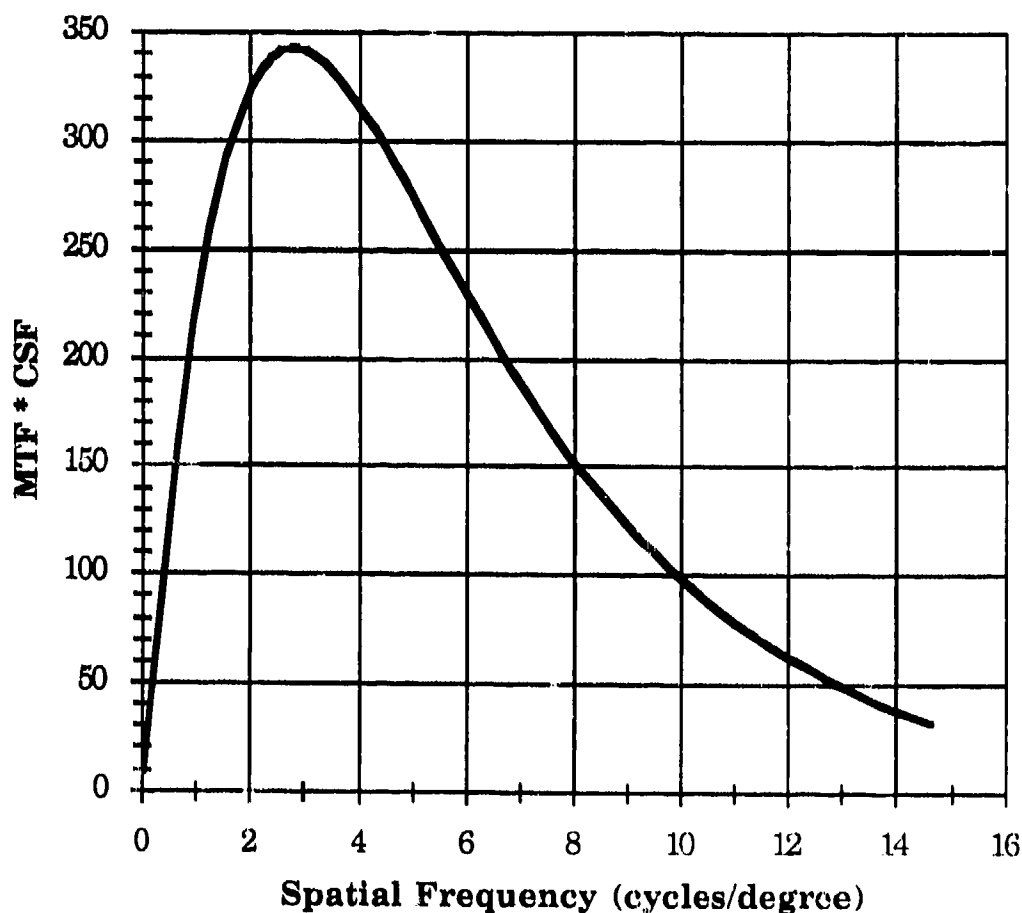


Figure 7. ICS integrand used in evaluation of standard conditions.

**3.2.3 SQRI Metric.** Computed SQRI values for the standard conditions are listed in Table 7. Once again, the three SQRI values correspond to metric calculations using each of the CTF models discussed in §2.4. The range of SQRI values across these CTF models is quite large (i.e., 137.606585 or 148% of the minimum SQRI value). As discussed for ICS metric, the variation in SQRI metric values stems from differences in the

CSF shape (i.e., low-pass versus band-pass perceptual models) as well as the multiplicative operations performed to combine the MTF and CSF values.

Table 7. Baseline SQRI Values for Standard Conditions<sup>1</sup>.

CTF Model	SQRI
Infante 1984	232.692399
Barten 1987	95.085814
Barten 1989	97.389434

Note 1. Metric values listed were determined with lower ( $v_l$  from Eq. 15b) and upper ( $v_u$  from Eq. 8b) limits of integration equal to 0.026856 and 14.697516 cycles per degree of visual angle, respectively.

The MTF curve used in the SQRI metric computation is shown in Figure 4 above, whereas the CSF curve is shown in Figure 6 above.

Figure 8 shows the SQRI integrand (i.e.,  $\frac{1}{v \ln 2} \sqrt{\frac{MTF(v)}{CTF(v)}}$ , in which the CTF was determined by Barten's 1989 model) used in the evaluation of the standard conditions. From Figure 8 it can be seen that the SQRI metric value is determined substantially by modulation at very low spatial frequencies. Indeed, the SQRI metric appears almost entirely dependent upon modulation below 1 cycle per degree of visual angle. The behavior of the SQRI integrand stems from the  $\left[\frac{1}{v}\right]$  term in the integrand — that is, the SQRI scaling factor approaches positive infinity as spatial frequency approaches zero. Thus, the SQRI metric indexes MTF and/or CTF changes at low spatial frequencies and de-emphasizes high frequency changes associated with these functions.

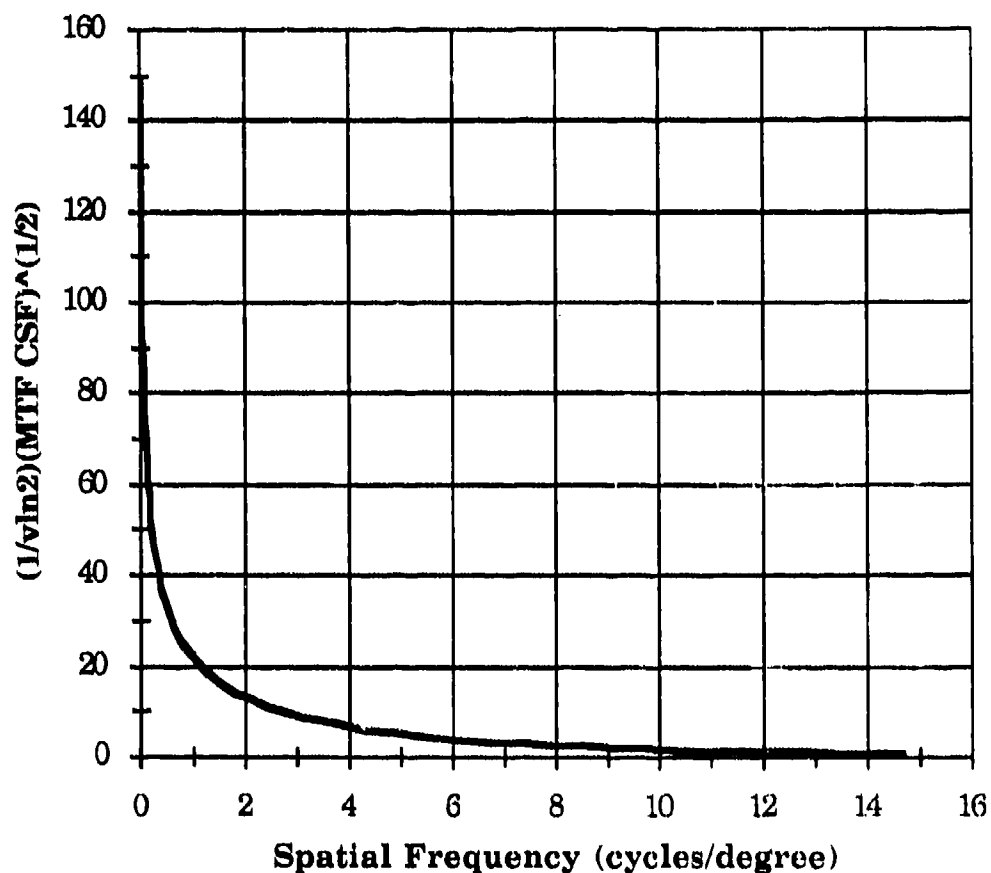


Figure 8. SQRI integrand used in evaluation of standard conditions.

### 3.3 COMPARISON OF NORMALIZED INTEGRANDS

To provide an initial summary of the analytical properties of the MTFA, ICS, and SQRI metrics, the normalized integrands of each metric are examined. Figure 9 plots the normalized metric integrands for the standard conditions as determined with Barten's 1989 CTF model. Since the MTF and CTF are constant across the integrand curves, the relative amplitude differences (i.e., vertical-axis disparities) among the curves at each spatial frequency reflects how the metrics differ in their "utilization" of MTF and CTF information.

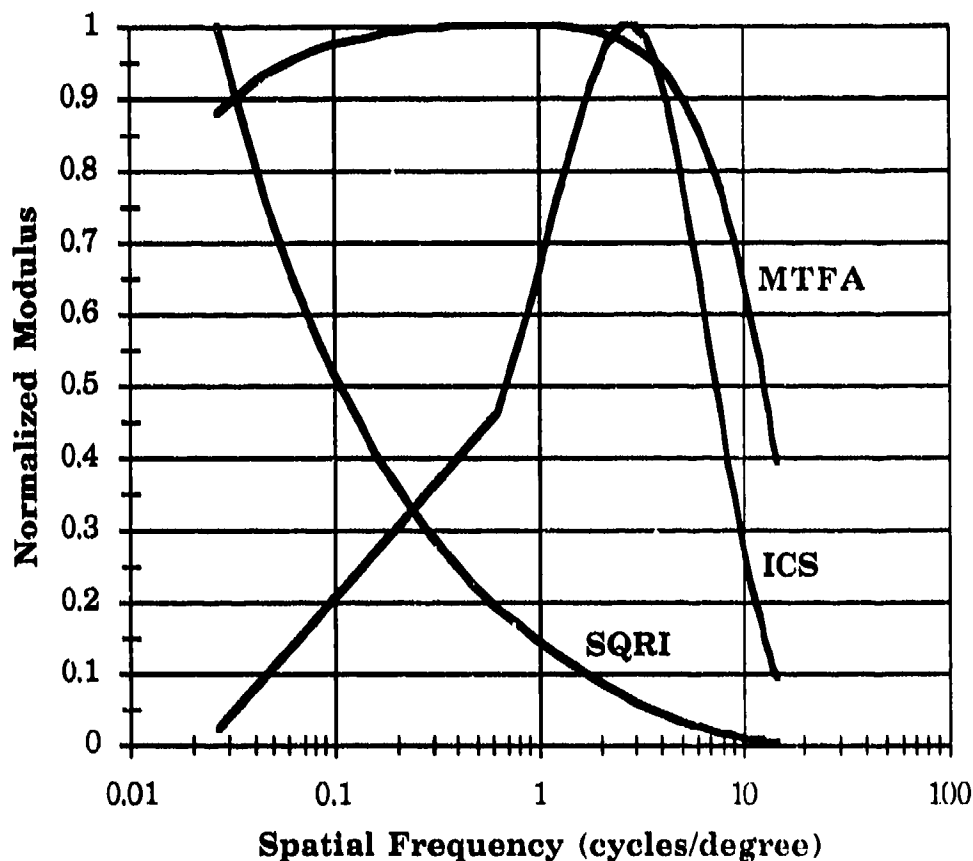


Figure 9. Normalized integrands for MTFA, ICS, and SQRI metrics used in evaluation of standard conditions.

Several properties of the image quality metrics for the standard conditions are evident in Figure 9. First, the MTFA metric is driven by MTF and CTF information within the 0.03–2.0 cycles per degree of visual angle passband. Second, the ICS metric integrand possesses a high-pass characteristic shape, indicating that it emphasizes MTF and CTF information near 3.0–4.0 cycles per degree of visual angle. Third, the SQRI metric integrand possesses a low-pass characteristic indicating that it emphasizes MTF and CTF information below 0.1 cycles per degree of visual angle.

### 3.4 MAXIMUM VALUES FOR IMAGE QUALITY METRICS

The numerical properties of the MTFA, ICS, and SQRI image quality metrics are explored further by determining their maximum values using each of the CTF models. The maximum value computations were performed for the standard conditions, with exceptions noted as follows. First, adaptation luminance level was set to an extremely high value (i.e., 100,000  $\text{cd/m}^2$ ) to increase utilization of MTF information in the metric computations. Second, the average display area was set to an extremely large value (i.e., 100  $\text{degree}^2$ ) to increase the spatial frequency integration range. Third, display resolution and addressability were set very high to produce a MTF of unity across the metric integration range. All other metric model parameters are defined as listed under the standard conditions.

Table 8 lists the maximum metric values computed with the three CTF models. As expected, the CTF models lead to different results. The Infante 1984 model produces higher values than Barten's models because it does not roll-off the CTF at lower spatial frequencies. The Barten 1989 model produces higher values than does the Barten 1987 model since it accounts for the effect of display size.

The maximum metric values serve as reference points for subsequent metric computations. That is, since alternate algorithms can be employed to determine metric quantities, the maximum value listed in Table 8 provides guidelines to assess computational errors for the standard conditions.

Table 8. Maximum Values for MTFA, ICS, and SQRI Metrics

CTF Model	MTFA	ICS	SQRI
Infante 1984	37.086425	7135.385204	280.329158
Barten 1987	50.549776	5686.687853	130.465216
Barten 1989	52.122453	6844.725702	140.879547

### 3.5 SENSITIVITY TO PARAMETER CHANGES

The primary use of image quality metrics by display engineers is to predict the impact of display design decisions on image quality. In this section, the image quality metrics are examined across parametric manipulations of the display device and observer parameters. The phrase "parametric manipulation" does not imply "factorial manipulation" of the relevant parameters. Rather, the parametric manipulations presented herein examine effects of the principle parameters at fixed or constant levels of other parameters. The effort required to examine joint or interaction effects among display device and observer parameters is reserved for future projects.

The computational algorithms used to generate the following results differ from the *Mathematica*<sup>TM</sup> algorithms used in previous sections of the report. For the following parametric manipulations, the C-language algorithms implemented on the Apple Macintosh and IBM PS-2 microcomputers were employed. The C-language algorithms exhibit greater computational speed than the *Mathematica*<sup>TM</sup> algorithms, and, thus, allowed parametric manipulations to be completed without excessive computer time. Extensive efforts were made to verify the accuracy of the C-language programs by comparing selected results with their corresponding *Mathematica*<sup>TM</sup> computations.

As explained in a later section of this report, several computational factors influence the accuracy of metric computations when using tabulated data arrays. For all parametric manipulations, several iterations of the metric computations were completed before selecting the "optimal" combination of computational factors that produce convergent metric values.

**3.5.1 Display Size.** The effect of display size on image quality is indexed in the image quality metrics by manipulation of the CTF (Barten's 1989 model only) as well as the lower limit of integration. In general, CTF values and the lower limit of integration decrease with increasing display size. As mentioned in §2.4.3, the display size value used in Barten's 1989

model equals the geometric mean of the horizontal and vertical screen extents, expressed in degrees of visual angle.

To examine the effect of display size on image quality, five different screen sizes were examined under the standard conditions. Table 9 lists the model parameters manipulated in this analysis, as well as those parameters held fixed at the levels defined by the standard conditions. For the numerical analysis, a 2048-element data array was used to tabulate a 76.8 mm horizontal simulated scan of the display screen.

Figures 10-A through 10-C show the effect of display size upon image quality as computed by the MTFA, ICS, and SQRI metrics, respectively. The ordinate (i.e., y-axis) scale range has been adjusted to about 20% of the maximum value determined for each metric under the standard conditions. That is, the MTFA range is 10 units (20% of 50), ICS range is 1400 units (20% of 7000), and the SQRI range is 30 units (20% of 150). This scaling procedure is intended to facilitate the comparison of sensitive to changes in display size across the three image quality metrics.

Table 9. Parameters for Display Size Computations.

Manipulated Parameters	Average Display Area (Degrees <sup>2</sup> )				
	13.84	25.81	33.00	45.00	53.95
Screen Height (mm)	107	210	280	500	600
Screen Width (mm)	142	280	380	500	800
Pixels Per Height	391	768	1024	1829	2194
Pixels Per Width	478	943	1280	1684	2695

Fixed Parameters	
Device Type	Monochrome CRT
Pixel Shape	Gaussian
Pixel Width	0.300 mm
Peak Luminance	100 cd/m <sup>2</sup>
Reflected Glare	20 cd/m <sup>2</sup>
Viewing Distance	500 mm
Adaptation Luminance	20 cd/m <sup>2</sup>

As seen in Figures 10-A through 10-C, the MTFA metric values remain relatively constant as display size increases, whereas both ICS and SQRI metric values increase with increasing display size. The change in metric value is 0.44% (7.902 vs. 7.937) for MTFA, 11.91% (2318.8 vs. 2595.2) for ICS, and 21.65% (86.14 vs. 104.79) for SQRI. These findings stem from the fact that the MTFA metric responds to changes in the CTF through a linear subtraction operation, while the ICS and SQRI respond to CTF changes through nonlinear multiplication operations.

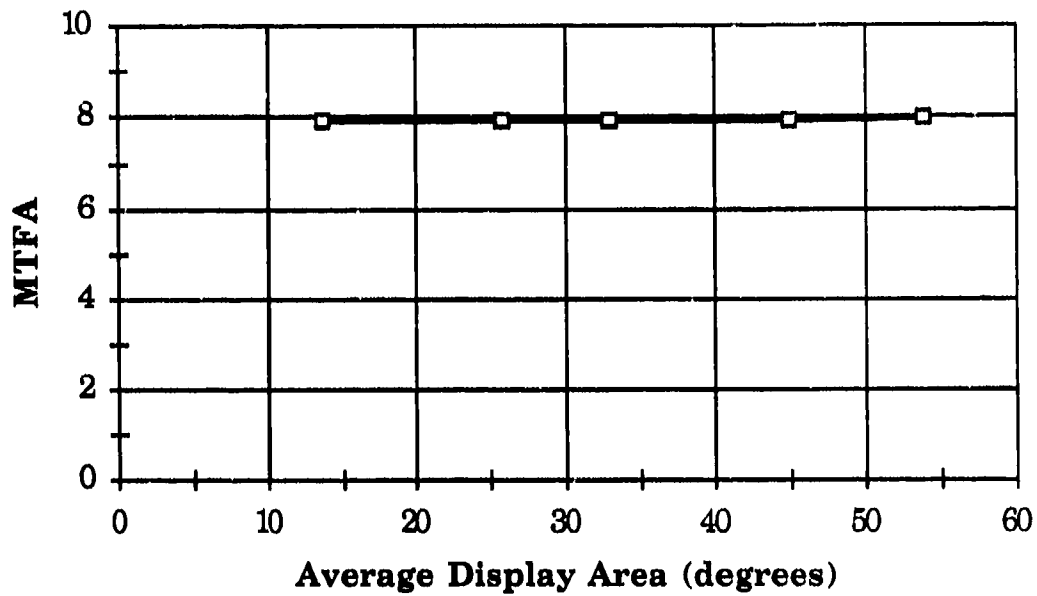


Figure 10-A. Effect of display size on the MTFA image quality metric.

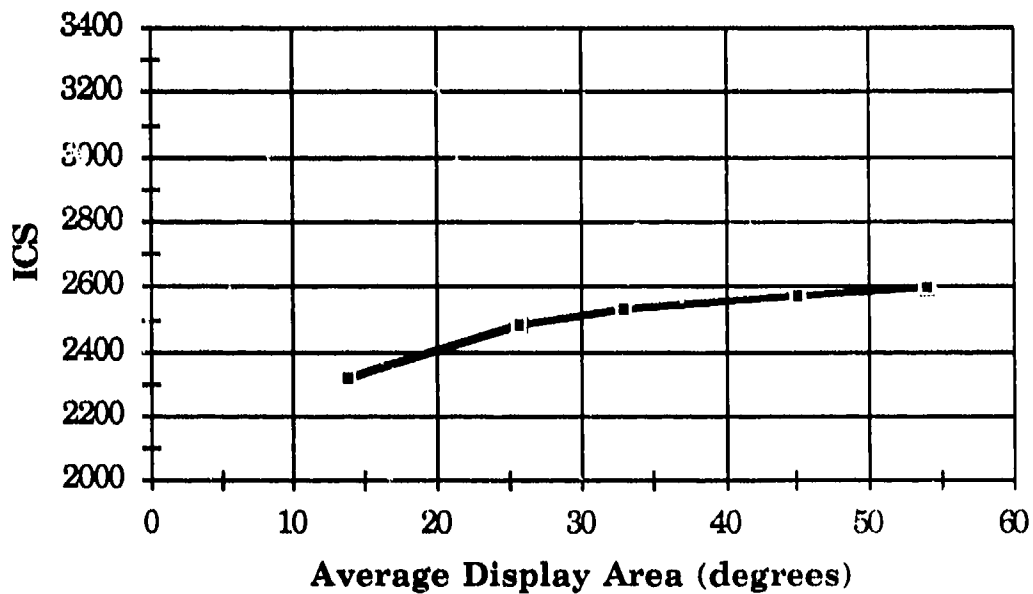


Figure 10-B. Effect of display size on the ICS image quality metric.

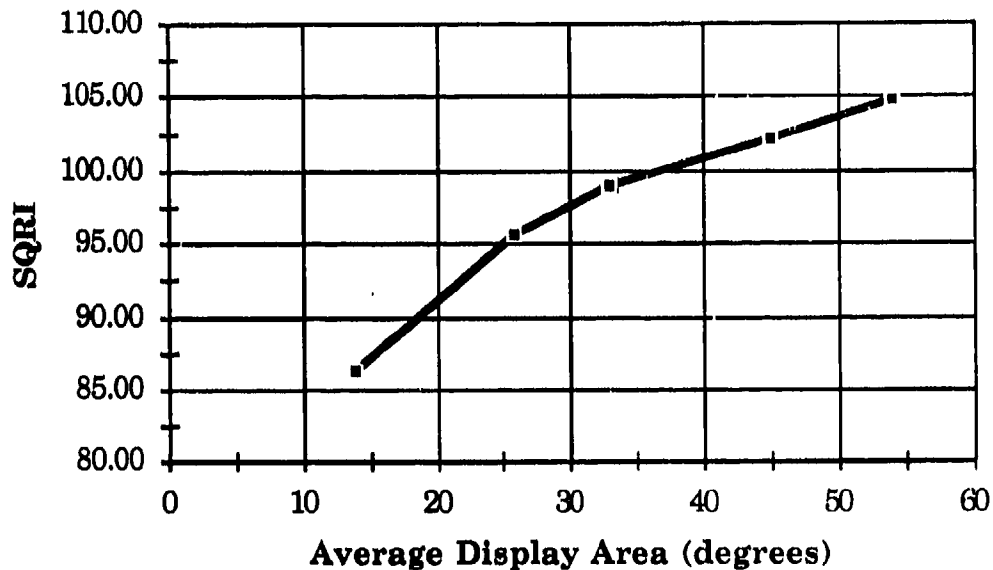


Figure 10-C. Effect of display size on the SQRI image quality metric.

**3.5.2 Resolution/Addressability.** The effect of display resolution and addressability on image quality is indexed in the image quality metrics by manipulation of pixel width and the Nyquist (upper) limit of integration. In general, the area under the MTF increases with smaller pixel widths (i.e., increasing resolution) and smaller pixel separations (i.e., increasing addressability). For most actual display systems, however, pixel width and addressability are not orthogonal parameters. That is, pixel width and pixel addressability typically are varied together — as pixel width decreases, pixel addressability increases. A commonly-practiced engineering guideline for the design of monochrome CRT displays is to maintain resolution approximately equal to addressability, as expressed in the following Resolution-to-Addressability Ratio (RAR) criterion (Murch and Beaton, 1986):

$$\frac{\text{Pixel Resolution}}{\text{Pixel Addressability}} \approx 1 \quad (\text{Eq. 28})$$

To examine the effect of display resolution and addressability on image quality, 10 levels of pixel width were examined under the standard

conditions. For each pixel width level, the RAR value was maintained at a constant 1.01; thus, the number of pixels varied along with pixel width. Table 10 lists the model parameters manipulated in this analysis, as well as those parameters held fixed at the levels defined by the standard conditions. For the numerical analysis, a 2048-element data array was used to tabulate the simulated scan data; however, the effective period of the measurement increased from 25.6 mm to 256 mm with increasing pixel width.

Table 10. Parameters for Resolution/Addressability Computations

Manipulated Parameters	Resolution (mm - FWHM)				
	0.1	0.2	0.3	0.4	0.5
Pixels Per Height	3072	1536	1024	768	614
Pixels Per Width	3840	1920	1280	960	768

Manipulated Parameters (cont.)	Resolution (mm - FWHM)				
	0.6	0.7	0.8	0.9	1.0
Pixels Per Height	512	439	384	341	307
Pixels Per Width	640	549	480	427	384

Fixed Parameters	
Device Type	Monochrome CRT
Pixel Shape	Gaussian
Screen Height	280 mm
Screen Width	380 mm
Peak Luminance	100 cd/m <sup>2</sup>
Reflected Glare	20 cd/m <sup>2</sup>
Viewing Distance	500 mm
Adaptation Luminance	20 cd/m <sup>2</sup>

Figures 11-A through 11-C show the effect of resolution and addressability upon image quality as computed by the MTF<sub>A</sub>, ICS, and SQRI

metrics, respectively. The ordinate (i.e., y-axis) range has been adjusted to about 42% of the maximum value of each metric under the standard conditions. This scaling procedure is intended to facilitate the comparison of cases sensitive to changes in display resolution/addressability across the three image quality metrics.

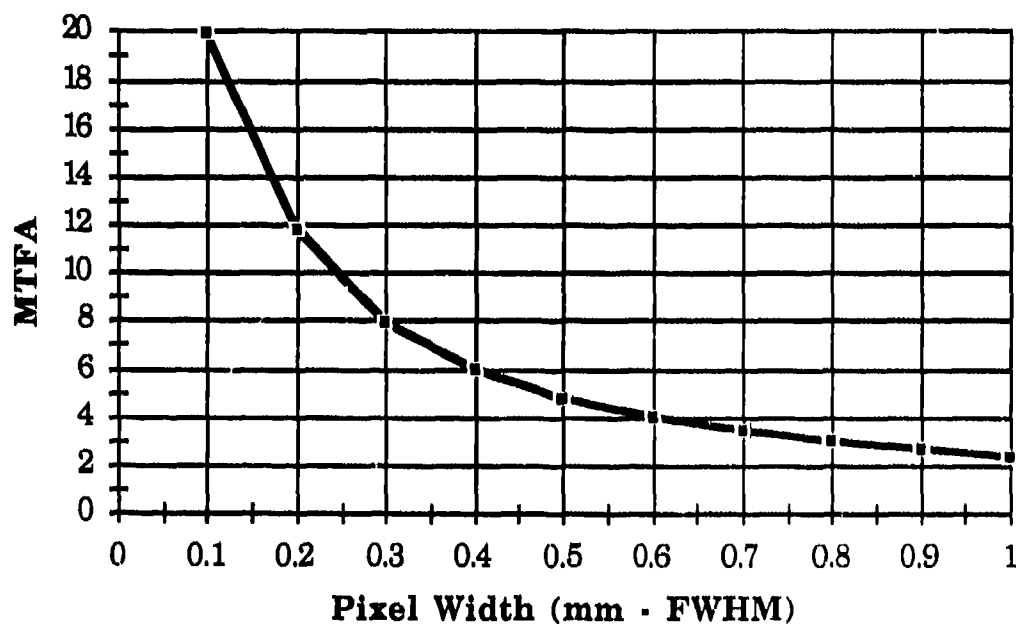


Figure 11-A. Effect of resolution/addressability on the MTFA image quality metric.

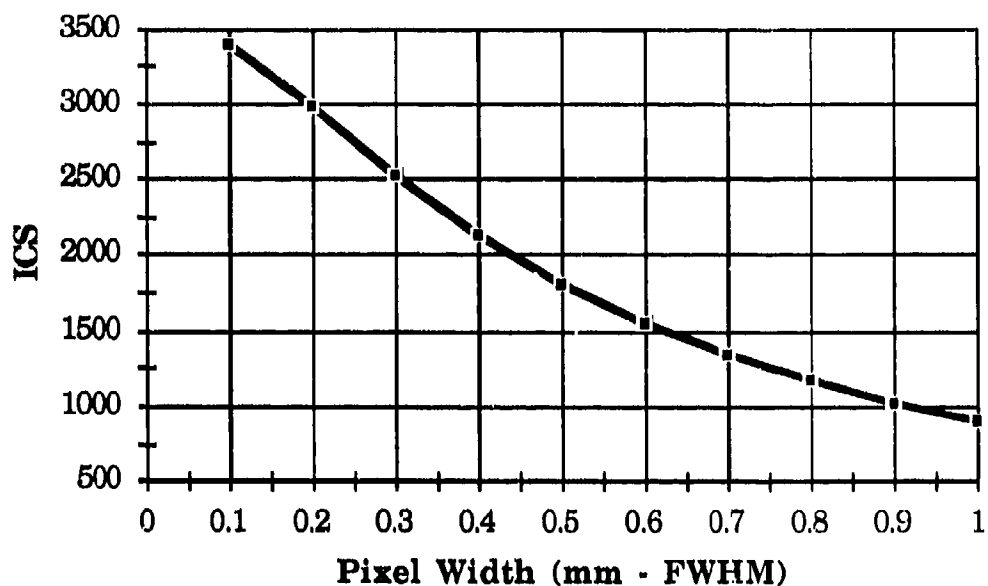


Figure 11-B. Effect of resolution/addressability on the ICS image quality metric.

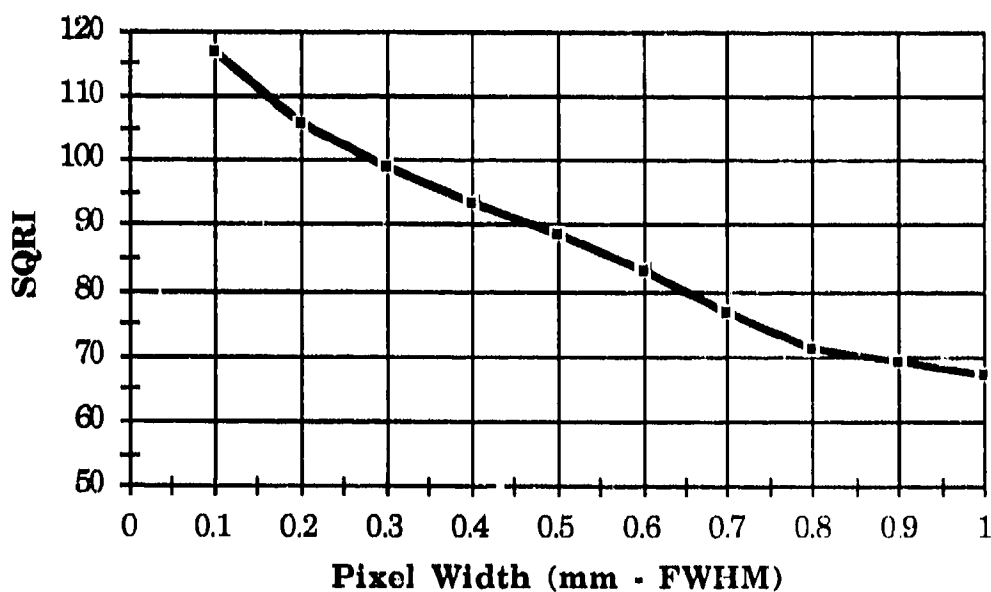


Figure 11-C. Effect of resolution/addressability on the SQRI image quality metric.

As seen in Figures 11-A through 11-C, the MTFA, ICS, and SQRI metric values decrease with increasing pixel width. The change in metric value is 746.08% (2.357 vs. 19.942) for MTFA, 278.95% (895.6 vs. 3393.9) for ICS, and 74.37% (67.02 vs. 116.86) for SQRI. These findings illustrate the fact that all three metrics are sensitive to changes in the resolution/addressability of the display system.

**3.5.3 Peak, Glare, and Adaptation Luminance.** The effects of peak display luminance, reflected glare luminance, and adaptation luminance on image quality are indexed in the image quality metrics by manipulation of the display MTF as well as observer CTF.

In general, peak display luminance and reflected glare luminance exert interdependent effects on the depth of modulation available from a display screen. Specifically, with increasing peak display luminance, the effect of increasing reflected glare luminance (i.e., loss of modulation) is reduced. The joint effects of peak luminance and reflected glare luminance are taken into account in the image quality metrics by a scaling factor applied to the display MTF, as given by Eq. 17. As a matter of convenience, though, the effects of peak display luminance and reflected glare luminance can be parameterized by a simple Peak-to-Glare Ratio (PGR), given as:

$$\text{PGR} = \frac{L_{\text{peak}}}{L_{\text{reflected glare}}} \quad (\text{Eq. 29})$$

Additionally, the observer CTF is affected by adaptation luminance. That is, with increasing adaptation levels, observer's CTF decreases. Barten's 1987 and 1989 CTF models are parameterized by adaptation luminance to account for this general perceptual effect. Unfortunately, there are theoretical issues yet to be solved in this aspect of image quality modelling.

A precise definition of adaptation luminance is not available for use in image quality metric computations. From visual science experiments (e.g.,

van Meeteren, 1973), an observer's CTF is known to decrease with increasing space-averaged luminance across sinusoidal grating patterns. However, the measurement of space-averaged luminance does not generalize uniquely to scenes of varying textual, graphical, and pictorial content. Thus, some researchers adopt a peak display luminance-based index (cf., Westerink and Roufs, 1989) of CTF adaptation level, while other workers adopt an average scene luminance-based index (cf., Barten, 1989a,b,c,d).

Moreover, it is logical that reflected glare luminance, in addition to peak display (or average scene) luminance, contributes to CTF adaptation level. Since luminance intensity of light sources combine in an additive manner, reflected glare luminance can be expected to add to the luminance of visual scenes, and, thereby, increase CTF adaptation levels. The relationships among peak (average) luminance, reflected glare luminance, and CTF adaptation level have not been examined through visual science experiments.

Due to the unclear luminance-based influences upon CTF adaptation level, the effects of peak display luminance and reflected glare luminance are examined separately from the effect of adaptation luminance.

To study the effects of display peak display luminance and reflected glare luminance on image quality, 10 levels of reflected glare luminance were examined under the standard conditions. For each reflected glare luminance level, the peak display luminance was maintained at a constant  $100 \text{ cd/m}^2$ . Table 11 lists the model parameters manipulated in this analysis, as well as those parameters held fixed at the levels defined by the standard conditions. For the numerical analysis, a 2048-element data array was used to tabulate the simulated scan data.

Table 11. Parameters for Peak-To-Glare Luminance Ratio Computations

Manipulated Parameters	Peak-To-Glare Luminance Ratio				
	0.0	0.2	0.4	0.6	0.8
Reflected Glare ( $\text{cd/m}^2$ )	0	20	40	60	80

Manipulated Parameters (cont.)	Peak-To-Glare Luminance Ratio				
	1.0	1.2	1.4	1.6	1.8
Reflected Glare ( $\text{cd/m}^2$ )	100	120	140	160	180

Fixed Parameters	
Device Type	Monochrome CRT
Pixel Shape	Gaussian
Screen Height	280 mm
Screen Width	380 mm
Pixels Per Height	1024
Pixels Per Width	1280
Peak Luminance	$100 \text{ cd/m}^2$
Viewing Distance	500 mm
Adaptation Luminance	$20 \text{ cd/m}^2$

Figures 12-A through 12-C show the effect of PGR on image quality as computed by the MTFA, ICS, and SQRI metrics, respectively. The ordinate (i.e., y-axis) range has been adjusted to about 50% of the maximum value determined for each metric under the standard conditions.

As seen in Figures 12-A through 12-C, the MTFA, ICS, and SQRI metric values decrease with increasing peak-to-glare luminance ratio. The change in metric value is 370.46% (2.366 vs. 11.131) for MTFA, 359.99% (768.9 vs. 3536.9) for ICS, and 114.48% (54.55 vs. 117.00) for SQRI. These findings illustrate the fact that all three metrics are sensitive to changes in the resolution/addressability of the display system.

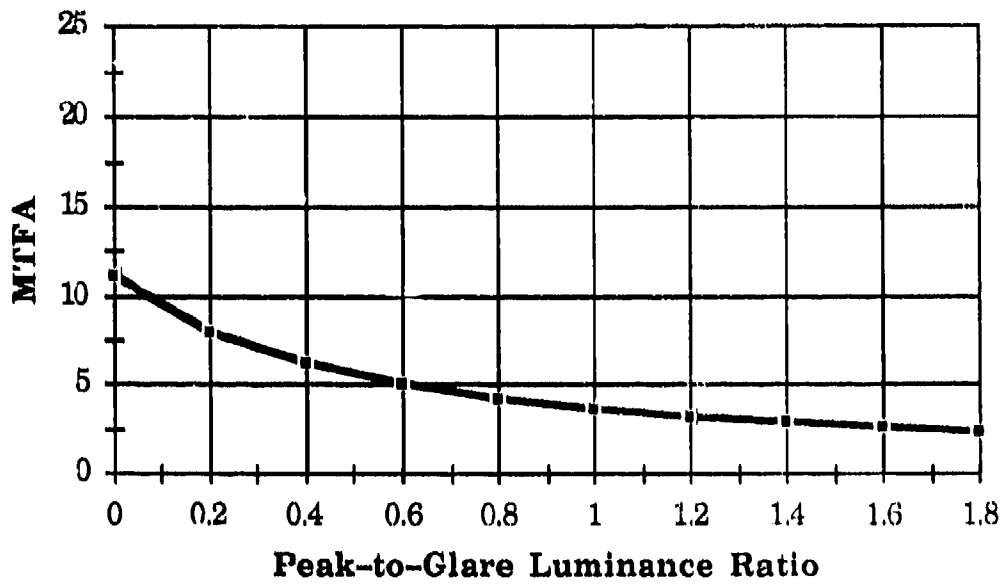


Figure 12-A. Effect of peak-to-glare luminance ratio on the MTFA image quality metric.

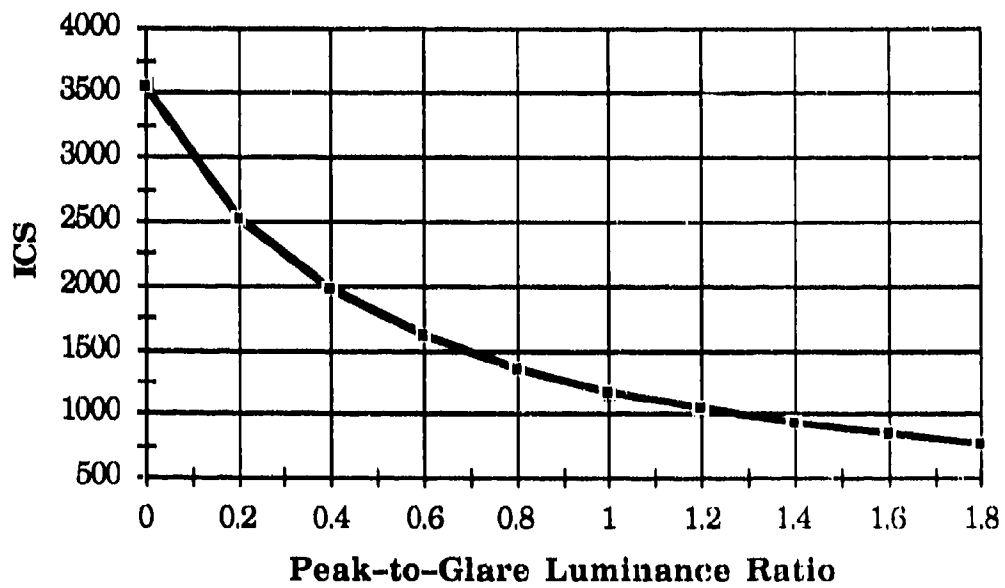


Figure 12-B. Effect of peak-to-glare luminance ratio on the ICS image quality metric.

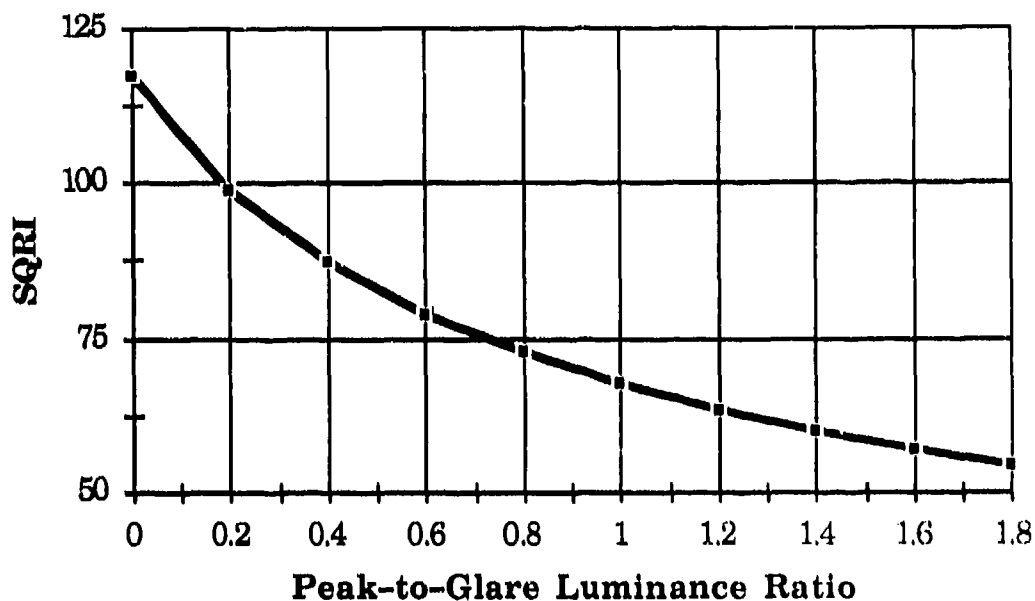


Figure 12-C. Effect of peak-to-glare luminance ratio on the SQRI image quality metric.

To investigate the effect of adaptation luminance on image quality, 5 levels of adaptation luminance were examined under the standard conditions. Table 12 lists the model parameters manipulated in this analysis, as well as those parameters held fixed at the levels defined by the standard conditions. For the numerical analysis, a 2048-element data array was used to tabulate the simulated scan data.

Figures 13-A through 13-C show the effect of adaptation luminance upon image quality as computed by the MTFA, ICS, and SQRI metrics, respectively. The ordinate (i.e., y-axis) range has been adjusted to about 50% of the maximum value determined for each metric under the standard conditions. Note that the abscissa (i.e., x-axis) scale in Figures 13-A through 13-C is logarithmic in order to show metric value differences across four orders of magnitude of adaptation luminance.

Table 12. Parameters for Adaptation Luminance Computations.

Manipulated Parameters	Condition				
	1	2	3	4	5
Adaptation Glare ( $\text{cd/m}^2$ )	0.1	1.0	10.0	100.0	1000.0

Fixed Parameters	
Device Type	Monochrome CRT
Pixel Shape	Gaussian
Screen Height	280 mm
Screen Width	380 mm
Pixels Per Height	1024
Pixels Per Width	1280
Peak Luminance	100 $\text{cd/m}^2$
Reflected Glare	20 $\text{cd/m}^2$
Viewing Distance	500 mm
Adaptation Luminance	20 $\text{cd/m}^2$

As seen in Figures 13-A through 13-C, the MTFA, ICS, and SQRI metric values increase with increasing adaptation luminance. The change in metric value is 15.93% (6.862 vs. 7.955) for MTFA, 736.78% (443.2 vs. 3708.6) for ICS, and 94.60% (56.33 vs. 109.62) for SQRI. These findings point out that the ICS is most sensitive in adaptation luminance, SQRI is moderately sensitive, and MTFA is least sensitive to changes in adaptation level.

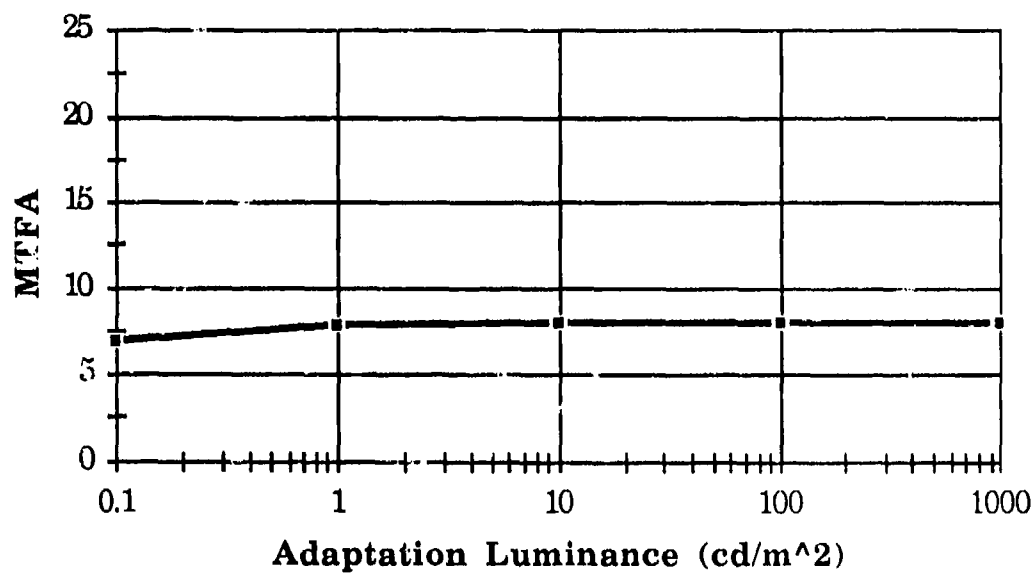


Figure 13-A. Effect of adaptation luminance ratio on the MTF image quality metric.

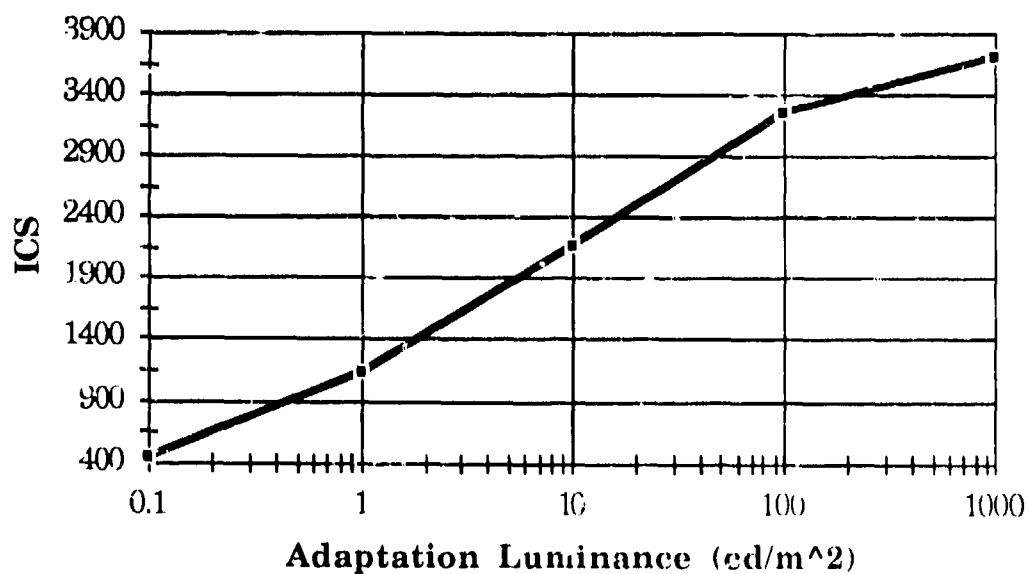


Figure 13-B. Effect of adaptation luminance ratio on the ICS image quality metric.

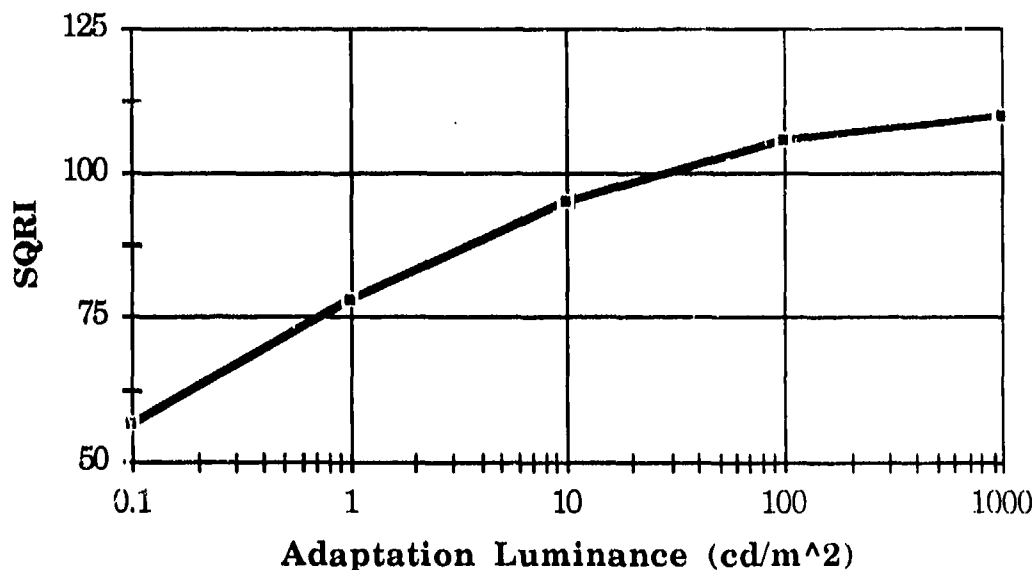


Figure 13-C. Effect of adaptation luminance ratio on the SQRI image quality metric.

**3.5.4 Viewing Distance.** Observer viewing distance affects the spatial frequency units used to scale the CTF and MTF. In general, spatial frequency increases with increasing viewing distance. It should be appreciated, however, that angular spatial frequency changes as a transcendental function (i.e., arc tangent) of viewing distance. Nevertheless, increasing the viewing distance tends to increase the “effective” bandwidth of the display MTF with respect to angular spatial frequency units.

Eight levels of viewing distance were examined under the standard conditions. Table 13 lists the model parameters manipulated as well as held fixed in this analysis. For the numerical analysis, a 2048-element data array was used to tabulate the simulated scan data.

Table 13. Parameters for Viewing Distance Computations

Manipulated Parameter	Condition			
	1	2	3	4
Viewing Distance (mm)	300	400	500	600

Manipulated Parameter (cont.)	Condition			
	5	6	7	8
Viewing Distance (mm)	700	800	900	1000

Fixed Parameters	
Device Type	Monochrome CRT
Pixel Shape	Gaussian
Screen Height	280 mm
Screen Width	380 mm
Pixels Per Height	1024
Pixels Per Width	1280
Peak Luminance	100 cd/m <sup>2</sup>
Reflected Glare	20 cd/m <sup>2</sup>
Adaptation Luminance	20 cd/m <sup>2</sup>

Figures 14-A through 14-C show the effect of viewing distance upon image quality as computed by the MTFA, ICS, and SQRI metrics, respectively. The ordinate (i.e., y-axis) range has been adjusted to about 25% of the maximum value determined for each metric under the standard conditions.

As seen in Figures 14-A through 14-C, the MTFA, ICS, and SQRI metric values increase with increasing viewing distance. The change in metric value is 224.23% (4.767 vs. 15.456) for MTFA, 65.18% (1857.4 vs. 3068.0) for ICS, and 8.51% (92.51 vs. 100.38) for SQRI. These findings illustrate a dramatic difference in trend among the metrics with respect to the viewing distance parameter. That is, the MTFA metric increases abruptly with increasing viewing distance, whereas the ICS metric values are

negatively-accelerating with increasing viewing distance, and the SQRI metric value reach an asymptotic value at an intermediate viewing distance.

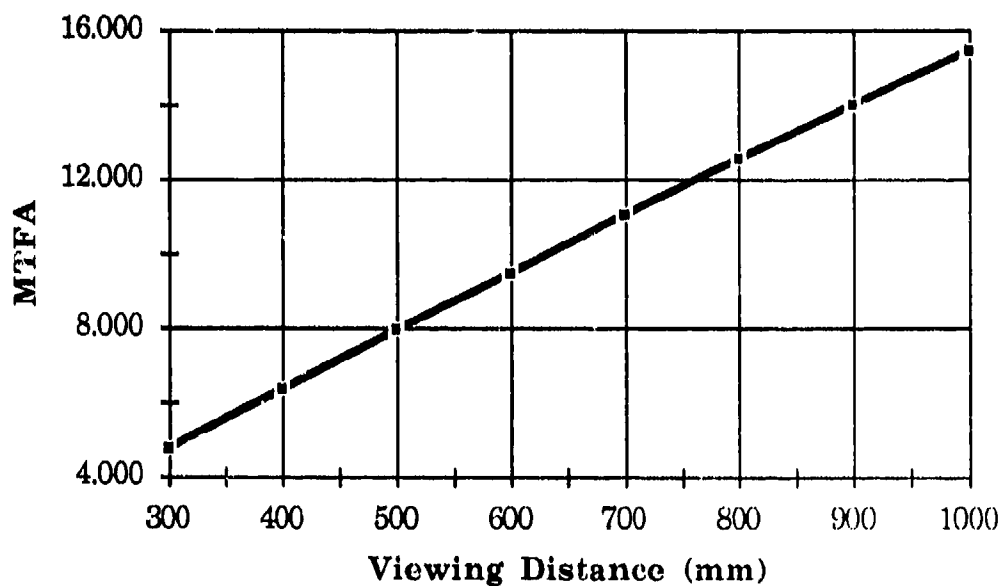


Figure 14-A. Effect of viewing distance on the MTFA image quality metric.

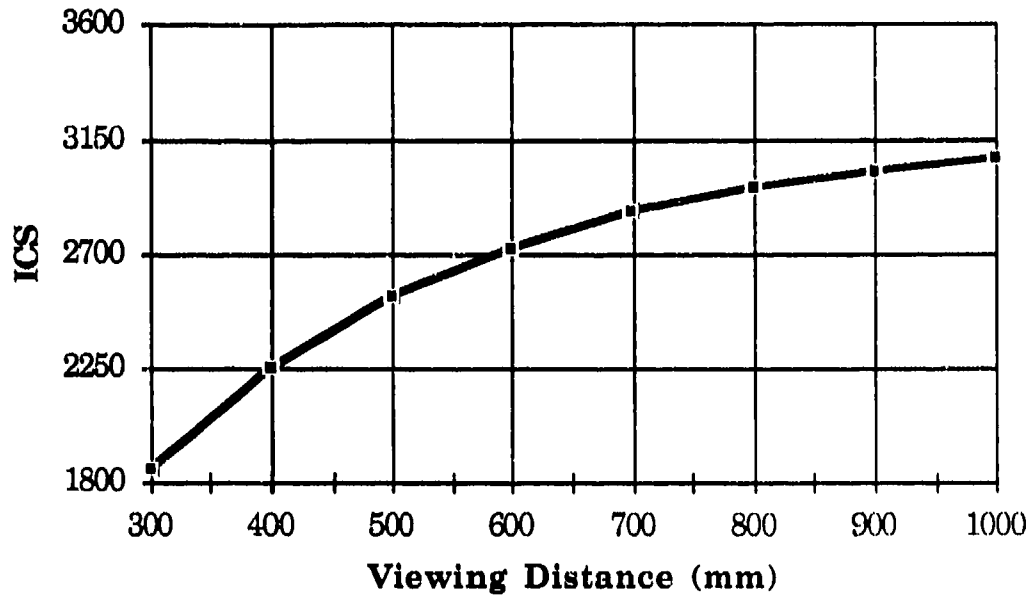


Figure 14–B. Effect of viewing distance on the ICS image quality metric.

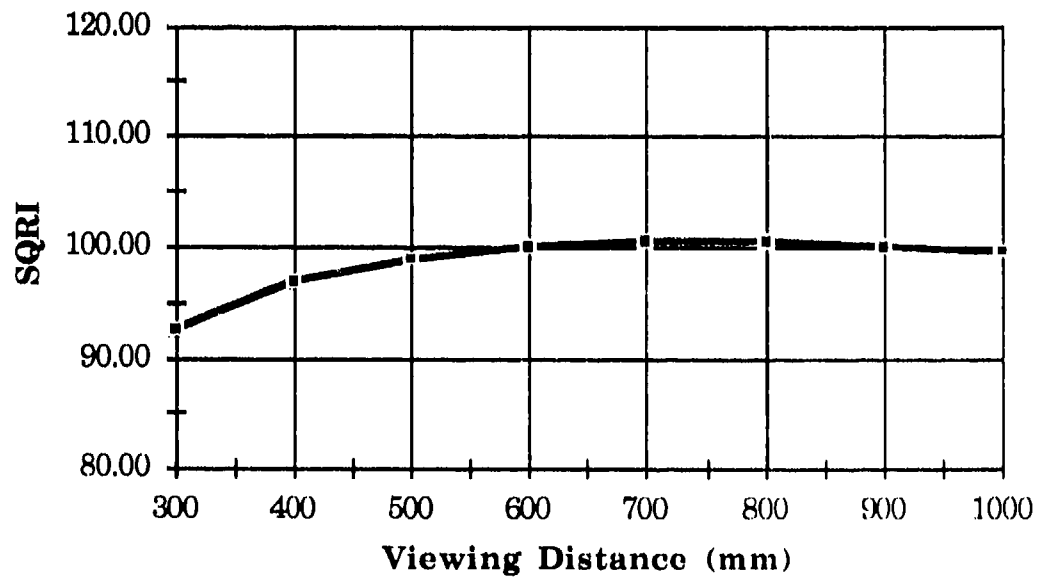


Figure 14–C. Effect of viewing distance on the SQRI image quality metric.

### 3.6 EMPIRICAL METRIC COMPUTATIONS

This section of the report examines the behavior of the MTFA, ICS, and SQRI image quality metrics computed from tabulated data arrays.

Although the MTFA, ICS, and SQRI image quality metrics are defined by closed-form integral equations, most applications of the metrics rely upon empirical techniques to approximate the analytical integrals. Typically, photometric measurement procedures are used to collect tabulated data arrays containing discrete samples of the display LSF. Next, the sampled LSF is subjected to a discrete Fourier transform to approximate MTF data at a finite number of spatial frequency values. Then, instead of solving integrals, discrete summations based on the sampled MTF and CTF data are evaluated for the image quality metric values.

**3.6.1 Empirical Metric Expressions.** To compute the MTFA, ICS, and SQRI metrics from tabulated data, the corresponding integral expressions must be replaced by discrete summations. From the Limit of Summation Theorem in calculus, the value of a summation approaches its corresponding integral value as the discrete forward difference (i.e., summation interval) approaches zero. Thus, one type of error inherent in discrete summation is related directly to the size of the sampling interval between adjacent data points in the tabulated array.

The following definitions are provided for the discrete MTFA, ICS, and SQRI metrics:

$$\text{MTFA} = \sum_{v_l}^{v_u} \text{MTF}(v) - \text{CTF}(v) \Delta v \quad (\text{Eq. 30})$$

$$\text{ICS} = \sum_{v_l}^{v_u} \frac{\text{MTF}(v)}{\text{CTF}(v)} \Delta v \quad (\text{Eq. 31})$$

$$SQRI = \frac{1}{\ln 2} \sum_{v_l}^{v_u} \frac{1}{v} \sqrt{\frac{MTF(v)}{CTF(v)}} \Delta v \quad (\text{Eq. 32})$$

in which,

$\Delta v$  denotes the discrete summation interval in cycles per degree of visual angle.

**3.6.2 Computational Issues.** There are numerous issues associated with the photometric measurement of LSFs from visual display devices. Although the reader who is interested in conducting photometric measurements should familiarize oneself with these issues (see, Beaton, 1988), many of the procedural issues are beyond the purposes of this report. Rather, in the following paragraphs, several issues concerning the use of discrete summations to approximate the integral definitions of image quality metrics are discussed.

**3.6.2.1 Number of Samples.** Number of samples ( $N_{LSF}$ ) refers to the total count of discrete luminance measurements collected across the LSF. Generally, larger  $N_{LSF}$  are preferred. However, there are two costs incurred with large numbers of LSF samples. First, computation time required to perform the discrete Fourier transform increases with increasing number of samples. Second, the amount of computer memory used to store the LSF increases with increasing number of samples.

**3.6.2.2 LSF Sampling Interval.** LSF sampling interval ( $\Delta d_{LSF}$ ) refers to the spatial separation or distance between adjacent measurement points across the LSF. At each sampled point, the LSF luminance is "averaged" across the two-dimensional extent of the measurement aperture. Typically, the size of a square, rectangular, or circular measurement aperture used is much smaller than the LSF width.

The LSF sampling interval has an important effect on MTFs computed from measurement data. That is, from the Nyquist sampling theory, the highest spatial frequency component uniquely represented in a discrete MTF analysis is given by

$$\tilde{\omega}_{Ny} = \frac{1}{2 \Delta d_{LSF}} \quad (\text{Eq. 33})$$

in which

$\tilde{\omega}_{Ny}$  denotes the Nyquist limit of the discrete MTF analysis (cycles per unit sampling distance).

Note that  $\tilde{\omega}_{Ny}$  is not the Nyquist limit of the display system ( $\omega_u$  in Eq. 8a).

**3.6.2.3 LSF Scan Period.** LSF scan period ( $P_{LSF}$ ) refers to the total spatial extent sampled in the LSF measurement. The LSF period is given by

$$P_{LSF} = \Delta d_{LSF} N_{LSF}. \quad (\text{Eq. 34})$$

Note that  $P_{LSF}$  is expressed in same distance units as  $\Delta d_{LSF}$  (e.g., mm).

The LSF scan period affects the computed MTF data. Specifically, given a discrete MTF array, denoted as

$$\text{MTF}(i), \text{ for } i = \{0, 1, 2, \dots, (N_{LSF}/2)\}, \quad (\text{Eq. 35})$$

the spatial frequency value (in cycles per distance units) corresponding to the  $i$ th array index is given by

$$\tilde{\omega} = \frac{i}{\Delta d_{LSF} N_{LSF}}. \quad (\text{Eq. 36})$$

Therefore, the MTF sampling interval (i.e., separation between adjacent spatial frequency amplitude values) is given by

$$\Delta\tilde{\omega} = \frac{1}{P_{LSF}}. \quad (\text{Eq. 37})$$

In other words, the LSF sampling period determines the size of the spatial frequency increments in the MTF analysis. Note that  $\Delta\tilde{\omega}$  also corresponds to the fundamental or lowest spatial frequency estimate above DC (i.e., 0 cycles per distance unit) computed in the discrete MTF analysis.

**3.6.2.4 Lower Spatial Frequency Limit.** For any visual display screen with finite extent, the first spatial frequency above DC that may be evaluated depends upon display size (width or height). In other words, the lower limit of integration (summation) in an image quality metric is related inversely to the spatial display extent (see Eq. 14a). However, in empirical metric evaluations, the spatial extent represented in the tabulated LSF array may be much less than the display size. That is,

$$P_{LSF} \ll DS \quad (\text{Eq. 38})$$

and, therefore,

$$\omega_l \ll \Delta\tilde{\omega}. \quad (\text{Eq. 39})$$

In these cases, the LSF measurement procedure has utilized a scan period too short to accurately assess the MTF amplitude at the lower spatial frequency limit. Consequentially, the accuracy of empirical metrics computed from the tabulated LSF data is degraded.

Specifically, in the evaluation of empirical metrics one must determine the MTF array index corresponding to the lower limit of summation (i.e., MTF ( $\omega_l$ ) in Eq. 35). It is unlikely, however, that the MTF array contains the lower limit exactly, as implied by Eq. 38. Therefore, the MTF array index corresponding to a spatial frequency (in cycles per degree of visual angle) equal to or greater than the lower limit is given by:

$$i_l = \vec{\text{int}} \left[ \frac{\pi N \Delta d_{\text{LSF}}}{180 \arctan \left[ \frac{DS}{D} \right]} \right] \quad (\text{Eq. 40})$$

in which

$\vec{\text{int}}$  denotes an integer round-up operation (e.g.,  
 $\vec{\text{int}}[2.4] = 3$ ).

The integer round-up of the lower limit of integration (summation) has special significance in the computation of the SQRI metric. As shown in §3.2.3., the SQRI metric value is determined largely by MTF and CTF information at the lowest spatial frequencies. However, due to the  $\left[ \frac{1}{\omega} \right]$  scaling term, the SQRI metric is undefined at  $\omega = 0$  cycles per degree of visual angle (i.e.,  $i = 0$  in Eq. 36). Therefore, algorithms for empirical evaluation of the SQRI metric are forced to avoid integer round-offs resulting in the selection of the DC spatial frequency term.

Unfortunately, the consequence of safe-guarding against selection of DC spatial frequency also is problematic in empirical evaluations of the SQRI metric. That is, the integer round-up operation usually results in selection of the angular frequency corresponding to  $\Delta\tilde{\omega}$  (i.e.,  $i = 1$  in Eq. 36). From Eq. 39 above,  $\Delta\tilde{\omega}$  is a much higher frequency than  $\omega_l$ . Thus, empirical evaluations of the SQRI metric are prone to serious computational errors unless the LSF scan period exactly matches the linear dimension of the display screen under evaluation.

**3.6.2.5 Upper Spatial Frequency Limit.** For discretely sampled displays (i.e., display screens consisting of discrete pixels), the highest spatial frequency depends on pixel addressability. In other words, the upper limit of integration (summation) for an image quality metric is related inversely to twice the pixel separation (see Eq. 8a). However, in empirical metric evaluations, the spatial increment between samples in the

tabulated LSF array may be much less than the distance between adjacent display pixels. That is,

$$\Delta d_{\text{LSF}} \ll A \quad (\text{Eq. 41})$$

and, therefore,

$$\omega_u \ll \tilde{\omega}_{\text{Ny}}. \quad (\text{Eq. 42})$$

In these cases, the LSF measurement procedure has used a sampling interval unnecessarily small given the bandwidth limits of the display device.

Nevertheless, the MTF array index corresponding to the upper limit (e.g., MTF( $\nu$ ) in Eq. 35) is given by:

$$i_1 = \overleftarrow{\text{int}} \left[ \frac{\pi N \Delta d_{\text{LSF}}}{180 \arctan \left[ \frac{2A}{D} \right]} \right] \quad (\text{Eq. 43})$$

in which

$\overleftarrow{\text{int}}$  denotes an integer round-down operation (e.g.,  
 $\overleftarrow{\text{int}}[2.4] = 2$ ).

For MTFA image quality metric, special consideration is needed to determine the upper limit of integration (summation). In addition to the display Nyquist constraint mentioned above, the upper limit of integration for the MTFA is bounded by the MTF and CTF cross-over point. In other words, the MTFA upper limit of integration is the spatial frequency at which  $\text{MTF}(\nu) - \text{CTF}(\nu) = 0$ , provided that spatial frequency is less than the Nyquist limit for the display system.

**3.6.2.6 Removing Glare Offset.** With few exceptions, visual display workstations are located in environments with finite amounts of ambient light. When sufficiently intense, the ambient light produces

measurable amounts of reflected glare luminance from the display screen. Prior to computing a MTF from a LSF measured in the presence of ambient light, it is imperative to remove the reflected glare luminance from the LSF data. Otherwise, the reflected glare luminance distorts the MTF analysis results.

For example, a uniform reflected glare field effectively adds a rectangular waveform to the LSF waveform. The MTF computed from this compound waveform contains spatial frequency components associated with the LSF as well as a sinc (i.e.,  $\frac{\sin(x)}{x}$ ) function, since the sinc function is the forward Fourier transform of a rectangular function.

Under conditions of uniform reflected glare, the ambient level offset value may be estimated from the leading and trailing ends of the LSF data. The reflected glare offset is subtracted from the LSF data prior to the MTF operation, and, then, it is used to scale the MTF data in accord with Eq. 17.

**3.6.3 Empirical Metric Computations.** To investigate the behavior of the empirical MTFA, ICS, and SQRI metrics, the computational parameters of  $N_{LSF}$ ,  $\Delta d_{LSF}$ , and  $P_{LSF}$  were manipulated. It should be appreciated that empirical evaluations of metrics are based on measured LSF data obtained with different lens magnifications, sampling intervals, and scan periods. These measurement parameters are related to the  $N_{LSF}$ ,  $\Delta d_{LSF}$ , and  $P_{LSF}$  computational parameters studied here. Thus, the computational findings presented in this section of the report mimic results obtainable with various photometric equipment configurations.

For the empirical metric computations, the C-language algorithms were used instead of the *Mathematica*<sup>TM</sup> algorithms because of their greater computational speed. Moreover, the standard conditions were used to set display device and human observer parameters in the metric models. Under the standard conditions, the C-language algorithms using  $N_{LSF} = 2048$  points,  $\Delta d_{LSF} = 0.0375$  mm, and  $P_{LSF} = 76.8$  mm yield results identical to the *Mathematica*<sup>TM</sup> algorithms.

Table 14 lists the computational parameters used to simulate the various photometric measurement systems. The values in Table 14 are scan periods listed as a function of lens magnification and total number of sample points. The relations among the computational parameters is summarized as

$$P_{LSF} = \frac{\Delta d_{LSF}}{MAG} N_{LSF}, \quad (\text{Eq. 44})$$

in which

MAG denotes the lens magnification factor.

Table 14. Computational Parameters for Empirical Metric Evaluations

P <sub>LSF</sub> (mm)		N <sub>LSF</sub>			
MAG	Δd <sub>LSF</sub> (mm)	256	512	1024	2048
1	0.037500	9.6	19.2	38.4	76.8
2	0.018750	4.8	9.6	19.2	38.4
4	0.009375	2.4	4.8	9.6	19.2
8	0.004688	1.2	2.4	4.8	9.6

**3.6.3.1 Empirical MTFA Metric.** Table 15 and Figure 15 present the empirical MTFA metric values computed for each combination of N<sub>LSF</sub> and MAG under the standard display conditions. As shown in Table 15, the range of variation in empirical MTFA values is 0.517 units. Using the Mathematica™ result for the standard conditions as the "correct" metric value, the percent error observed in the range of MTFA values is 6.51%. Note that the empirical MTFA metric expression yields values that are lower than the correct metric value.

From these data, the empirical MTFA metric appears to be relatively insensitive to changes in the N<sub>LSF</sub> and MAG computational parameters. For a fixed MAG value, the errors associated with the empirical MTFA metric

decrease with increasing  $N_{LSF}$ . Conversely, for a fixed  $N_{LSF}$  value, the empirical MTFA errors increase with increasing MAG. This pattern of results indicates that MTFA errors are minimized when  $N_{LSF}$  is large and MAG is low.

Table 15. Empirical MTFA Values Computed Across  $N_{LSF}$  and MAG

Correct MTFA = 7.940036								
$N_{LSF}$	MAG							
	1X	% Error	2X	% Error	4X	% Error	8X	% Error
256	7.868	0.91	7.816	1.56	7.703	2.99	7.414	6.63
512	7.896	0.55	7.868	0.91	7.816	1.56	7.703	2.99
1025	7.920	0.25	7.896	0.55	7.868	0.91	7.816	1.56
2048	7.931	0.11	7.920	0.25	7.896	0.55	7.868	0.91

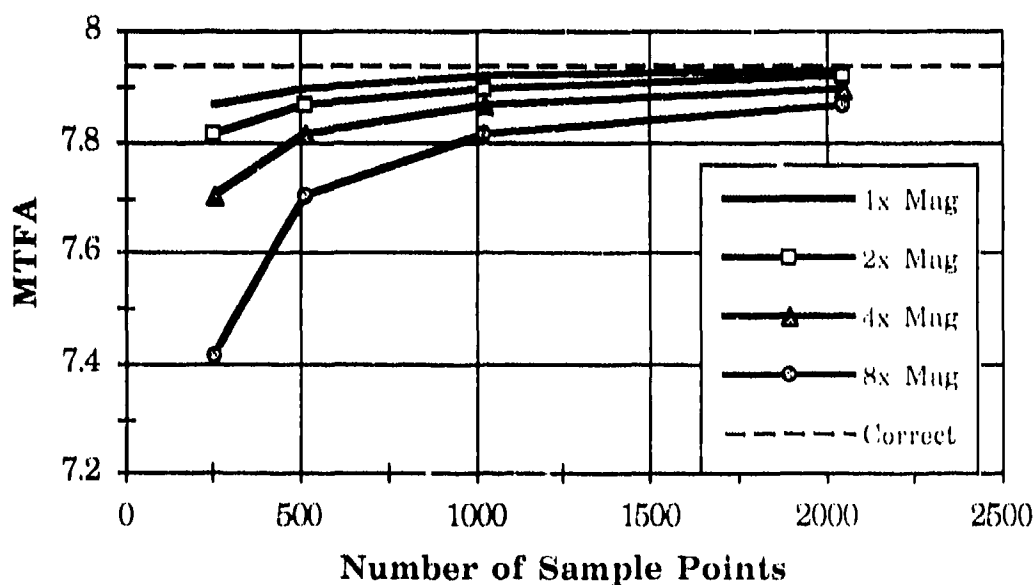


Figure 15. Empirical MTFA metric values as a function of number of samples and lens magnification. Note that the ordinate (y-axis) range is scaled to about 10% of the correct MTFA value.

**3.6.3.2 Empirical ICS Metric.** Table 16 and Figure 16 present the empirical ICS metric values computed for each combination of  $N_{LSF}$  and MAG under the standard conditions. As shown in Table 16, the range of variation in empirical ICS values is 1086.9 units. In comparison to the Mathematica™ result for the standard conditions, the range of variation in the empirical ICS values corresponds to a percent error of 43.0%. Across the conditions examined, the empirical ICS metric yields values lower than the correct metric value.

From these data, it is apparent that the empirical ICS metric is sensitive to changes in the  $N_{LSF}$  and MAG computational parameters. For a fixed MAG value, the empirical ICS metric errors decrease with increasing  $N_{LSF}$ . Conversely, for a fixed  $N_{LSF}$  value, ICS errors increase with increasing MAG. This pattern of results indicates that ICS errors are minimized when  $N_{LSF}$  is large and MAG is low.

Table 16. Empirical ICS Values Computed Across  $N_{LSF}$  and MAG

Correct ICS = 2527.49								
$N_{LSF}$	MAG							
	1X	% Error	2X	% Error	4X	% Error	8X	% Error
256	2503.4	0.95	2442.7	3.35	2202.4	12.86	1439.5	43.05
512	2519.1	0.33	2503.4	0.95	2442.7	3.35	2202.4	12.86
1025	2524.5	0.12	2519.1	0.33	2503.4	0.95	2442.7	3.35
2048	2526.4	0.04	2524.5	0.12	2519.1	0.33	2503.4	0.95

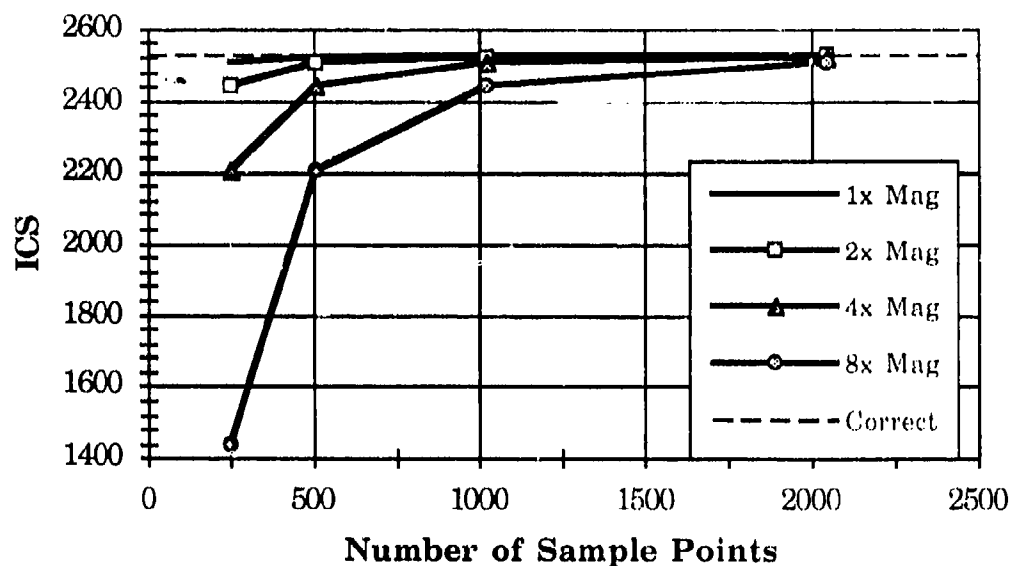


Figure 16. Empirical ICS metric values as a function of number of samples and lens magnification. Note that the ordinate (y-axis) range is scaled to about 50% of the correct ICS value.

**3.6.3.2 Empirical SQRI Metric.** Table 17 and Figure 17 present the empirical SQRI metric values computed for each combination of  $N_{LSF}$  and MAG under the standard conditions. As shown in Table 16, the range of variation in empirical SQRI values is 463.26 units. The range of variation in the empirical SQRI values corresponds to a percent error of 475.68% with respect to the "correct" SQRI value determined with the *Mathematica*™ algorithms. Across the conditions examined, the empirical SQRI metric yields values higher than the correct metric value.

The empirical SQRI metric is extremely sensitive to changes in the  $N_{LSF}$  and MAG. For a fixed MAG value, the errors in empirical SQRI metric decrease with increasing  $N_{LSF}$ . Conversely, for a fixed  $N_{LSF}$  value, SQRI errors increase with increasing MAG. These trends indicate that SQRI errors are minimized when  $N_{LSF}$  is large and MAG is low.

Table 17. Empirical SQRI Values Computed Across  $N_{LSF}$  and MAG

Correct SQRI = 97.389								
$N_{LSF}$	MAG							
	1X	% Error	2X	% Error	4X	% Error	8X	% Error
256	137.2	-40.88	191.91	-97.06	310.46	-	562.14	-
						218.78		477.21
512	112.84	-15.87	137.2	-40.88	191.91	-97.06	310.46	-
								218.78
1025	102.67	-5.42	112.84	-15.87	137.2	-40.88	191.91	-97.06
2048	98.88	-1.53	102.67	-5.42	112.84	-15.87	137.2	-40.88

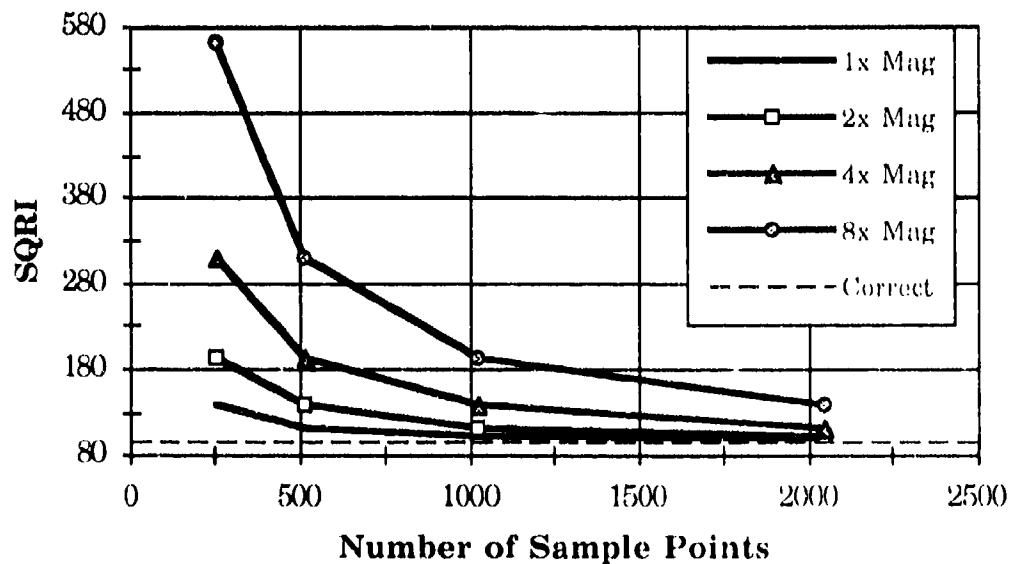


Figure 17. Empirical SQRI metric values as a function of number of samples and lens magnification. Note that the ordinate (y-axis) range is scaled to about 500% of the correct SQRI value.

## 4.0 PERFORMANCE CORRELATIONS

This section of the report presents an investigation of the statistical correlations between the image quality metrics and observed human performance under varying display device and viewing conditions.

### 4.1 WESTERINK AND ROUFS (1988)

**4.1.1 Description of Experiment.** This experiment assessed subjective image quality judgments of projected color slides across a range of system resolutions and display sizes. Resolution was defined operationally as the spatial frequency coinciding with the -6 db (i.e., 25% of peak) MTF point, and it was manipulated by defocusing the projector lens across seven steps ranging in MTF cut-offs from 2.7 to 38.0 cycles per degree of visual angle. Display size was defined as the linear extent of the rectangular picture area and it was manipulated by using slide media of varying size.

During the experiment, observers viewed each pictorial scene for 15 sec from a 2900 mm viewing distance. The average scene luminance was about  $30 \text{ cd/m}^2$  and observers were light adapted to this same luminance level. The ambient luminance reflected from the projection screen was about  $5 \text{ cd/m}^2$ . A 100-point scale (ranging from 0.1 to 10.0) was used to collect the subjective judgments.

**4.1.2 Metric v. Performance Correlations.** Using the parameters and data graphs reported in Westerink and Roufs (1988), the MTFA, ICS, and SQRI were metrics computed and, then, compared to human performance results reported for each viewing condition in the experiment.

Before performing the metric computations, it was necessary to re-parameterize the resolution values reported by Westerink and Roufs (1988).

Since the authors specify the -6 dB MTF cut-off point in cycles per degree of visual angle, these values were used to compute the 50% width of a Gaussian LSF. Using Eq. 5 for the MTF of a Gaussian LSF, the 50% width is given as

$$s = \sqrt{\frac{-4 \ln 2 \ln 0.25}{\pi \omega_{-6 \text{ dB}}^2}} \quad (\text{Eq. 45})$$

in which

$\omega_{-6 \text{ dB}}$  denotes the MTF cut-off spatial frequency in cycles per millimeter.

Before solving Eq. 45 for each 50% width value, the angular MTF cut-off frequencies reported by Westerink and Roufs were converted into linear frequency units by

$$\omega_{-6 \text{ dB}} = \frac{180 \nu_{-6 \text{ dB}}}{\pi D} \quad (\text{Eq. 46})$$

Table 18 lists the 50% width calculations performed for the resolutions levels used by Westerink and Roufs (1988). Note that these authors did not explicitly cite the MTF cut-off frequencies used in the experiment. Therefore, the MTF cut-off frequencies were determined by digitizing photo-enlargements of the data plots provided in their report.

Table 18. 50% Width Calculations for Westerink and Roufs (1988).

v-6 dB	$\omega$ -6 dB	50% LSF Width (mm)
40.071445	0.791698	0.788244
27.777554	0.548806	1.137109
20.509969	0.405219	1.540036
14.767671	0.291767	2.138868
8.5554331	0.169031	3.691934
4.09734	0.080952	7.708927
2.7447323	0.054228	11.5079

Table 19 summarizes the computational parameters used in the MTFA, ICS, and SQRI metric computations for the Westerink and Roufs (1988) study.

Table 19. Computational Parameters for Westerink and Roufs (1988)

Display Device Parameters	Value
Device Type	Slide Projector
Screen Height	2400, 7200, 4800, 9200 mm
Screen Width	2400, 7200, 4800, 9200 mm
Pixels Per Height	$\infty$
Pixels Per Width	$\infty$
Pixel Shape	Gaussian
Pixel Width (FWHM)	(see Table 18)
Average Luminance	20 cd/m <sup>2</sup>
Reflected Glare	5 cd/m <sup>2</sup>
Observer Parameters	Value
Viewing Distance	2900 mm
Adaptation Luminance	30 cd/m <sup>2</sup>

**4.1.2.1 MTFA Metric.** Figure 18 presents a scattergram of the image quality judgments and MTFA metric values across the resolution and display size conditions reported in Westerink and Roufs (1988). From Figure 18, it can be seen that subjective image quality increases with increasing MTFA values.

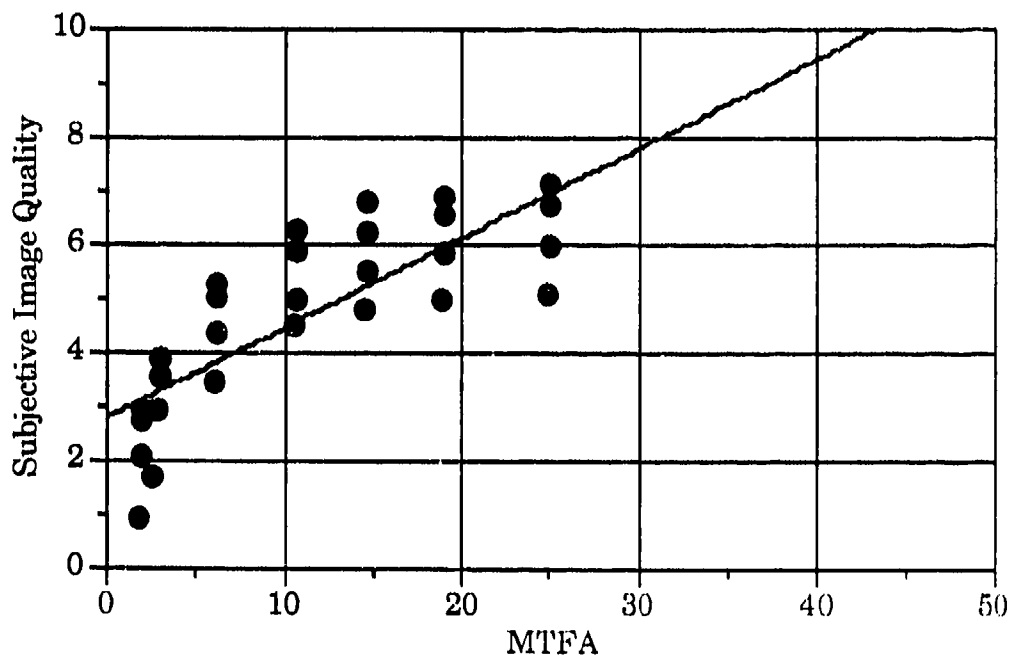


Figure 18. Scattergram of subjective image quality judgments reported in Westerink and Roufs (1988) and empirically computed MTFA metric values.

The linear regression of MTFA values on subjective image quality judgments, as given by

$$\Psi_{IQ} = 2.789 + (0.166 \text{ MTFA}) \quad (\text{Eq. 47})$$

where

$\Psi_{IQ}$  denotes the subjective image quality judgment.

Eq. 47 is plotted in Figure 18 as a straight line. The statistical fit of the linear regression is  $r^2 = 0.639$ , indicating that a linear relationship accounts for 63.9% of the observed variance between subjective quality and MTFA values. However, by inspection of the data trend in Figure 18, it is clear that a linear relationship does not describe the relationship between subjective image quality judgments and MTFA values. Rather, a linear relationship

appears to exist between logarithmically transformed subjective image quality and MTFA values.

**4.1.2.2 ICS Metric.** Figure 19 presents a scattergram of the image quality judgments and ICS metric values across the resolution and display size conditions reported in Westerink and Roufs (1988). From Figure 19, it can be seen that subjective image quality increases with increasing ICS values.

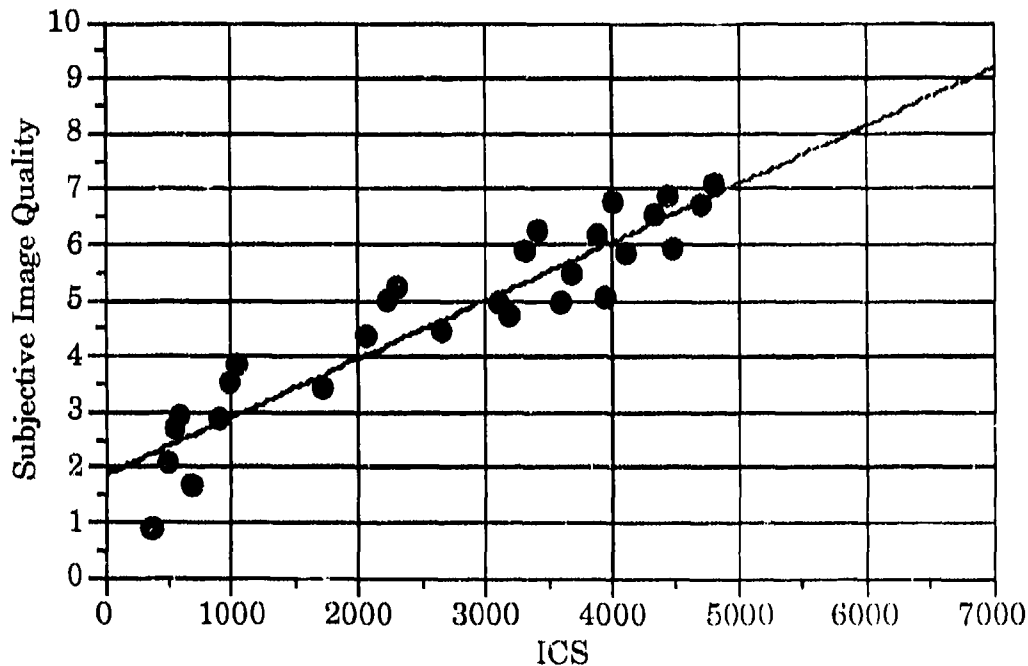


Figure 19. Scattergram of subjective image quality judgments reported in Westerink and Roufs (1988) and empirically computed ICS metric values.

The linear regression of ICS values on subjective image quality judgments, as given by

$$\Psi_{IQ} = 1.876 + (1.044\text{E-}3 \text{ ICS}). \quad (\text{Eq. 48})$$

Eq. 48 is plotted in Figure 19 as a straight line. The statistical fit of the linear regression is  $r^2 = 0.872$ , indicating that a linear relationship accounts for 87.2% of the observed variance in the subjective quality and ICS values. Inspection of Figure 19 suggests that a linear trend reasonably describes the relationship between subjective image quality judgments and ICS values.

**4.1.2.3 SQRI Metric.** Figure 20 presents a scattergram of the image quality judgments and SQRI metric values across the resolution and display size conditions reported in Westerink and Roufs (1988). From Figure 20, it can be seen that subjective image quality increases with increasing SQRI values.

The linear regression of SQRI values on subjective image quality judgments, as given by

$$\Psi_{IQ} = -1.848 + (7.312E-2 \text{ SQRI}). \quad (\text{Eq. 49})$$

Eq. 49 is plotted in Figure 20 as a straight line. The statistical fit of the linear regression is  $r^2 = 0.984$ . From Figure 20, it is clear that a linear relationship accurately describes the relationship between subjective image quality judgments and SQRI values.

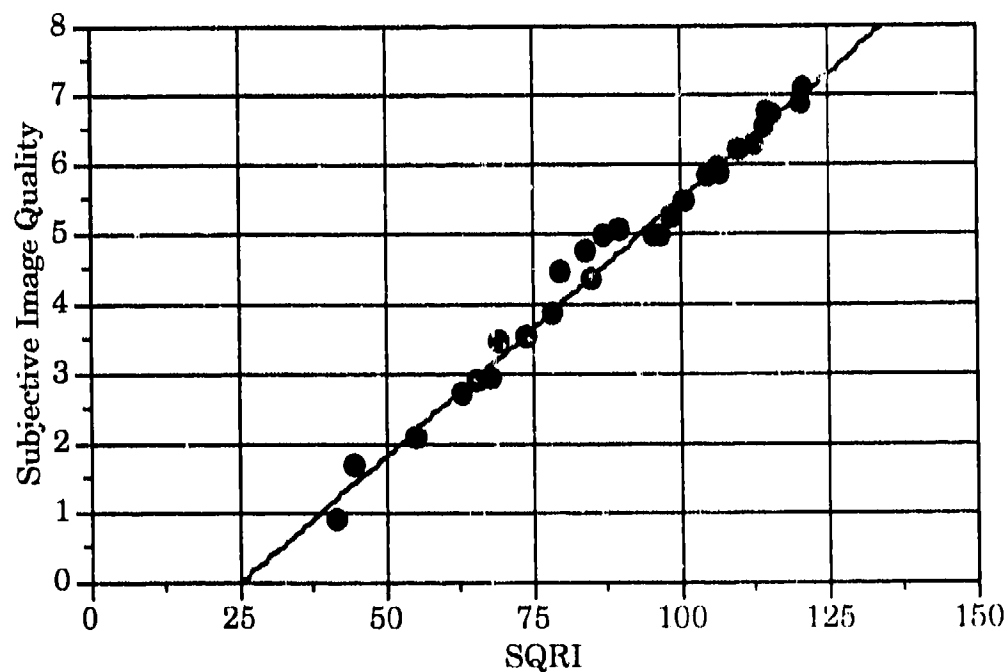


Figure 20. Scattergram of subjective image quality judgments reported in Westerink and Roufs (1988) and empirically computed SQRI metric values.

## 4.2 VAN DER ZEE AND BOESTEN (1980)

**4.2.1 Description of Experiment.** This experiment assessed subjective image quality judgments of projected color slides across a range of scene luminance and display size levels. Luminance was defined as the peak luminance of the scene and it was manipulated across seven levels ranging 69.0 to 500.0  $\text{cd/m}^2$  by neutral density filters placed into the projection light path. Display size was manipulated across three levels ranging from 4.2 to 20 degrees of visual angle by using slide media of varying size.

During the experiment, 29 observers viewed each pictorial scene for 15 sec from a 2900 mm viewing distance. A five-point scale was used to collect the subjective judgments. Observers were light adapted to 25.0  $\text{cd/m}^2$ . The ambient luminance reflected from the projection screen was about 0.25  $\text{cd/m}^2$ . Resolution of the projection display system (i.e., projector and screen) was not specified by the authors.

**4.2.2 Metric v. Performance Correlations.** Using the parameters reported by van der Zee and Boesten (1980), the MTFA, ICS, and SQRI metrics were computed for each viewing condition in the experiment. The C-language algorithms were used for the metric computations.

Before performing the metric computations, it was necessary to select a resolution value for the projection system used by van der Zee and Boesten. Since these authors did not specify a resolution value, an attempt was made to estimate resolution from prior work conducted by Barten (1990a,b). That is, since Barten (1990a,b) reports an SQRI metric evaluation of van der Zee and Boesten's data, an attempt was made to iterate the empirical SQRI metric on the resolution parameter until Barten's SQRI values were replicated. Unfortunately, this approach proved to be difficult as explained below.

Barten (1990a,b) reports that the luminance levels used by van der Zee and Boesten were 7, 9, 16, 20, 36, and 50  $\text{cd/m}^2$ . However, in their original paper, van der Zee and Boesten report peak luminance levels of 69, 93, 157, 200, 365, and 500  $\text{cd/m}^2$ . Although Barten (1990a,b) advocates the use of

adaptation luminance levels equal to twice the average scene luminance, the factor-of-ten difference in the reported luminance values appears too conservative.

Despite the discrepancy mentioned above, the SQRI model was iteratively solved with varying resolutions and Barten's reported luminance values. This procedure led to a resolution specification of 0.20 mm, which replicates Barten's results well. Then, since Barten apparently used incorrect luminance values, new estimates of the adaptation luminance were computed for the MTFA, ICS, and SQRI computations based upon van der Zee and Boesten's luminance values. That is, the adaptation luminance was set to one-half of the peak luminance values reported by van der Zee and Boesten.

It was also necessary to determine the sizes of the square projection screens used by van der Zee and Boesten. Table 20 lists linear sizes computed from the angular subtense of the screens and viewing distance.

Table 20. Screen Size Calculations for van der Zee and Boesten (1988)

Degrees	Millimeters
4.20	212.96
5.20	263.92
8.40	428.23
10.50	537.48
12.60	648.23
16.00	831.56
20.00	1055.51

Table 21 lists the computational parameters used to evaluate the MTFA, ICS, and SQRI metrics for the van der Zee and Boesten (1980) study.

Table 21. Computational Parameters for van der Zee and Boesten (1980)

Display Device Parameters	Value
Device Type	Slide Projector
Screen Height	(see Table 20)
Screen Width	(see Table 20)
Pixels Per Height	$\infty$
Pixels Per Width	$\infty$
Pixel Shape	Gaussian
Pixel Width (FWHM)	0.2 mm
Peak Luminance	69 to 365 cd/m <sup>2</sup>
Reflected Glare	0.25 cd/m <sup>2</sup>

Observer Parameters	Value
Viewing Distance	2900 mm
Adaptation Luminance	25 cd/m <sup>2</sup>

**4.2.2.1 MTFA Metric.** Figure 21 presents a scattergram of the image quality judgments and MTFA metric values across the luminance and display size conditions reported in van der Zee and Boesten (1980). From Figure 21, it can be seen that subjective image quality tends to increase with increasing MTFA values.

The linear regression of MTFA values on subjective image quality judgments, as given by

$$\Psi_{IQ} = -5.521 + (1.285E-1 \text{ MTFA}), \quad (\text{Eq. 50})$$

Eq. 50 is plotted in Figure 21 as a straight line. The statistical fit of the linear regression is  $r^2 = 0.216$ . Inspection of Figure 21 suggests that a linear relationship weakly describes the relationship between the subjective image quality judgments and MTFA values. Indeed, the large dispersion of image quality judgments at each MTFA value indicates that the MTFA metric does not track the judgments well.

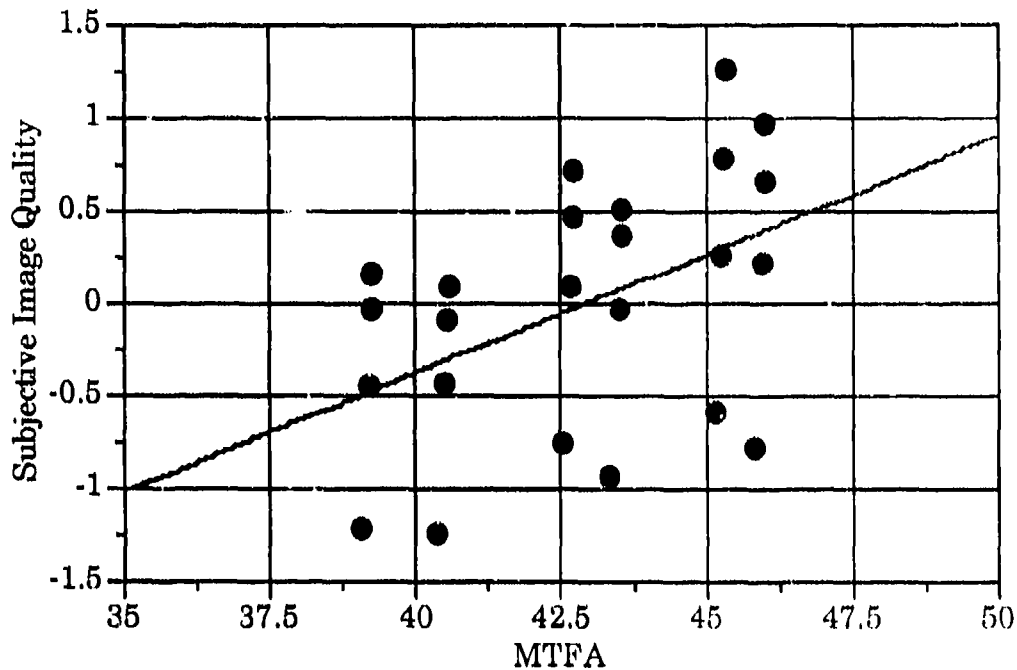


Figure 21. Scattergram of subjective quality judgments reported in van der Zee and Boesten (1980) and empirically computed MTFA metric values.

**4.2.2.2 ICS Metric.** Figure 22 presents a scattergram of the image quality judgments and ICS metric values across the luminance and display size conditions reported in van der Zee and Boesten (1980). From Figure 22, it can be seen that subjective image quality increases with increasing ICS values.

The linear regression of ICS values on subjective image quality judgments, as given by

$$\Psi_{IQ} = -4.276 + (6.920E-4 \text{ ICS}). \quad (\text{Eq. 51})$$

The statistical fit of Eq. 51 is  $r^2 = 0.676$ . Inspection of Figure 22 suggests that a linear relationship adequately describes the relationship between subjective image quality judgments and ICS values.

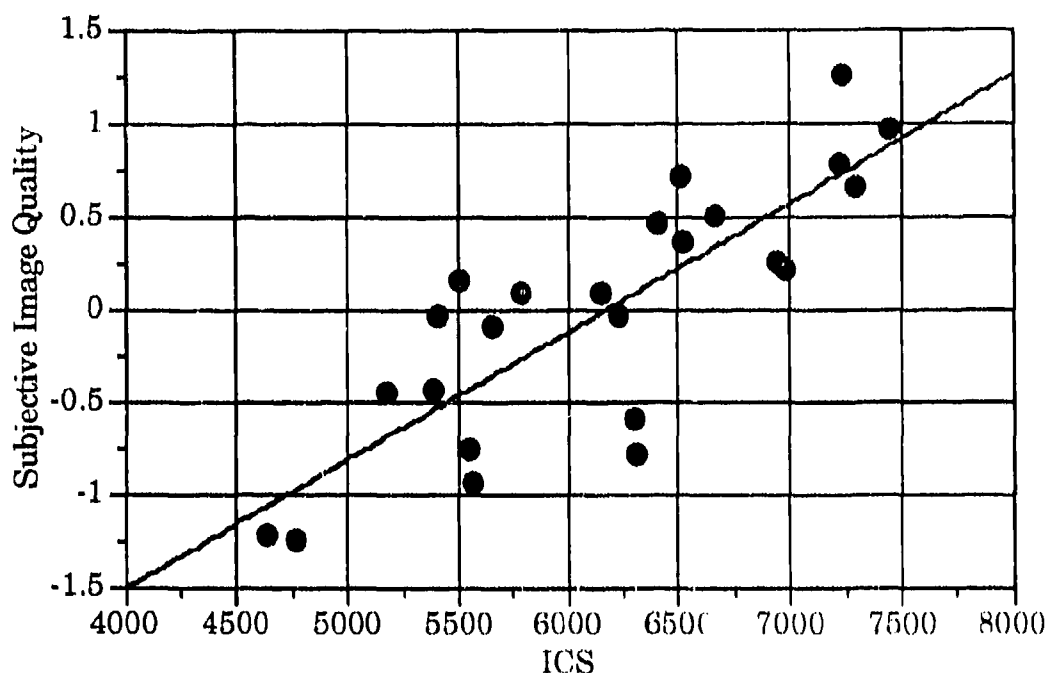


Figure 22. Scattergram of subjective image quality judgments reported in van der Zee and Boesten (1980) and empirically computed ICS metric values.

**4.2.2.2 SQRI Metric.** Figure 23 presents a scattergram of the image quality judgments and SQRI metric values across the luminance and display size conditions reported in van der Zee and Boesten (1980). From Figure 23, it can be seen that subjective image quality increases with increasing SQRI values.

The linear regression of SQRI values on subjective image quality judgments, as given by

$$\Psi_{IQ} = -4.122 + (3.092E-2 \text{ SQRI}). \quad (\text{Eq. 52})$$

The statistical fit of Eq. 51 is  $\bar{r}^2 = 0.892$ . Inspection of Figure 23 suggests that the relationship between these subjective image quality judgments and SQRI values is described well by the linear expression.

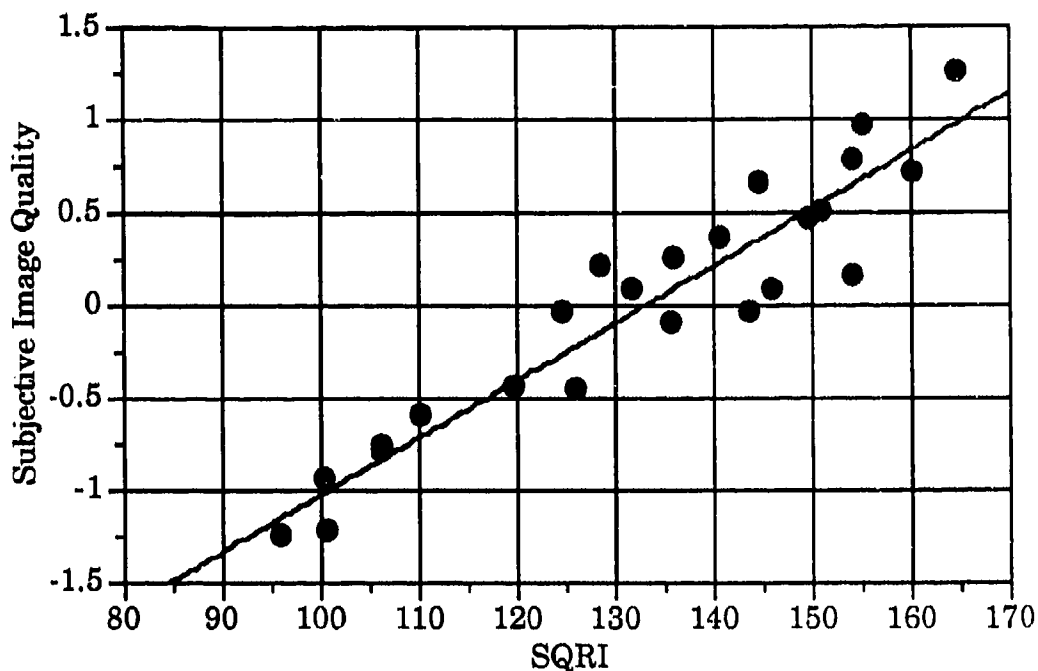


Figure 23. Scattergram of subjective image quality judgments reported in van der Zee and Boesten (1980) and empirically computed SQRI metric values.

### 4.3 KNOX (1987)

**4.3.1 Description of Experiment.** This experiment assessed subjective image quality judgments of raster-scanned text and graphics imagery across a range of resolution and addressability levels. Resolution was defined as the 50% LSF width, whereas addressability was defined as the separation between adjacent display pixels. The resolution and addressability were specified in terms of RAR which was manipulated across 12 levels ranging 0.5 to 4.0. The resolution and addressability of the CRT were computer-controlled through a digital interface to the CRT beam-focus and scan-deflection circuits.

During the experiment, 10 observers viewed each scene from about a 558 mm viewing distance. A 9-point scale was used to collect the subjective judgments. The observer's were light adapted to  $25.0 \text{ cd/m}^2$ . The ambient luminance reflected from the CRT screen was about  $1.0 \text{ cd/m}^2$ .

**4.3.2 Metric v. Performance Correlations.** Using the parameters reported by Knox (1987), the MTFA, ICS, and SQRI metrics were computed for each resolution condition in the experiment. The C-language algorithms were used for the metric computations.

Before performing the metric computations, it was necessary to recompute the experimental levels reported by Knox (1987) in terms of display resolution, addressability, and display size. Since the author specifies 50% LSF width (i.e., resolution) and RAR, it was a simple matter to compute addressability from these values. Table 22 lists the 16 resolution and addressability combinations used in the experiment. Moreover, since the number of pixel per screen dimension remained fixed, the horizontal and vertical display extents were determined directly from the addressability levels. Table 23 lists the four screen sizes used in the experiment.

Table 22. Resolution/Addressability Ratio Calculations for Knox (1987)

RAR				
50% LSF (mm)	Addressability (mm)			
	0.127	0.169	0.212	0.254
0.127	1.00	0.75	0.60	0.50
0.254	2.00	1.50	1.20	1.00
0.381	3.00	2.25	1.80	1.50
0.508	4.00	3.01	2.40	2.00

Table 23. Display Size Calculations for Knox (1987)

Addressability (mm)	Horizontal (mm)	Vertical (mm)
	(1280 pels)	(1024 pels)
0.127	162.56	130.05
0.169	216.32	173.06
0.212	271.36	217.09
0.254	325.12	260.10

Table 24 summarizes the computational parameters used in the MTFA, ICS, and SQRI metric computations for the Knox (1987) study.

Table 24. Computational Parameters for Knox (1987)

Display Device Parameters	Value
Device Type	Monochrome CRT
Screen Height	(see Table 23)
Screen Width	(see Table 23)
Pixels Per Height	1024
Pixels Per Width	1280
Pixel Shape	Gaussian
Pixel Width (FWHM)	(see Table 22)
Average Luminance	68.52 cd/m <sup>2</sup>
Reflected Glare	1.0 cd/m <sup>2</sup>

Observer Parameters	Value
Viewing Distance	558.8 mm
Adaptation Luminance	68.52 cd/m <sup>2</sup>

**4.3.2.1 MTFA Metric.** Figure 24 presents a scattergram of the image quality judgments and MTFA metric values across the resolution and addressability conditions reported in Knox (1987). From Figure 24, it can be seen that subjective image quality increases with increasing MTFA values.

The linear regression of MTFA values on subjective image quality judgments, as given by

$$\Psi_{IQ} = 2.301 + (1.551E-1 \text{ MTFA}). \quad (\text{Eq. 53})$$

Eq. 53 is plotted in Figure 24 as a straight line. The statistical fit of the linear regression is  $r^2 = 0.474$ . Inspection of Figure 24 suggests that a linear relationship weakly describes the relationship between the subjective image quality judgments and MTFA values.

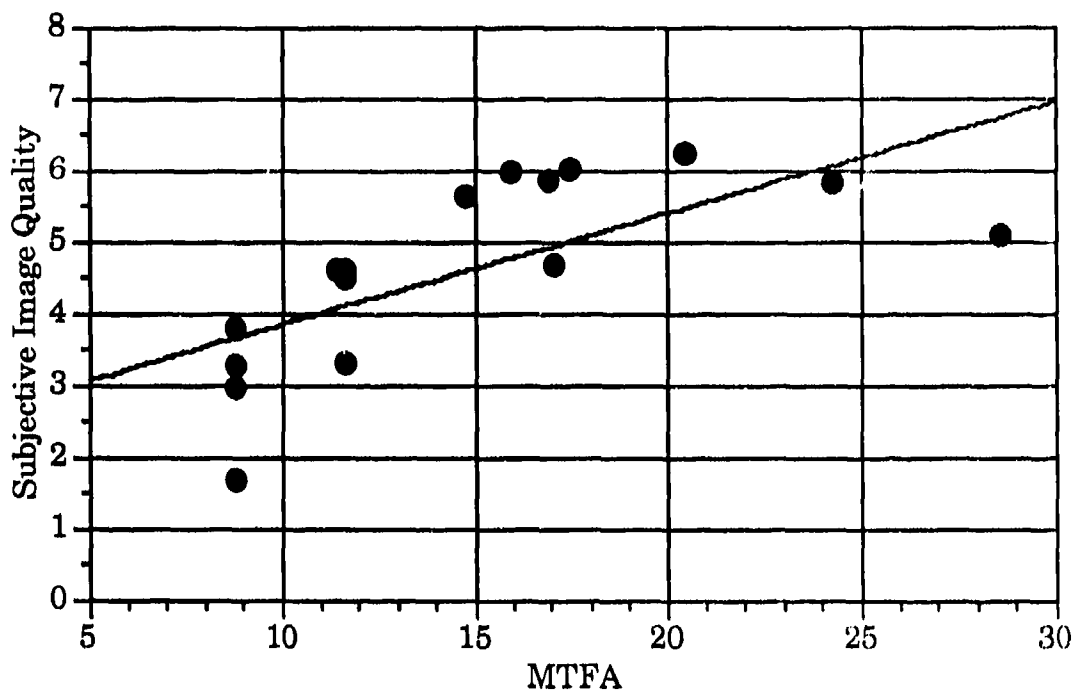


Figure 24. Scattergram of subjective image quality judgments reported in Knox (1987) and empirically computed MTFA metric values.

**4.3.2.2 ICS Metric.** Figure 25 presents a scattergram of the image quality judgments and ICS metric values across the resolution and addressability conditions reported in Knox (1987). From Figure 25, it can be seen that subjective image quality increases with increasing ICS values.

The linear regression of ICS values on subjective image quality judgments, as given by

$$\Psi_{IQ} = -1.382 + (1.315E-3 \text{ ICS}). \quad (\text{Eq. 54})$$

Eq. 54 is plotted in Figure 25 as a straight line. The statistical fit of the linear regression is  $r^2 = 0.777$ . Inspection of Figure 25 suggests that a linear relationship adequately describes the relationship between subjective image quality judgments and ICS values.

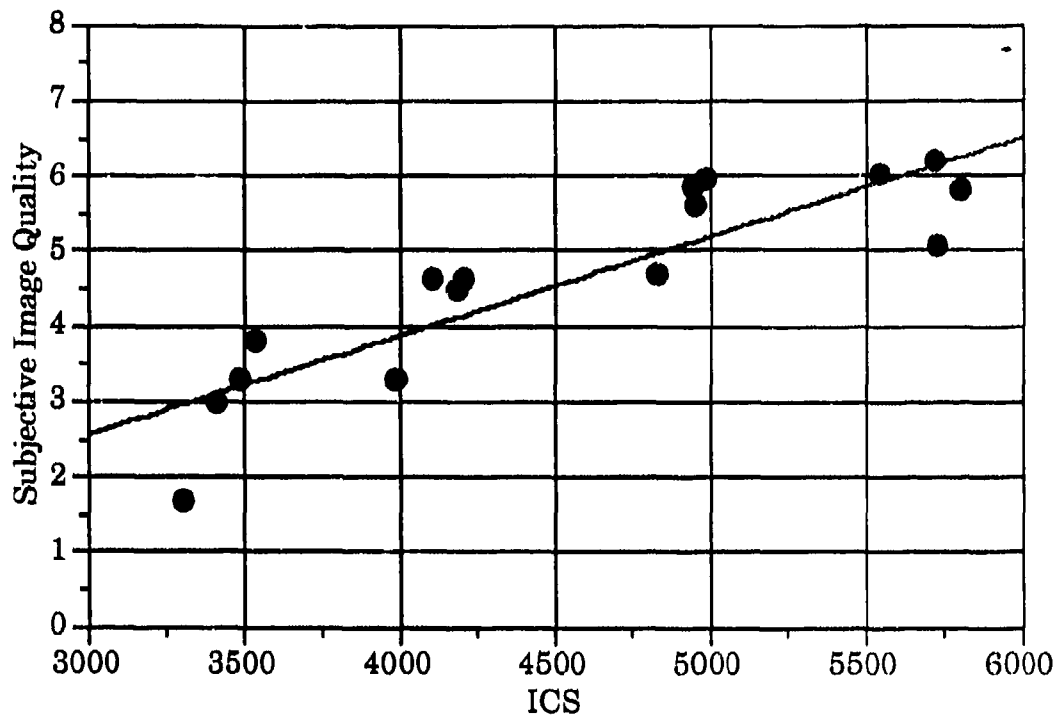


Figure 25. Scattergram of subjective image quality judgments reported in Knox (1987) and empirically computed ICS metric values.

**4.3.2.3 SQRI Metric.** Figure 26 presents a scattergram of the image quality judgments and SQRI metric values across the resolution and addressability conditions reported in Knox (1987). From Figure 26, it can be seen that subjective image quality increases with increasing SQRI values.

The linear regression of SQRI values on subjective image quality judgments, as given by

$$\Psi_{IQ} = -12.494 + (1.422E-1 \text{ SQRI}). \quad (\text{Eq. 55})$$

The statistical fit of the linear regression is  $r^2 = 0.860$ . The trend in Figure 26 suggests that the relationship between subjective image quality judgments and SQRI values is described well by a linear expression.

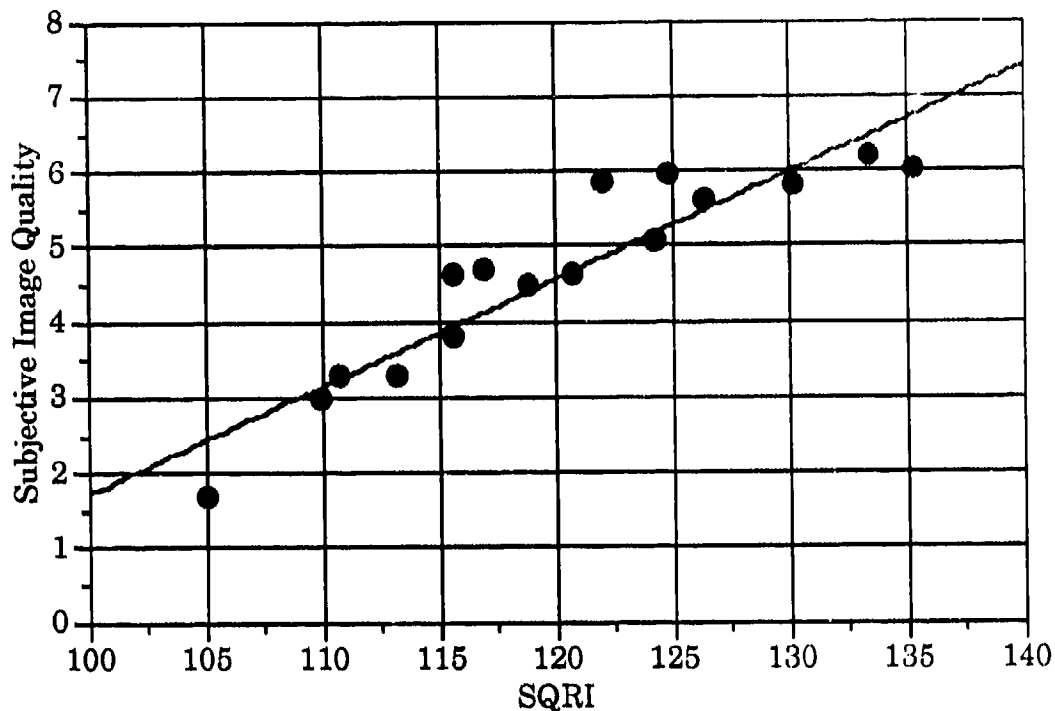


Figure 26. Scattergram of subjective image quality judgment reported Knox (1987) and empirically computed SQRI metric values.

#### 4.4 BEATON (1984)

**4.4.1 Description of Experiment.** This experiment assessed subjective image quality judgments of raster-scanned aerial imagery across a range of resolution and static noise levels. Resolution was defined as the 50% width of the imaging system MTF, and it was manipulated across five levels ranging 69.0 to 500.0  $\text{cd/m}^2$  by digital imaging processing techniques. The effects of static noise levels are not considered in this report.

During the experiment, 10 observers viewed each aerial scene from about a 762 mm viewing distance. A 10-point scale was used to collect the subjective judgments. Observers were light adapted to 25.0  $\text{cd/m}^2$ . The ambient luminance reflected from the CRT screen was about 1.0  $\text{cd/m}^2$ .

**4.4.2 Metric v. Performance Correlations.** Using the parameters reported by Beaton (1984), the MTF<sub>A</sub>, ICS, and SQRI metrics were computed

for each resolution condition in the experiment. The C-language algorithms were used for the metric computations.

Before performing the metric computations, it was necessary to re-parameterize the resolution values reported by Beaton (1984). Since the author specifies the 50% MTF point in normalized cycles per pixel, these values were used to compute the 50% width of a Gaussian LSF. As reported in §4.1.2 above, the conversion from MTF to LSF width is straightforward for Gaussian functions. Table 25 lists the 50% width calculations performed for the resolutions levels used by Beaton (1984).

Table 25. 50% Width Calculations for Beaton (1984)

50 % MTF (cyc/pel)	50% LSF (mm)
0.902	0.447477
2.331	1.156395
4.464	2.214563
8.747	4.339332
17.325	8.594824

Table 26 summarizes the computational parameters used in the MTFA, ICS, and SQRI metric computations for the Beaton (1984) study.

**4.4.2.1 MTFA Metric.** Figure 27 presents a scattergram of the image quality judgments and MTFA metric values across the resolution conditions reported in Beaton (1984). From Figure 27, it can be seen that subjective image quality increases with increasing MTFA values.

The linear regression of MTFA values on subjective image quality judgments, as given by

$$\Psi_{IQ} = 5.330 + (3.039E-1 \text{ MTFA}). \quad (\text{Eq. 56})$$

Eq. 56 is plotted in Figure 27 as a straight line. The statistical fit of the linear regression is  $r^2 = 0.544$ . Inspection of Figure 27 suggests that a linear

relationship poorly describes the curvilinear relationship between the subjective image quality judgments and MTFA values.

Table 26. Computational Parameters for Beaton (1984)

Display Device Parameters	Value
Device Type	Monochrome CRT
Screen Height	254 mm
Screen Width	254 mm
Pixels Per Height	512
Pixels Per Width	512
Pixel Shape	Gaussian
Pixel Width (FWHM)	(see Table 25)
Average Luminance	25.0 cd/m <sup>2</sup>
Reflected Glare	1.0 cd/m <sup>2</sup>

Observer Parameters	Value
Viewing Distance	550 mm
Adaptation Luminance	25.0 cd/m <sup>2</sup>

**4.4.2.2 ICS Metric.** Figure 28 presents a scattergram of the image quality judgments and ICS metric values across the resolution conditions reported in Beaton (1984). From Figure 28, it can be seen that subjective image quality increases with increasing ICS values.

The linear regression of ICS values on subjective image quality judgments, as given by

$$\Psi_{IQ} = 5.442 + (7.667E-4 \text{ ICS}). \quad (\text{Eq. 57})$$

Eq. 57 is plotted in Figure 28 as a straight line. The statistical fit of the linear regression is  $r^2 = 0.549$ . Inspection of Figure 28 suggests that a linear relationship poorly describes the curvilinear relationship between subjective image quality judgments and ICS values.

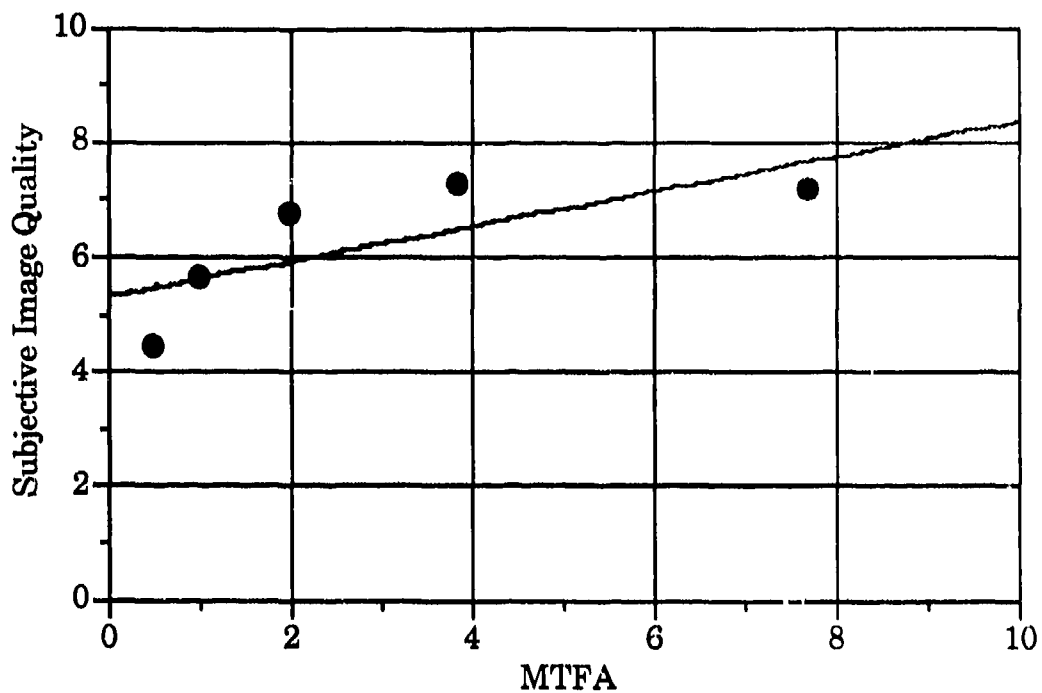


Figure 27. Scattergram of subjective image quality judgments reported in Beaton (1984) and empirically computed MTFA metric values.

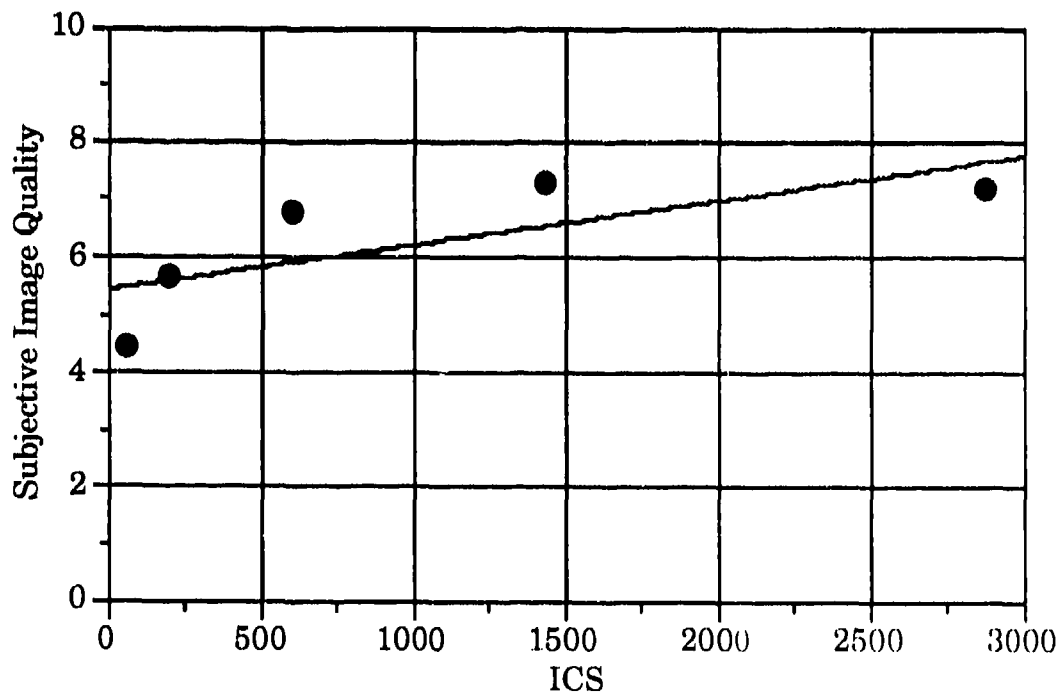


Figure 28. Scattergram of subjective image quality judgments reported in Beaton (1984) and empirically computed ICS metric values.

**4.4.2.3 SQRI Metric.** Figure 29 presents a scattergram of the image quality judgments and SQRI metric values across the resolution conditions reported in Beaton (1984). From Figure 29, it can be seen that subjective image quality increases with increasing SQRI values.

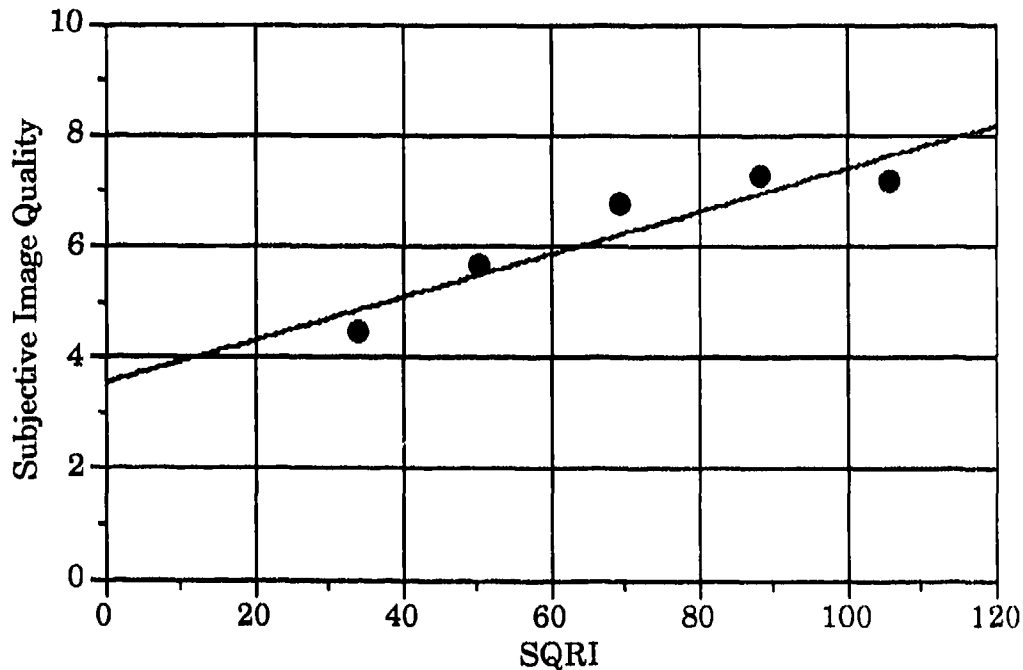


Figure 29. Scattergram of subjective image quality judgment reported Beaton (1984) and empirically computed SQRI metric values.

The linear regression of SQRI values on subjective image quality judgments, as given by

$$\Psi_{IQ} = 3.537 + (3.869E-2 \text{ SQRI}). \quad (\text{Eq. 58})$$

Eq. 58 is plotted in Figure 29 as a straight line. The statistical fit of the linear regression is  $r^2 = 0.859$ . The trend in Figure 29 suggests that a linear relationship adequately describes the relationship between subjective image quality judgments and SQRI values. A curvilinear trend remains apparent in these data, however.

## 4.5 HUNTER (1988)

**4.5.1 Description of Experiment.** This experiment assessed subjective image quality judgments of raster-scanned text imagery across numerous ambient glare levels and display resolutions. Ambient glare was defined in terms of the illuminance on the screen, and it was manipulated across three levels: Dark (~0 lux), 650 lux diffuse, and 650 lux specular.

Display resolution was defined in terms of the 50% LSF width, and it was manipulated by pixel-replication techniques and the use of diffusing anti-glare filters. Two levels of pixel-replication were employed: (1) none, which consisted of the unmodified CRT pixel (high-resolution) and (2) a 2-by-2 pixel replication, which consisted of four pixels arranged in a square matrix and, then, defocused to preserve the Gaussian LSF shape (low-resolution).

The high- and low-resolution conditions were manipulated further by placement of anti-glare filter across the CRT faceplate. Sixteen anti-glare filters were used which had various transmissivity and first-surface characteristics (i.e., polished, etched, optically-coated, and mesh).

A total of 32 (i.e., 16 filters X 2 pixel sizes) resolution levels were used in the experiment. Each resolution level was specified in terms of the 50% LSF width as determined by microphotometric measurements.

During the experiment, observers viewed each text screen from about a 558 mm viewing distance. A 9-point scale was used to collect the subjective judgments. It should be noted that the anti-glare filters affected the peak (average) luminance of the scenes as well as the observer's adaptation level.

**4.5.2. Metric v. Performance Correlations.** Using the parameters reported by Hunter (1987), the MTFA, ICS, and SQRI metrics were computed for each resolution condition in the experiment. The C-language algorithms were used for the metric computations.

Before performing the metric computations, it was necessary to estimate the reflected glare luminance, average scene luminance, and adaptation level. Since Hunter (1987) reports the peak luminance of the unfiltered display, the ambient illuminance, as well as the transmissivity and reflectivity values for the various filter, these values were used to determine the parameter settings of the image quality models. The reflected glare luminance was derived as

$$G_{\text{reflected}} = \frac{I R}{\pi}, \quad (\text{Eq. 59})$$

the average scene luminance was estimated as

$$L_{\text{ave}} = \frac{T L_{\text{peak}}}{2}, \quad (\text{Eq. 60})$$

and the adaptation level was estimated as

$$L_{\text{adapt}} = T L_{\text{peak}} + G \quad (\text{Eq. 61})$$

in which

$G$	denotes the reflected glare luminance,
$L_{\text{ave}}$	denotes the average scene luminance,
$L_{\text{adapt}}$	denotes the adaptation luminance level,
$L_{\text{peak}}$	denotes the peak luminance of the unfiltered display ( $40 \text{ cd/m}^2$ ),
$T$	denotes a filter transmissivity value,
$I$	denotes an ambient illumination level, and
$R$	denotes a filter reflectivity value.

Table 27 summarizes the computational parameters used in the MTFA, ICS, and SQRI metric computations for the Hunter (1988) study.

Table 27. Computational Parameters for Hunter (1988)

Display Device Parameters	Value
Device Type	Monochrome CRT
Screen Height	100 mm
Screen Width	200 mm
Pixels Per Height	512 (low) or 1024 (high)
Pixels Per Width	1024 (low) or 2048 (high)
Pixel Shape	Gaussian
Pixel Width (FWHM)	0.363 – 0.667 mm
Average Luminance	12.49 – 124.73 cd/m <sup>2</sup>
Reflected Glare	0.06 – 88.00 cd/m <sup>2</sup>

Observer Parameters	Value
Viewing Distance	558.8 mm
Adaptation Luminance	12.49 – 124.73 cd/m <sup>2</sup>

**4.5.2.1 MTFA Metric.** Figure 30 presents a scattergram of the image quality judgments and MTFA metric values across the low-resolution conditions reported in Hunter (1988).

The linear regression of MTFA values on subjective image quality judgments, as given by

$$\Psi_{IQ} = 5.873 + (2.347E-1 \text{ MTFA}). \quad (\text{Eq. 62})$$

Eq. 62 is plotted in Figure 30 as a straight line. The statistical fit of the linear regression is  $r^2 = 0.132$ . Inspection of Figure 30 suggests that a linear relationship does not exist between the subjective image quality judgments and MTFA values.

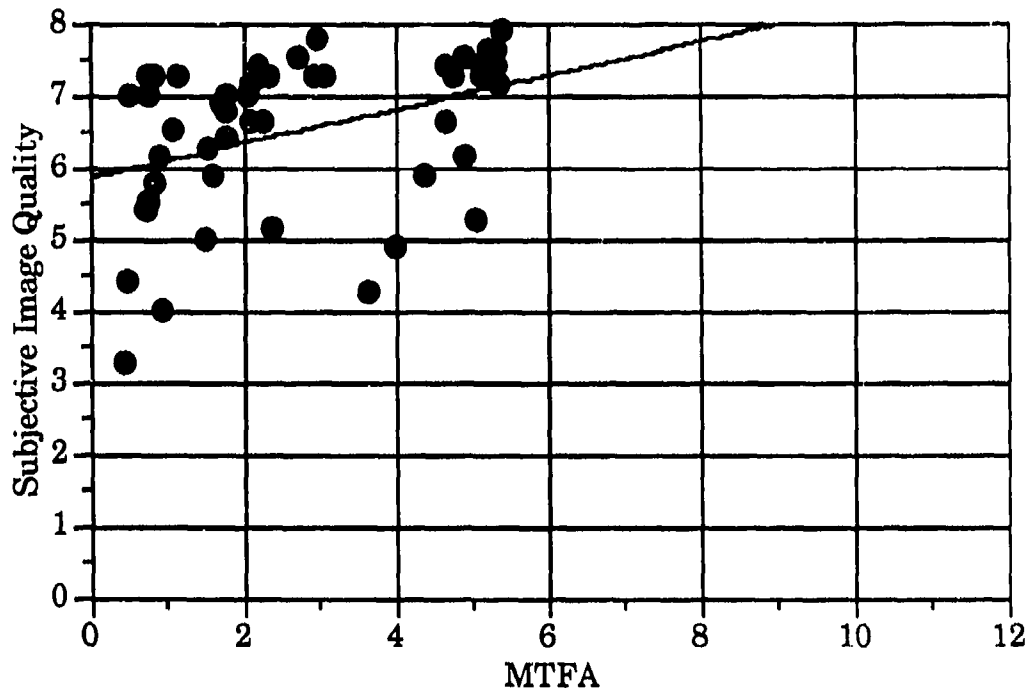


Figure 30. Scattergram of subjective image quality judgments reported in Hunter (1988) and empirically computed MTF metric values for the low-resolution display condition.

Figure 31 presents a scattergram of the image quality judgments and MTF metric values across the high-resolution conditions reported in Hunter (1988). The linear regression of MTF values on subjective image quality judgments, as given by

$$\Psi_{IQ} = 4.296 + (3.262E-1 \text{ MTF}). \quad (\text{Eq. 63})$$

The statistical fit of Eq. 63 is  $r^2 = 0.414$ . Inspection of Figure 31 suggests that a weak linear relationship exists between the subjective image quality judgments and MTF values.

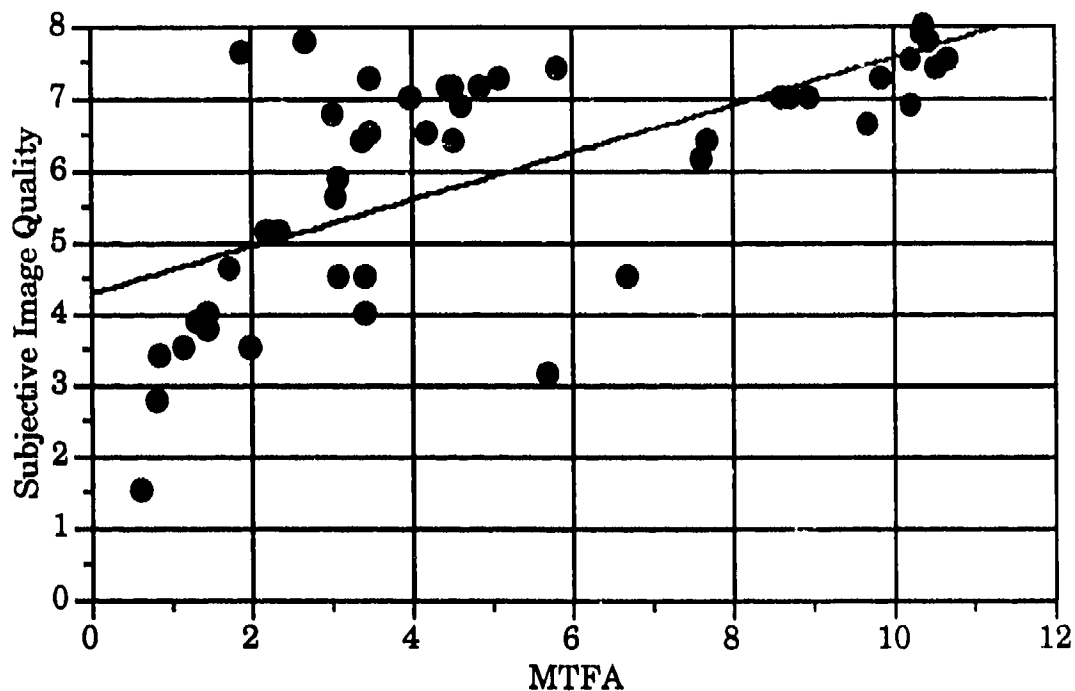


Figure 31. Scattergram of subjective image quality judgments reported in Hunter (1988) and empirically computed MTFA metric values for the high-resolution display condition.

**4.5.2.2 ICS Metric.** Figure 32 presents a scattergram of the image quality judgments and ICS metric values across the low-resolution conditions reported in Hunter (1988). The linear regression of ICS values on subjective image quality judgments is given by

$$\Psi_{IQ} = 5.794 + (7.253E-4 \text{ ICS}). \quad (\text{Eq. 64})$$

Eq. 64 is plotted in Figure 32 as a straight line. The statistical fit of the linear regression is  $r^2 = 0.145$ . Inspection of Figure 32 suggests that a linear relationship does not describe the relationship between subjective image quality judgments and ICS values.

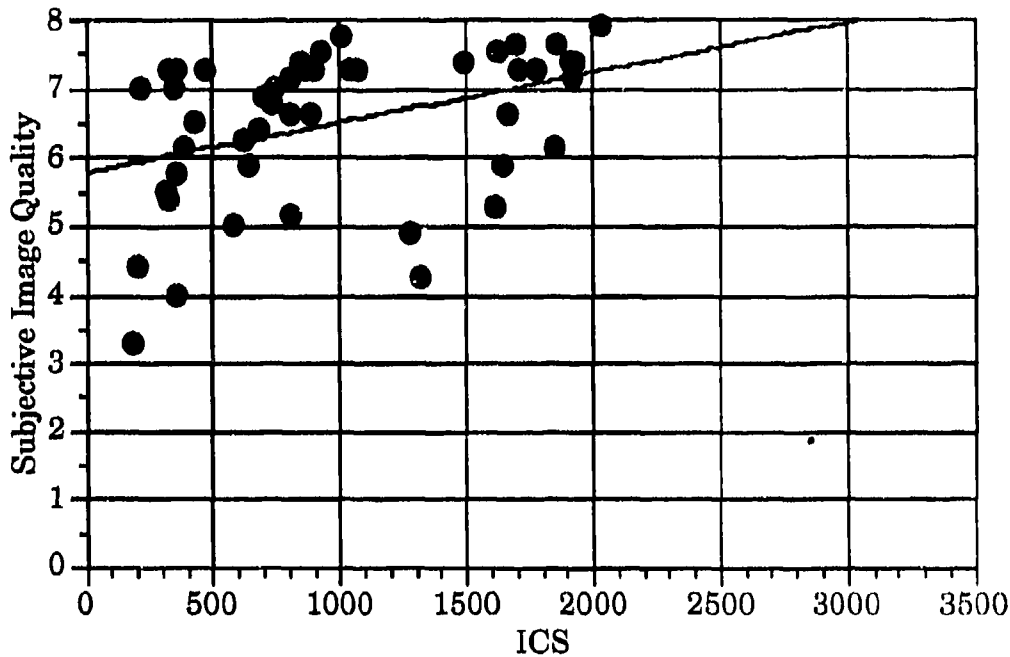


Figure 32. Scattergram of subjective image quality judgments reported in Hunter (1988) and empirically computed ICS metric values for the low-resolution display condition.

Figure 33 presents a scattergram of the image quality judgments and ICS metric values across the high-resolution conditions reported in Hunter (1988). The linear regression of ICS values on subjective image quality judgments is given by

$$\Psi_{IQ} = 4.106 + (1.130E-3 \text{ ICS}). \quad (\text{Eq. 65})$$

Eq. 65 is plotted in Figure 33 as a straight line. The statistical fit of the linear regression is  $r^2 = 0.416$ . Inspection of Figure 33 suggests that a linear relationship adequately roughly models the relationship between subjective image quality judgments and ICS values.

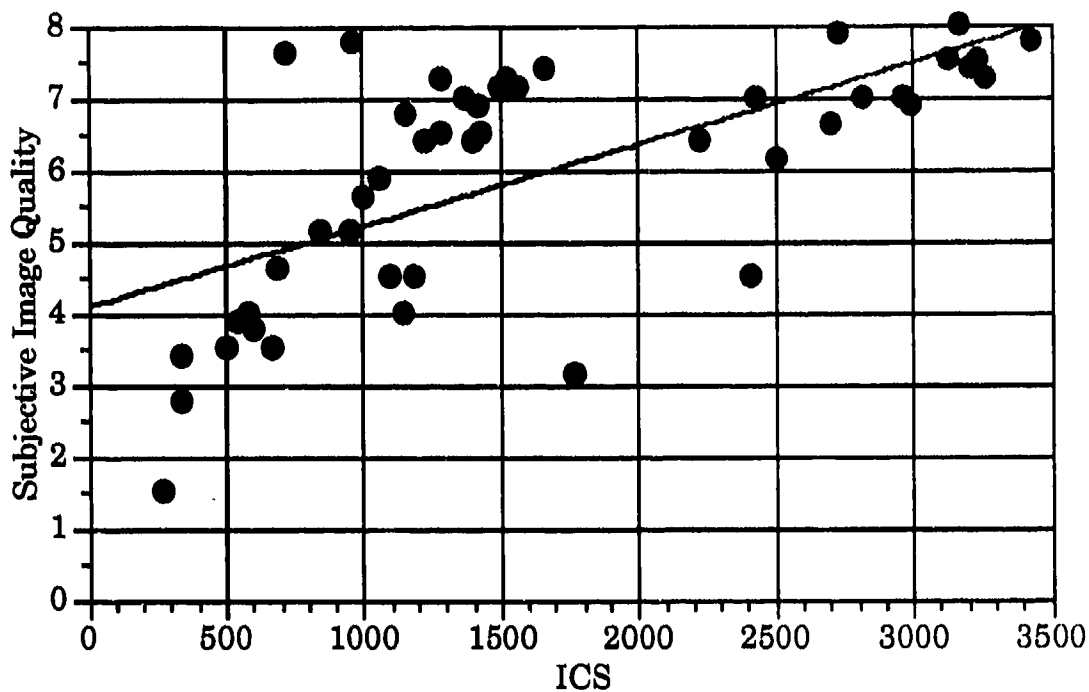


Figure 33. Scattergram of subjective image quality judgments reported in Hunter (1988) and empirically computed ICS metric values for the high-resolution display condition.

**4.5.2.3 SQRI Metric.** Figure 34 presents a scattergram of the image quality judgments and SQRI metric values across the low-resolution conditions reported in Hunter (1988). The linear regression of SQRI values on subjective image quality judgments, as given by

$$\Psi_{IQ} = 5.160 + (1.990E-2 \text{ SQRI}). \quad (\text{Eq. 66})$$

The statistical fit of Eq. 66 is  $r^2 = 0.153$ . Figure 34 suggests that the relationship between subjective image quality judgments and SQRI values is not described by a linear trend.

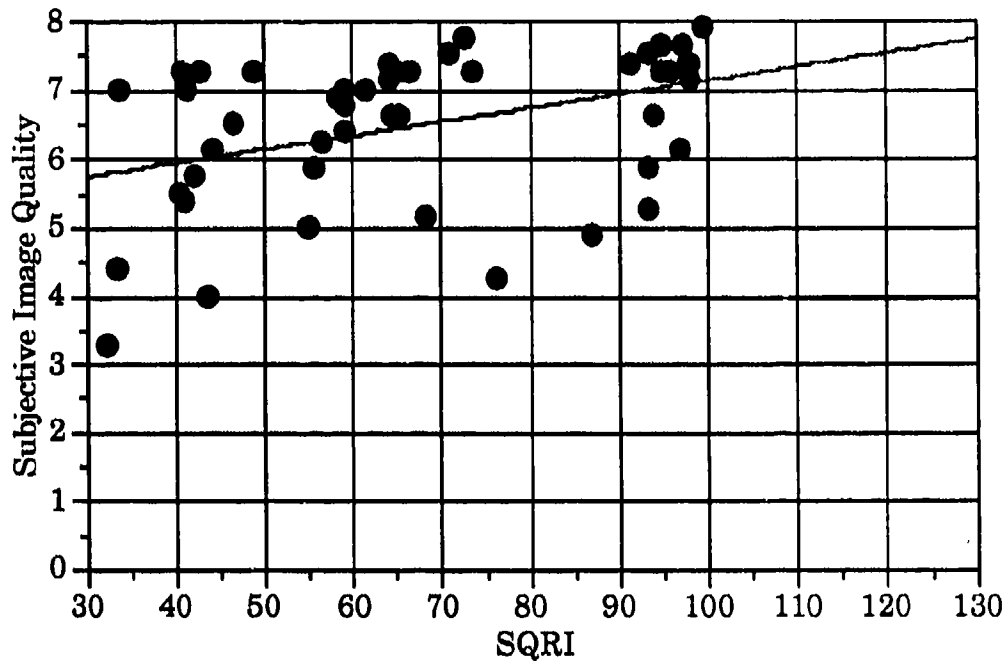


Figure 34. Scattergram of subjective image quality judgment reported Hunter (1988) and empirically computed SQRI metric values for the low-resolution display conditions.

Figure 35 presents a scattergram of the image quality judgments and SQRI metric values across the high-resolution conditions reported in Hunter (1988). The linear regression of SQRI values on subjective image quality judgments, as given by

$$\Psi_{IQ} = 2.520 + (4.378E-2 \text{ SQRI}). \quad (\text{Eq. 67})$$

Eq. 67 is plotted in Figure 35 as a straight line. The statistical fit of the linear regression is  $r^2 = 0.419$ . Figure 35 suggests that the relationship between subjective image quality judgments and SQRI values is not described well by a linear trend.

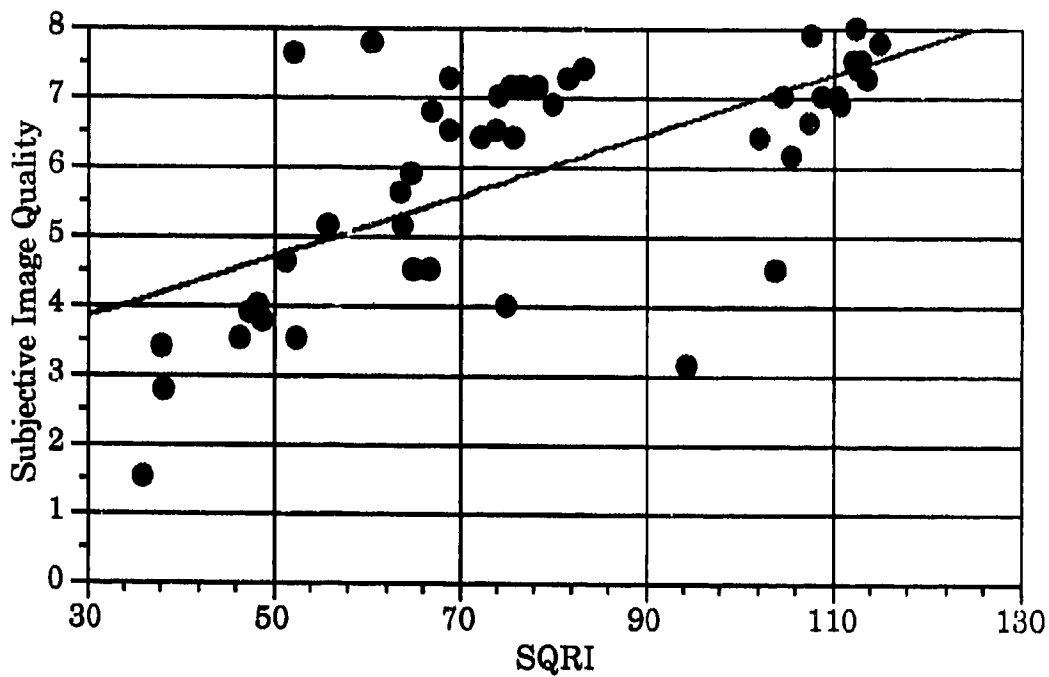


Figure 35. Scattergram of subjective image quality judgment reported Hunter (1988) and empirically computed SQRI metric values for the high-resolution display conditions.

## 5.0 CONCLUSIONS

In general, the MTFA, SQRI, and ICS metrics use the same quantitative information concerning the display system and human observer — that is, the MTF and CTF. However, the three metrics utilize the quantitative information in different manners. The differences in analytical formulation among the MTFA, ICS, and SQRI metrics can produce dramatically different predictions of image quality across various display device and viewing conditions.

As indicated in the analytical section of this report, the MTFA metric weights a relatively broad spatial frequency passband of MTF and CTF information. The weighting emphasizes MTF and CTF information within a passband located in the region of lowest contrast thresholds for the human visual system. Although the passband location is suitable, the MTFA metric value does not change substantially with CTF shifts due to its linear subtraction formulation. As a consequence, the MTFA metric does not index several important device and viewing condition parameters that are known to affect perceived image quality levels. The most notable parameters in this regard include display size and adaptation level.

The ICS metric emphasizes MTF and CTF information at higher spatial frequencies. Since the ICS metric formulation is based on a multiplicative combination of MTF and CTF information, this metric is responsive to subtle variations in either the MTF or CTF at the higher spatial frequencies. Thus, the ICS metric is well-suited to index changes in resolution and addressability, since the effect of these parameters tends to influence higher frequency portions of the MTF passband.

The SQRI metric is very responsive to MTF and CTF changes at low spatial frequencies. This property of the SQRI metric accounts for its capacity to index changes in display size, viewing distance, and the luminance-dependent perceptual phenomena. Moreover, the compressive weighting of MTF and CTF information applied by the SQRI accounts for its capacity to index suprathreshold changes in display and viewing condition parameters.

Aside from these general remarks, it is important to consider the "practical" issues associated with the computation of the image quality metrics. In this vein, the MTFA metric is robust to computational parameter settings that mimic the operational characteristics of display measurement systems. That is, the LSF sampling interval and scan period exert minimal influences on the computed MTFA values. This is an important property of any "accepted" image quality metric, since the empirical measurement and numerical processing environment of users can not be well-specified and controlled.

Similar to the MTFA metric, the ICS metric is well-behaved under a broad range of computational parameter settings. While the ICS metric is influenced significantly by LSF sampling interval and scan period, computational errors can be held to acceptable levels with easily obtained increases in the number of sample points and scan length.

The SQRI metric exhibits high sensitivity to computational parameters. Indeed, the SQRI errors are very difficult to control and are large in magnitude. The SQRI computational errors arise from the lower spatial frequency limits of the integral, which can not be achieved readily in tabulated data arrays. Indeed, due to the magnitude of SQRI errors observed in this work, it is reasonable to suspect the validity of any SQRI metric value computed from tabulated data or simplistic numerical integration techniques.

With an accurate computation of the three metrics, it is apparent that the SQRI predicts image quality better than the ICS metric which, in turn, predicts better than the MTFA metric. This statement, however, is based on the observed statistical regressions for subjective image quality judgments of "higher" quality images, such as projected color slides. For "lower" quality images, such as those produced by raster-scanned CRTs, it is not entirely clear that the image quality predictions differ substantially among the MTFA, ICS, and SQRI metrics. Inspection of analyses for Beaton (1984) and Hunter (1988) points up the fact that no one metric accounts for substantially greater amounts of variance in the data.

In conclusion, the SQRI metric is recommended over the ICS and MTFA when evaluated by closed-form techniques or sophisticated numerical integration algorithms. On the other hand, the SQRI metric is not recommended for general-purpose use with tabulate data arrays, since the computational environment of users can not be controlled. For general-purpose use, either the ICS or MTFA metrics offer easily achieved computational accuracy with reasonable image quality predictions across select display and viewing condition parameters.

## 6.0 REFERENCES

- American National Standard for Human Factors Engineering of Visual Display Terminal Workstations. ANSI/HFS 100-1988, Santa Monica: Human Factors Society, 1988.
- Beaton, R. J. A human-performance based evaluation of quality metrics for hard-copy and soft-copy digital imaging systems. Unpublished doctoral dissertation, Virginia Polytechnic Institute and State University, Blacksburg, VA, 1984.
- Beaton, R. J. Display Measurements. Society for Information Display, Tutorial Notes, 1988.
- Bracewell, R. N. The Fourier transform and its applications. McGraw-Hill: New York, 2nd Edition, 1986.
- Murch, G. M. and Beaton, R. J. Matching display characteristics to human visual capacity. In Bulletin 3: Scientific Programme and Abstracts: Work with Visual Display Units, Stockholm, 1986.
- Barten, P. G. J. The SQRI method: A new method for the evaluation of visible resolution on a display, Proceedings of the Society for Information Display, 28(3), 253-262, 1987.
- Barten, P. G. J. Effect of picture size and definition on perceived image quality, IEEE Proceedings of the International Display Research Conference, 142-145, 1988.
- Barten, P. G. J. Subjective image quality of HDTV pictures. Proceedings of the 9th International Display Research Conference, Japan Display'89, October 16-18, Kyoto, 598-601, 1989 (a).
- Barten, P. G. J. The effects of picture size and definition on perceived image quality. IEEE Transactions on Electron Devices, 36(9), 1865-1869, 1989 (b).

- Barten, P. G. J. The square root integral (SQRI): A new metric to describe the effects of various display parameters on perceived image quality. Proceedings of the Society for Photographic Instrumentation Engineers, Human Vision, Visual Processing, and Digital Display, Los Angeles, 1077, 73-82, 1989 (c).
- Barten, P. G. J. Evaluation of CRT displays with the SQRI method. Proceedings of the Society for Information Display Engineers, 30, 9-14, 1989 (d).
- Barten, P. G. J. The effects of glass transmission on the subjective image quality of CRT pictures. Proceedings of the 10th International Display Research Conference, EURODISPLAY'90, Amsterdam, The Netherlands, 336-339, 1990 (a).
- Barten, P. G. J. Evaluation of subjective image quality with the square-root integral method. Journal of the Optical Society of America (A), 7, 2024-2031, 1990 (b).
- Barten, P. G. J. Evaluation of the effect of noise on subjective image quality. Proceedings of the Society for Photographic Instrumentation Engineers, Unpublished manuscript, 1991.
- Bergland, G. D. and Doland, M. T. Fast Fourier Transform Algorithms. Programs for Digital Signal Processing. IEEE Press Book (1979) pp1.2-1 to 1.2-18.
- Borough, H. C., Fallis, R. F., Warnock, R. H., and Britt, J. H. Quantitative determination of image quality. Boeing Company Report D2-114058-1, 1967.
- Carlson, C. R. Sine-wave threshold contrast-sensitivity function: Dependence on display size. RCA Review, 43, 675-683, 1982.
- Carlson, C. R. and Cohen, R. W. A simple psychophysical model for predicting the visibility of display information. Proceedings of the Society for Information Display, 21, 1980.

- Farley, W. W. Determination of monochrome display MTFs in the presence of glare. Society for Information Display Digest, Baltimore, 212-215, 1989.
- Hoekstra, J., van der Goot, D. P. A., van den Brink, G., and Bilsen, F. A. The influence of the number of cycles upon the visual contrast threshold for spatial sine wave patterns. Vision Research, 14, 1974.
- Hunter, M. Unpublished doctoral dissertation, Virginia Polytechnic Institute and State University, Blacksburg, VA, 1988.
- Infante, C. Proceedings of the Society for Information Display, 1984
- Jesty, L. C. The relation between picture size, viewing distance, and picture quality, IEE Proceedings, 425-439, 1958.
- Knox, S. T. Resolution and addressability requirements for digital CRT's. SID Digest, 18, 26-29, 1987.
- Snyder, H. L. Image quality and observer performance, In L. M. Biberman (ed.), Perception of displayed information. New York: Plenum, 1973.
- Snyder, H. L. Human visual performance and flat panel display image quality. Human Factors Laboratory Technical Report, HFL-80/ONR-80-1, Virginia Polytechnic Institute and State University, Blacksburg, 1980.
- Snyder, H. L. Image quality: Measures and visual performance. In, L. E. Tannas (ed.), Flat panel displays and CRTs, New York: Van Nostrand Reinhold, 1985.
- van der Zee, E. and Boesten, M. H. W. A. The influence of luminance and size on the image quality of complex scenes, IPO Annual Progress Report, 15, 69-75, 1980.
- van Meeteren, A. Visual aspects of image intensification. Ph.D. Dissertation, Univ. of Utrecht, The Netherlands, 1973.

- van Nes, F. L. and Bouman, M. A. Spatial modulation transfer in the human eye. *Journal of the Optical Society of America*, 57, 1967.
- Westerink, J. H. D. M. and Roufs, J. A. J. A local basis for perceptually relevant resolution measures. *SID Digest*, 19, 360-363, 1988.
- Westerink, J. H. D. M. and Roufs, J. A. J. Subjective image quality as a function of viewing distance, resolution, and picture size. *SMPTE Journal*, 98 (2), 113-119, 1989.